CONTENTS

Regular contribution

14th International School and Symposium
on Synchrotron Radiation in Natural Science
09-14 June 2019, Zakopane, Poland

Organized by Polish Synchrotron Radiation Society
in cooperation with Adam Mickiewicz University, Poznań, Poland

Welcome to the 14th International School and Symposium on Synchrotron Radiation in Natural Science

On behalf of the Organizing Committee and International Scientific Advisory Committee, we are pleased to welcome you to the 14th International School and Symposium on Synchrotron Radiation in Natural Science (ISSRNS 2019) organized by the Polish Synchrotron Radiation Society (PTPS) in cooperation with the A. Mickiewicz University in Poznań in Zakopane (Poland). The goal of our biennial meeting organized from 1992, is to bring together scientists and students working with synchrotron radiation and new participants interested in using synchrotron radiation and laser-based techniques.

This year our conference is organized in Belvedere hotel (Zakopane). This beautiful place is located in Podhale region (Tatra mountains, the southern part of Poland), and is known as the center of Goral culture and also an excellent place for sports and recreation activities. There is long tradition, that ISSRNS is an exchange place of information on recent developments in the field of the construction of accelerators, insertion devices, and other synchrotron instrumentation as well as applications of synchrotron radiation in industry and science. The topics of ISSRNS 2019 cover main areas of applications of synchrotron radiation:

- X-ray imaging, nanoimaging, holography and nanotomography,
- macromolecular crystallography of complex systems,
- XFEL sources, time-resolved and ultrafast techniques
- X-ray diffraction studies of materials at extreme conditions,
- *in situ* synchrotron studies of novel materials,
- scattering techniques in structural analysis of new materials and biological macromolecules,
- design and development of instrumentation for synchrotrons and free electron lasers,
- applications of X-ray fluorescence, X-ray absorption, and photoelectron spectroscopies in material science and biophysics,
- X-ray magnetic dichroism,
- development and application of laser-based sources of radiation (in collaboration with Laserlab-Europe)
- other applications of synchrotron radiation in nanosciences and soft matter physics.

We would like to thank all lecturers for accepting our invitations to show the results of their exciting studies. We also thank all the participants for preparing oral and poster presentations. We wish you a fruitful and stimulating conference.

Organizers

PROGRAMME

Sunday, 09 June 2019			
14^{00}-19^{00}	Registration and Reception		
15^{00}-15^{10}	Opening Address		
15^{10}-15^{50}	Special speaker	Wladek Minor	Synchrotron Radiation - Foundation for the Golden Age of Structural Biology
15^{50}-16^{30}	L-01	Marcin Nowotny	Crystallographic studies of the mechanism of proteins involved in genome stability
16^{30}-17^{00}	Coffee Break		
17^{00}-17^{40}	L-02	Magdalena Kowalska	Beta-NMR with CERN accelerators: from nuclear physics to biology
17^{40}-18^{00}	O-01	Jakub Szlachetko	Core-level spectroscopy triggered by femtoseconds X-ray pulses
18^{00}-18^{20}	O-02	Pawel Grochulski	Review of Health Research at the Canadian Light Source
18^{20}-18^{40}	O-03	Tomasz Wysokinski	Introducing monochromatic Microbeam Radiation Therapy (m-MRT) modality
18^{40}-19^{00}	O-04	Slawomir Skruszewicz	XUV coherence tomography with nanoscale resolution driven by broadband XUV sources
19^{15}-…	Barbecue		

Monday, 10 June 2019			
8^{00}-9^{00}	Registration and Reception		
9^{00}-9^{40}	L-03	Armin Wagner	Tender X-rays – New colours for macromolecular crystallography
9^{40}-10^{20}	L-04	Michael Hanfland	Molecular solids at high pressure, structural changes and stability
10^{20}-11^{00}	L-05	Damian Paliwoda	Matter at Extremes: Toward New Functional Materials Synthesized at High Pressure
11^{00}-11^{40}	Coffee Break		
11^{40}-12^{20}	L-06	Nikolay Mezentsev	Superconductivity for light generation
12^{20}-12^{40}	O-05	Gesa Richter	Integrative Structural Characterization of Biopharmaceuticals by Small-Angle X-Ray Scattering (SAXS)
12^{40}-13^{00}	O-06	Maciej Jankowski	Synchrotron X-ray diffraction investigation of graphene on liquid copper
13^{00}-14^{20}	Lunch		
14^{20}-15^{00}	L-07	Marek Stankiewicz	Synchrotron SOLARIS – present and future research options
15^{00}-15^{40}	L-08	Sebastian Glatt	High-Resolution single particle Cryo-EM How Poland can take part in the ongoing resolution revolution in structural biology
15^{40}-16^{00}	O-07	Krzysztof Woźniak	Successful Experimental Quantitative Charge Density Feasibility Study of Grossular Under High Pressure
16^{00}-16^{30}	Coffee Break		

SOLARIS Special Session			
16^{30}-16^{40}		Alicja Górkiewicz	How to apply for a beamtime at SOLARIS Synchrotron?
16^{40}-17^{00}	O-08	Adriana Wawrzyniak	SOLARIS operation status
17^{00}-17^{20}	O-09	Marcin Zając	The first experimental results from PEEM/XAS beamline at Solaris
17^{20}-17^{40}	O-10	Maciej Kozak	SOLCRYS - new SAXS/XRD beamline for NCPS Solaris
17^{40}-18^{00}	O-11	Tomasz Kołodziej	SOLCRYS beamline at SOLARIS
18^{00}-18^{20}	O-12	Barbara Wolanin	XMCD beamline status
18^{20}-18^{40}	O-13	Magdalena Szczepanik-Ciba	PHELIX – a new beamline at SOLARIS synchrotron
18^{40}-19^{00}	O-14	Natalia Olszowska	UARPES - high resolution photoelectron spectroscopy beamline at NSRC Solaris - Current state
19^{00}-20^{00}	Dinner		

Tuesday, 11 June 2019

9^{00}-9^{40}	L-09	Saša Bajt	Development of multilayer Laue lenses and their applications
9^{40}-10^{20}	L-10	Andrei V. Petukhov	Nanoparticles and their self-assembly in 1D and 2D: SAXS, GISAXS and XRR
10^{20}-11^{00}	L-11	Eleonora Shtykova	The role and potential benefits of protein structural disorder in viral replication machinery: study and modeling from synchrotron SAXS data
11^{00}-11^{40}	Coffee Break		
11^{40}-12^{20}	L-12	Krzysztof Banas	Comparison of bulk and microscale infrared characterisation of stratum corneum - key aspects of hyperspectral data processing
12^{20}-13^{00}	L-13	Per Johnsson	Laser-Driven High-Order Harmonic Generation Successful Experimental Quantitative Charge Density Feasibility Study of Grossular Under High Pressure
13^{00}-14^{20}	Lunch		
14^{20}-15^{00}	L-14	Lutz Kirste	Synchrotron X-ray Diffraction Rocking Curve Imaging of the Defect Structure of GaN Substrates
15^{00}-15^{40}	L-15	Britta Redlich	IR and THz spectroscopy with the FELIX free electron laser: From astrochemistry to condensed matter physics
15^{40}-16^{00}	O-15	Henryk Fiedorowicz	X-ray absorption spectroscopy using laser plasma soft X-ray sources
16^{00}-16^{20}	O-16	Karol A. Janulewicz	Nanometer resolution optical coherence tomography (OCT) using a compact laser plasma soft X-ray source
16^{20}-16^{40}	O-17	Maciej Dendzik	Ultra-fast core-level dynamics in semiconducting WSe_2
16^{40}-17^{15}	Coffee Break		
17^{15}-19^{00}	General Assembly of the Polish Synchrotron Radiation Society		
19^{00}-20^{00}	Dinner		
20^{00}-22^{00}	Poster Session		

Wednesday, 12 June 2019

9^{00}-9^{40}	L-16	Agnieszka Banas	Nanoscale characterisation of chemical speciation in CNT based composites - advantages and pitfalls of photothermal infrared spectroscopy in light of data processing
9^{40}-10^{20}	L-17	Matthias Bauer	Establishment of XAS, XES and HERFD-XAS for sustainable chemistry applications
10^{20}-11^{00}	L-18	Michael Sztucki	Probing the structure and dynamics of soft matter by synchrotron radiation
11^{00}-11^{40}	Coffee Break		
11^{40}-12^{20}	L-19	Vaclav Holy	Anomalous x-ray scattering and DAFS spectroscopy on nanoparticles in metallic single crystals
12^{20}-13^{00}	L-20	Krystyna Jabłońska	Influence of metal oxides surface stoichiometry on their physical and chemical properties – XAS and XPS studies
13^{00}-14^{20}	Lunch		
14^{20}-19^{00}	Conference Excursion		
19^{00}-20^{00}	Conference Dinner		

Thursday, 13 June 2019

9^{00}-9^{40}	L-21	Dmitry Khakhulin	Combining femtosecond hard X-ray scattering and spectroscopy to study photochemical dynamics in solution: instrumentation and recent results
9^{40}-10^{20}	L-22	Josef Hormes	Low energy X-ray absorption spectroscopy
10^{20}-11^{00}	L-23	Hiromitsu Tomizawa	Synchronization between XFEL and Petawatt laser
11^{00}-11^{40}	Coffee Break		
11^{40}-12^{20}	L-24	Dino Jaroszynski	The laser plasma wakefield accelerator as a versatile radiation source for applications
12^{20}-13^{00}	L-25	Subhendu Kahaly	Attosecond High Harmonic Sources at ELI-ALPS and the opportunities
13^{00}-14^{20}	Lunch		
14^{20}-15^{00}	L-26	Toshiya Senda	Automation and the DB system in the MX beamlines of Photon Factory
15^{00}-15^{40}	L-27	Elzbieta Trzop	From molecular switching to material transformation: revisiting the spin crossover with ultrafast pump-probe techniques
15^{40}-16^{20}	L-28	Miroslaw Gilski	Macromolecular Xtallography Raw Data Repository MX-RDR
16^{20}-16^{50}	Coffee Break		
Session A			
16^{50}-17^{10}	O-18A	Robert Nietubyć	Photon beams and experimental stations at the PolFEL free electron laser facility
17^{10}-17^{30}	O-19A	Edyta Piskorska-Hommel	The structure evolution of the self-regenerative doubly doped CeO

17^{30}-17^{50}	O-20A	Piotr Maj	Structural insight into thymidylate synthase inhibition by N^4-OH-dCMP
17^{50}-18^{10}	O-21A	Michał Nowakowski	Cr $K\beta_{1,3}$ RXES reveals heterogeneity of Cr binding site types in various artificial lipid membranes
18^{10}-18^{30}	O-22A	Izabela Biało	X-ray studies of charge correlations in cuprates under extreme conditions
18^{30}-18^{50}	O-23A	Katarzyna M. Sowa	3D Multipoint-projection X-ray microscopy
18^{50}-19^{10}	O-24A	Joanna Stępień	XNLD as the means of studying near surface crystallographic structure in pristine and TM doped single crystals bismuth chalcogenides
Session B			
16^{50}-17^{10}	O-25B	Małgorzata Zienkiewicz-Strzałka	SAXS investigation of nanostructure - property relationship of composite materials
17^{10}-17^{30}	O-26B	Ryszard Sobierajski	Ultrafast crystallization of thin film metallic glasses: an X-ray diffraction study
17^{30}-17^{50}	O-27B	Anna Wolska	XAFS study on the Co(II), Ni(II) and Cu(II) complexes with chlorophenoxy herbicides
17^{50}-18^{10}	O-28B	Diana Kalinowska	Local atomic environment of Cu and Ag ions of new bioactive 1,5-disubstituted tetrazole complexes investigated using multi–technique approach methodology
18^{10}-18^{30}	O-29B	Krzysztof Tyrala	The off-resonant excitations and two-photon absorption cross-sections Z-dependence for the 3d elements
18^{30}-18^{50}	O-30B	Klaudia Wojtaszek	Changes in the structure of XAS spectra and kinetics of phase transformation for thermally oxidized titanium at different temperatures
18^{50}-19^{10}	O-31B	Anna Wach	Electronic structure of photocatalysts probed by means of X-ray spectroscopy techniques
18^{50}-19^{10}	Dinner		
Friday, 14 June 2019			
9^{00}-9^{40}	L-29	Wojciech Tabiś	Charge correlations and the Fermi surface reconstruction in cuprate superconductors
9^{40}-10^{20}	L-30	Tomasz Giela	Characterization and measurement of magnetic materials using X-Ray and Threshold Photoemission Electron Microscopy
10^{20}-10^{40}	O-32	Michał Taube	Structural and biophysical studies of the plant m6A methyltransferase complex
10^{40}-11^{00}	Closing Remarks		
11^{00}-11^{30}	Coffee and snacks		
11^{30}- …	Departure		

L-00 **Sunday, 09.06., 15^{10}-15^{50}**

Synchrotron radiation - Foundation for the golden age of structural biology

W. Minor[1]*

[1]*Department of Molecular Physiology and Biological Physics University of Virginia, Charlottesville, Virginia 22903, USA*

*e-mail: wladek@iwonka.med.virginia.edu

The past two decades have witnessed tremendous progress regarding the description of life on a macromolecular level, making the 21st century the era of biomedical science. The combination of synchrotron radiation with new methodologies for structure determination have brought an avalanche of macromolecular structures. Crystal structures inspire new hypotheses and experiments to probe biological macromolecules regarding molecular mechanisms, plausible binding modes, and the feasibility of small molecule agents to serve as scaffolds for lead compounds.

The improvement of the resolution and quality of macromolecular structures, especially complexes of macromolecular structures with biomedically important small molecule ligands, is critical for further expansion of structural biology. The new approaches require not only better and more careful refinement protocols but also better synchrotron experiments. The ways to obtain better structures will be discussed in details.

L-01 **Sunday, 09.06., 15^{50}-16^{30}**

Mechanisms of specific DNA recognition in DNA repair

M. Nowotny[1]*

[1]*Laboratory of Protein Structure, International Institute of Molecular and Cell Biology, 02-109 Warsaw, Poland*

*e-mail: mnowotny@iimcb.gov.pl

DNA molecules constantly undergo chemical modifications, also termed damage, which can distort the genetic information. Cells possess effective and sophisticated mechanisms to find and repair such DNA modifications. This talk will describe the use of integrative structural biology approaches involving protein crystallography, modelling, electron microscopy (EM) and molecular dynamics (MD) to decipher the molecular mechanisms of DNA repair.

One general pathway for DNA repair in nucleotide excision repair (NER). In bacterial NER UvrA protein detects the damage and recruits UvrB helicase for damage verification. UvrC cuts out a fragment of the damaged DNA strand. Our crystal structures of UvrA-DNA complex showed that the protein finds the site of DNA damage indirectly by sensing the deformation of the double helix induced by the chemical modification. Using a combination of EM, modelling and biochemical methods we showed that UvrA then recruits two UvrB molecules each loaded on a different DNA strand. UvrB uses its weak helicase activity to translocate toward the lesion. The UvrB molecule that travels on the damaged strand gets stalled at the site of DNA modification. This then drives precise and strand-specific DNA incision by UvrC. Hence, this mechanism explains how indirect and inherently imprecise damage localization is converted into precise DNA cuts.

Holliday junctions (HJs) are four-way DNA structures which act as intermediates in homologous recombination, another important DNA repair pathway. HJs are subsequently removed through actions of nucleases termed resolvases. RuvC is a canonical bacterial resolvase, which introduces two symmetric cuts into the HJ. These two cuts are coordinated: the first one greatly accelerates the second. RuvC preferentially cleaves DNA at A/TTT↓C/G cognate sequences. We found that in the crystal structure of protein-DNA complex the substrate was not properly positioned at active sites. This was attributable to protein-induced conformational tension at the exchange point of the HJ. Cleavage requires easing of this tension through high-energy states with protein-assisted base flipping. This was much easier for the T↓C/G sequence of the second half of the consensus. The mechanism of conformational tension was also used for cleavage coordination as the first nick relaxed the substrate, which accelerated the second cut. This unique mechanism is an example of a different mode of nucleic acid recognition in DNA repair.

L-02 **Sunday, 09.06., 17^{00}-17^{40}**

Beta-NMR with CERN accelerators: from nuclear physics to biology

M. Kowalska[1]*

[1]*UNIGE/CERN, Physics Department, 1121 Geneva, Switzerland*

*e-mail: Kowalska@cern.ch

The CERN laboratory is well known for LHC, the biggest accelerator in the world and particle physics discoveries. However, CERN is also host to several smaller-scale laboratories which use the particles provided by its full accelerator chain. One of these is the CERN-ISOLDE facility, where over 1000 radioactive isotopes can be produced, out of around 3000 discovered until now.

Our ISOLDE-based project is devoted to a special type of Nuclear Magnetic Resonance, called beta-NMR, which can be up to 10 orders of magnitude more sensitive than conventional NMR and which we aim at using for the first time in chemistry and biology. This is possible thanks to the use of lasers to polarize spins close to 100% combined with efficient detection of beta particles, because beta emission from spin-polarized nuclei is asymmetric in space.

In chemistry and biochemistry classical NMR is currently the most versatile and powerful spectroscopic technique for characterization of molecular structure and dynamics in solution. However, the low sensitivity leads to relatively large amounts of sample, imposing constraints on the systems that may be explored. In addition, not all elements are easily accessible, as the most abundant isotopes display no or poor response. beta-NMR addresses these limitations by improving significantly the sensitivity but also introducing many new NMR nuclei with properties complementary to those already available. It brings however challenges very similar to those present at synchrotron-radiation facilities: the need to be coupled to a large-scale online facility, the requirement of high vacuum in the region in front and even around the sample, and the need for a close-to vertical sample orientation.

Within our project we have addressed the above challenges in our dedicated laser-polarization and beta-NMR beamline that we commissioned in 2016. Metal isotopes which have been already used for beta-NMR studies in solid samples include 8,9,11Li, 11Be, 25-28Na, and 23,29,31Mg. First studies on 26Na in liquid samples were performed by our team in December 2017. Soon to be polarized are several K, Ca, Rb, Cu and Zn isotopes [1]. Our first biological studies concern the interaction of Na and K cations with DNA G-quadruplexes, present for example in telomers [3]. At a later stage we plan to investigate the interaction of Cu and Zn with different proteins.

This contribution will cover the principles of beta-NMR, the experimental setup and technical solutions and the scientific topics we have covered and plan to cover.

[1] A. Jancso *et al.*, *J. Phys. G: Nucl. Part. Phys.* **44** (2017) 064003.

[2] M. Kowalska *et al.*, *J. Phys. G: Nucl. Part. Phys*. **44** (2017) 084005.

[3] M. Kowalska *et al*, *CERN-INTC-2017-071 ; INTC-P-521* (2017).

L-03 **Monday,10.06., 9^{00}-9^{40}**

Long-wavelength crystallography – Exploiting anomalous dispersion from light elements

A. Wagner[1;2]*, R. Duman[1;2], V. Mykhaylyk[1;2], K. el Omari[1;2] and C. Orr[1;2]

[1]*Diamond Light Source, Harwell Science and Innovation Campus, Chilton, Didcot OX11 0DE, United Kingdom.*
[2]*Research Complex at Harwell, Rutherford Appleton Laboratory, Harwell Oxford, Didcot OX11 0FA, United Kingdom.*

Keywords: long-wavelength crystallography, macromolecular crystallography, anomalous dispersion

*e-mail: armin.wagner@diamond.ac.uk

Macromolecular crystallography is a very well established technique in structural biology, responsible for the majority of structures in the Protein Data Base (PDB). The majority of structures are determined using X-ray diffraction data from synchrotron beamlines. These beamlines typically operate in a wavelength range from 0.8 to 2 Å.

Anomalous dispersion is an effect which leads to intensity differences between reflections *hkl* and *–h-k-l*, so called Friedel pairs. This signal is typically small, but increases towards absorption edges of elements present in the crystal structure. The anomalous signal can be exploited to solve the crystallographic phase problem either by SAD (single-wavelength anomalous diffraction) or MAD (multi-wavelength anomalous diffraction) techniques. The most commonly used element utilised for this purpose is selenium with an absorption edge at a wavelength of around 0.98 Å. It is based on substituting the amino acid methionine with seleno-methionine. This works very well for bacterial expression systems, but can become laborious, expensive or even not feasible for expression systems from higher organisms. An alternative is using the intrinsic anomalous signal from sulphur present in the two amino acids cysteine and methionine. With the absorption edge of sulphur at a wavelength of 5.02 Å, however, these so-called native SAD experiments are very demanding, as for longer wavelengths the diffraction angles are increasing as is the absorption from the sample, sample mounts and even air. Beamline I23 at Diamond Light Source is currently the only beamline dedicated to long-wavelength MX, operating in a vacuum environment with a semi-cylindrical detector accessing wavelengths of up to 5.9 Å [1].

Long-wavelength X-rays are not only useful for native phasing experiments. With the absorption edges of Ca, K, Cl, S and P becoming accessible, anomalous contrast can be utilised to either assist model building at low resolution or identify these light elements unambiguously. These lighter atoms are for example important for ion gradients responsible for essential membrane transport mechanisms. Anomalous data was recently used to refine the occupancy of potassium cations in the NaK potassium channel [2]. In a similar study we investigated the role of potassium binding in the 70S ribosome structure from anomalous data collected above and below the potassium absorption edge [3].

In my presentation, I will introduce the basic ideas of native phasing and anomalous contrast, discuss the challenges arising when operating at wavelengths beyond 2 Å and show recent highlights from experiments covering a range of wavelengths all the way to the phosphorous edge at 5.78 Å.

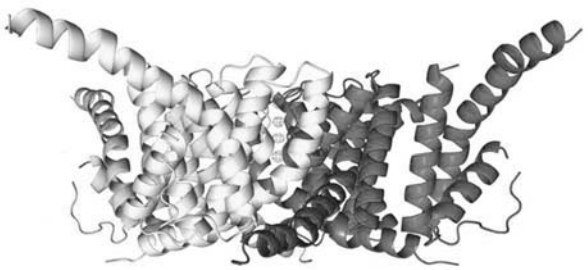

Figure 1. Anomalous difference fourier map (magenta mesh) indicating the four potassium positions in the NaK membrane channel

[1] A. Wagner *et al.*, *Acta Cryst. D***72** (2016) 430.
[2] P. S. Langan *et al.*, *Nat. Commun.* **9** (2018) 4540.
[3] A. Rozov *et al.*, *Nat. Commun.* (2019) *accepted*.

L-04 **Monday, 10.06., 9^{40}-10^{20}**

Molecular solids at high pressure, structural changes and stability

M. Hanfland[1]*

[1]*European Synchrotron Radiation Facility, B.P.220, F-38043 Grenoble Cedex, France*

Keywords: diamond anvil cell, single crystal diffraction, molecular systems synchrotron radiation

*e-mail: hanfland@esrf.fr

Recent technical advances have significantly added to the utility of single crystal X-ray diffraction experiments at high pressures [1]. New ways of supporting diamond anvils, like Boehler Almax anvils [2], have considerably increased the volume of accessible reciprocal space. Use of Helium or Neon as a pressure transmitting medium extends substantially the practicable pressure range. Fast electronic area detectors have noticeably decreased the data collection time and increased the accuracy.

We have studied several molecular systems with single crystal X-ray diffraction. Most data were collected on the new and improved ID15B beamline of the ESRF. It replaces ID09A which was a state of the art high pressure diffraction beamline carrying out monochromatic diffraction experiments with large area detectors.

One system extensively studied is arsenolite (As_4O_6) and its interaction with Helium [3]. At moderate pressure Helium can enter the molecular arsenolite crystal forming an intercalation compound with the stoichiometry As_4O_6 + 2He. Infiltration of the He pressure transmitting medium can be avoided by increasing the pressure rapidly to over 10 GPa permitting us to study the structural properties of arsenolite under quasi hydrostatic conditions to very high compressions (see *Figure 1*). Other systems studied are realgar (As_4S_4) and molecular sulphur (S_8). Intra- and intermolecular structural changes were determined with unprecedented accuracy. In particular no structural transitions or signs of amorphisation were observed in arsenolite and realgar for pressures approaching 40 GPa (V/V0 ~0.5). Above 40 GPa realgar becomes amorphous (see *Figure 2)*, while aresenolite remains crystalline to at least 45 GPa.

In Sulphur a series of symmetry lowering structural phase transitions starts at 16 GPa (see*Figure 3)*. No amorphisation is observed till 38 GPa, were the molecular S_8 phase transforms into the tetragonal spiral chain SII structure [4].

Single crystal diffraction permits an exhaustive characterization of the structural changes under pressure. Molecules in certain molecular solids compressed with a quasihydrostatic pressure transmitting medium as shown here for arsenolite, realgar and molecular sulphur can be surprisingly stable up to exceptionally high compressions.

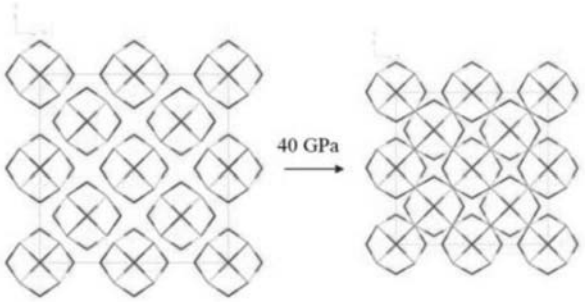

Figure 1. As_4O_6 under pressure

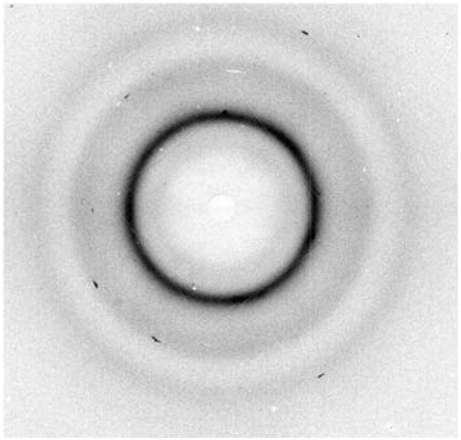

Figure 2. Amorphous realgar at 42 GPa

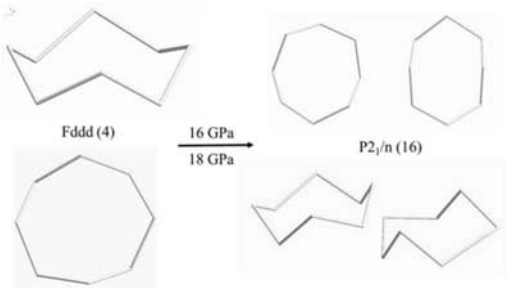

Figure 3. Symmetry lowering phase transition in sulphur (S_8)

Acknowledgements: Work done in collaboration with H. Müller. Arsenolite single crystals from P. A. Gunka.

[1] M. Merlini, M. Hanfland, *High Press. Res.* **33** (2013) 511.
[2] R. Boehler, K. DeHantsetters, *High Press. Res.* **24** (2004) 391.
[3] P. A. Gunka, M. Hapka, M. Hanfland *et al*., *ChemPhysChem* **19** (2018) 857-864.
[4] H. Fujihisa *et al.*, *PRB* **70** (2004) 13410.

L-05 **Monday, 10.06., 10^{20}-11^{00}**

Matter at extremes: Toward new functional materials synthesized at high pressure

D. Paliwoda[1]*

[1]*SOLARIS National Synchrotron Radiation Centre, Jagiellonian University, Czerwone Maki 98, 30-392 Kraków, Poland*

Keywords: high pressure synthesis, diamond anvil cell, single crystal diffraction, multi-anvil press, molecular crystals

*e-mail: damian.paliwoda@uj.edu.pl

Pressure is one of basic thermodynamic parameters, however its effect on chemical reactions, properties of materials and their structure remains relatively poorly understood, mainly due to the lack of experimental data and technical requirements. High pressure experiments could be conducted only in strong vessels with thick walls, capable of withstanding high pressure, but obscuring access to the sample.

The breakthrough in the high-pressure methods was the invention of a diamond anvil cell, DAC - a powerful tool for high pressure synthesis and in situ spectroscopic and structural investigations.

Here I will present a new route toward the synthesis of diamond-like 1D-sp^3-carbon nanostructures derived from benzene inside the 1-dimensional channels of periodic mesoporous silica SBA-15 at pressures above 20 GPa and room temperature. Inside the silica template, the 1D-sp^3-carbon nanostructures are spatially separated from each other preventing their aggregation at the high-pressure conditions. Small Angle and X-Ray Scattering data collected for SBA-15/benzene composite clearly shows that silica mesostructure retains its periodic order upon compression, while X-ray diffraction experiments allow to track pressure-induced structural transformations of benzene.

Acknowledgements: This work was supported by the EFree, an Energy Frontier Research Center of the US Department of Energy Office of Basic Energy Science (SC-0001057).

[1] M. Schwander, K. Partes, *Diamond and Rel. Mater.***20** (2011) 1287-1301.

[2] Y. Yu, L. Wu, J. Zhi, *Angew. Chem. Int. Ed.* **53** (2014) 2-28.

L-06 **Monday, 10.06., 11^{40}-12^{20}**

Superconductivity for light generation

N. Mezentsev[1]*

[1]*Budker Institute of Nuclear Physics, Novosibirsk, Russia*

*e-mail: mezentsev@inp.nsk.su

Superconducting (SC) magnets for light generation were introduced about forty years ago and since then have been extensively used at many synchrotron radiation (SR) facilities around the world. The technology of SC shifters, SC wigglers and SC undulators progressed significantly due to innovative designs and the use of novel materials. SC wigglers (SCW) have been established as reliable tools and are a standard attribute of any SR facility. They became the radiation source of choice for the majority of low- and medium-energy light sources. SCWs greatly increased the capabilities of these sources by extending the accessible radiation wavelength range down to one angstrom. Absolute majority of SCWs have been designed and built at Budker Insitute of Nuclear Physics, Novosibirsk, Russia.

Although the first superconducting undulator (SCU) was built almost at the same time as the first SCW, the progress in the development of SCUs was much slower compared with SCWs. This was mostly due to the fact that major investments went to the development and production of permanent magnet undulators. Recently there is a progress in creation of superconducting undulators in such centers as APS, KARA (ANKA), BINP, ASTeC, LBNL etc.

L-07 **Monday, 10.06., 14^{20}-15^{00}**

Synchrotron SOLARIS – present and future research options

M. Stankiewicz[1]*

[1]*SOLARIS National Synchrotron Radiation Centre, Jagiellonian University, Czerwone Maki 98, 30-392 Kraków, Poland*

*e-mail: m.j.stankiewicz@uj.edu.pl

National Synchrotron Radiation Centre SOLARIS in Kraków is the most modern and largest multidisciplinary research facility in Poland. The Centre was built between 2010 and 2015. The investment was co-financed by the European Union with funds from the European Regional Development Fund, as part of the Innovative Economy Operational Programme for 2007-2013.

As a strategic investment for the development of science, SOLARIS has been included on the Polish Roadmap for Research Infrastructures.

SOLARIS has been built using the ground-breaking design of magnetic double bend achromats developed at MAX-lab facility in Lund, Sweden, resulting in outstanding properties of generated synchrotron light which places SOLARIS firmly at the cutting edge of devices of this type. SOLARIS synchrotron operates at 1.5GeV energy with up to 500mA stored electron beam. It is powered by 600MeV S-band linac.

SOLARIS can provide synchrotron radiation for up to 18 beamlines from bending magnets and insertion devices. Within the scope of the project budget already two state of the art beamlines (PEEM/XAS and UARPES) have been constructed.

In April 2018 SOLARIS opened the first call for the external users for measurements at these beamlines. The talk will focus on the presentation of the current status of the of the center and ongoing and future development of SOLARIS infrastructure.

L-08 **Monday, 10.06., 15^{00}-15^{40}**

High-Resolution single particle Cryo-EM How Poland can take part in the ongoing resolution revolution in structural biology

S. Glatt[1,]*

[1]*Malopolska Centre of Biotechnology (MCB), Jagiellonian University Krakow, Gronostajowa 7a str, 30-387 Krakow, Poland*

Keywords: Cryo-EM, structural biology, macromolecular complexes

*e-mail: sebastian.glatt@uj.edu.pl

My talk will summarize the latest developments in the field of single particle Cryo-EM analyses and show our current progress to establish the “Krajowe Centrum Kriomikroskopii Elektronowej” at the Solaris synchrotron in Krakow. In detail, we are in the process of installing and commissioning a high-end Titan Krios G3i microscope, equipped with a BioQunatum energy filter and two direct electron detectors, namely a K3 and Falcon 3EC. The microscope constitutes the core module of an open-access facility for the whole structural biology community and I will describe our efforts to establish a fair and transparent evaluation system to grant access to the top scientists in Poland and CERIC-ERIC countries.

In addition, I will provide insights into our own research [1,2,3,4,5,6] based on Cryo-EM of macromolecular complexes to illustrate the potential of the technique.

All types of cellular RNAs are post-transcriptionally modified, constituting the so called "epitranscriptome". In particular, tRNAs and their anticodon stem loops represent major modification hotspots. The attachment of small chemical groups at the heart of the ribosomal decoding machinery can directly affect translational rates, reading frame maintenance, co-translational folding dynamics and overall proteome stability. The variety of tRNA modification patterns is driven by the activity of specialized tRNA modifiers and large modification complexes. Notably, the absence or dysfunction of these cellular machines is correlated with several human pathophysiologies, like cancer and neurodegenerative diseases. I will present our latest structural and biochemical analyses comparing the enzymatic core of the highly conserved Elongator complex in eukaryotes, bacteria and archaea. In addition, I will present data on Elongator's unfortunate role in human diseases and our data on the regulatory network surrounding this large macromolecular machine in eukaryotic cells. I aim to focus on our most recent work that has allowed us to understand this large RNA modification complex and its regulatory factors at atomic resolution using Cryo-EM.

Acknowledgements: This work was supported by an EMBO Installation grant, an OPUS10 grant (UMO-2015/19/B/NZ1/00343) from the National Science Centre and two grants (FIRSTTEAM/2016-1/2 and TEAM TECH CORE FACILITY/2017-4/6) from the Foundation for Polish Science

[1] Krutyhołowa R, Zakrzewski K, Glatt S, COSB 2019
[2] Krutyhołowa R *et al., NAR* 2019
[3] Lin TY *et al., Nature Comm* 2019
[4] Kojic M *et al*., *Nature Comm.* 2018
[5] Daudene*t al., EMBO Rep.* 2017
[6] Glatt *et al., Nature Struct Mol Biol*. 2016.

L-09 **Tuesday, 11.06., 9^{00}-9^{40}**

Development of multilayer Laue lenses and their applications

S. Bajt[1]*

[1]*Deutsches Elekronen Synchrotron (DESY), Notkestrasse 85, 22607Hamburg, Germany*

Keywords: multilayer Laue lenses, x-ray optics, multilayers, focusing, imaging

*e-mail: sasa.bajt@desy.de

Recent advances in X-ray sources combined with novel X-ray optics offer new opportunities to focus X-rays to nanometer spots sizes and unprecedented intensities, especially when combined with X-ray free electron lasers. Due to their large penetration depth and short wavelengths hard x-rays are ideal for imaging and studying internal properties, dynamics and structure of complex materials.

High precision X-ray optics is essential to take full advantage of ultra-bright X-ray sources. We will discuss different types of X-rays optics for imaging capable of achieving 10 nm resolution or lower but in particular about multilayer Laue lenses (MLLs).

The focusing behavior and efficiency of MLLs is described by dynamical diffraction theory. The depth-graded structures of these diffraction elements are fabricated by layer deposition. To achieve sub 10 nm resolution a nanometer fabrication precision is required. This demands extreme control of layer thickness, interface roughness and intrinsic stress in these multilayers. Other properties such as thermal stability and nanostructure of the layers play a significant role as well.

The resolution of an MLL is determined by the numerical aperture (NA), which is fixed by the range of angles over which the optics focuses X-rays of a certain wavelength, dependent in turn on the smallest layer thicknesses that can be fabricated. These lenses must be optically thick to achieve significant efficiency in the hard X-ray regime. Obtaining high aspect ratios is not a problem because a MLL is prepared by sputtering a multilayer onto a flat substrate, which is then sliced in a direction perpendicular to the layers to create a block of the desired depth. Because the structures are optically thick the condition of efficient diffraction is given by Bragg's law. So, in each point in the zone plate the layers have to simultaneously satisfy the Fresnel zone-plate formula and Bragg's condition. To achieve this, each layer must be tilted differently, resulting in a MLL where the layers are wedged along the optical path.

We are using different methods to achieve wedged layers including depositing the layer materials within the penumbra of a straight mask [1]. This allows us to fabricate wedged high-numerical aperture (NA) MLLs with high accuracy and control. Initial demonstration with one wedged lens produced a focus of 8 nm in 1D [2]. MLL works similarly as a cylindrical lens or one-dimensional zone plate meaning a MLL focuses X-rays only in one direction. Therefore, to achieve a focused spot two MLLs with slightly different focal lengths are required. Recently we demonstrated 2D focusing of 16 keV X-rays to 6.8 x 8.4 nm^2 [3].

Our MLLs have been successfully used with different types of x-ray sources [4]. Latest results on the development and performance of MLLs will be presented as well the future outlook of this state-of-the-art X-ray optics and their applications.

Figure 1. Multilayer Laue lens focuses light in one direction therefore two orthogonal lenses with slightly different focal lengths are needed to focus X-rays to a common focus

[1] M. Prasciolu *et al.,Opt. Express* **25** (2015) 15195.
[2] A. Morgan *et al.,Sci. Rep.* **5** (2015) 09892.
[3] S. Bajt *et al.,Light Sci. Appl.* **7** (2018) 17162.
[4] K. Murray *et al., Opt. Express* **27** (2019) 7120.

L-10 **Tuesday, 11.06., 9^{40}-10^{20}**

Nanoparticles and their self-assembly in 1D and 2D: SAXS, GISAXS and XRR

A.V. Petukhov[1;2]*

[1]*van 't Hoff laboratory for physical and colloid chemistry, Debye Institute for nanomaterials science, Utrecht University, the Netherlands*
[2]*Laboratory of physical chemistry, Eindhoven University of Technology, the Netherlands*

Keywords: colloids, nanoparticles, confinement

*e-mail: a.v.petukhov@uu.nl

Nanoparticles can self-assemble into various periodic superstructures that can be tuned by varying particle shape and their mutual interactions [1]. The resulting nanomaterials are shown to possess unprecedented electronic, optical and magnetic properties. In this talk, I would like to show some of our recent studies of the nanoparticles at interfaces or in 1D cylindrical confinement. Attention will be paid to information provided by synchrotron techniques, namely small- and ultra-small-angle x-ray scattering (SAXS / USAXS), grazing-incidence small- and wide-angle x-ray scattering (GISAXS/ GIWAXS), as well as x-ray reflectometry (XRR), which are schematically illustrated in Figure 1.

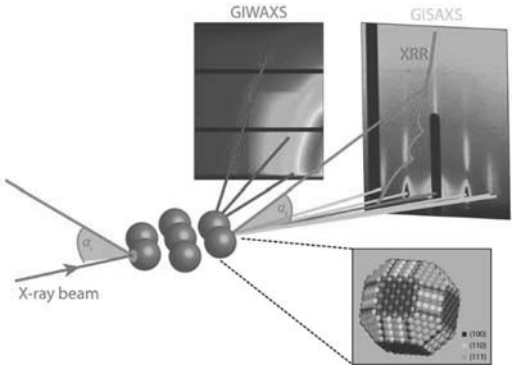

Figure 1. Sketch of the in-situ GISAXS, GIWAXS and XRR experiments. Adapted from Ref. [3]

One of the projects deals with the self-organisation of semiconductor PbSe quantum dots adsorbed at a liquid-air interface. The particles have a shape of truncated cubes (see inset in Figure 1) while the degree of truncation depends on the particle size. In particular, using *in-situ* GISAXS and GIWAXS we were able to follow the formation of a 2D square-like lattice by 5.3 nm nanoparticles [2]. More recently, we extended our study to examine the adsorption geometry of particles of different size ranging from about 5 to 10 nm. To this end, we applied a combination of synchrotron techniques. In particular, GIWAXS reveals the particle orientation at the surface, the in-plane interparticle structure is characterized by GISAXS while XRR gives access to the laterally-averaged density profile across the interface. Three characteristic adsorption geometries varying with the NC size are observed. Based on the experimental evidence and with support of simulation results we identify three-dimensional geometries for PbSe nanocrystals at the ethylene glycol surface and discuss the implications for superlattice formation [3].

Another example is the self-assembly of sugar and surfactant molecules into hollow microtubules. Their hierarchical microstructure spanning more than three orders of magnitude of spatial scales was characterized with high resolution SAXS and USAXS [4,5]. Moreover, we uncover the mechanism of this self-assembly process by time-resolved SAXS & USAXS measurements [6]. The hollow microtubules are used to confine colloids that self-assemble into a library of new 1D assemblies such as chains, zigzags, zippers and chiral chains. These assemblies are subsequently fixed using photo-induced crosslinking between particle surfaces [7].

Finally, I would like to discuss the structure of an unusual interface. Mixtures of colloids and non-adsorbing polymers are able to demix for purely entropic reasons. This phase separation at sufficiently high concentrations is induced by excluded volume entropy without any enthalpic contribution. The interface formed between the two phases sharing the same solvent is intrinsically rough as it cannot be smaller than the size of the colloids and polymer molecules. By applying the XRR technique to this buried interface, we were able to determine the density profile across the interface for different concentrations of the constituents. It is shown that by approaching the critical point, the contrast between the phases reduces and the interface becomes more diffuse [8].

Acknowledgements: The author gratefully acknowledges numerous contributions of many colleagues, students and postdocs from Utrecht University, which cannot be all listed here. In particular, Samia Ouhajji, Jasper Landman,Jaco Geuchies, and Daniel Vanmaekelbegh provided key contributions to this work. In addition, part of the work is performed in collaboration with Mark Vis (Eindhoven University of Technology, the Netherlands) and Linxiang Jiang (Jinan University, Guangzhou, China). Synchrotron experiments are made possible thanks to support and developments by the personnel of the Dutch-Belgian beamline BM-26 DUBBLE and public beamlines ID-10 and ID-2 of the European Synchrotron (ESRF) in Grenoble, France. In particular, I highly appreciate contributions of Oleg Konovalov, Thienchery Narayanan, Anatoly and Irina Snigirevs, and Daniel Hermida-Merino. This work was financially supported by the Netherlands Organization for Scientific Research (NWO). NWO and ESRF are acknowledged for granting beamtime.

[1] A. V. Petukhov *et al.*, *Curr. Opin. Colloid Interface Sci.* **20** (2015) 272.
[2] J. J. Geuchies *et al.*, *Nat. Mater.* **15** (2016) 1248.
[3] J. J. Geuchies *et al.*, *to be published*.
[4] S. Ouhajji *et al.*, *Soft Matter* **13** (2017) 2421.
[5] S. Yang *et al.*, *Nat. Comm.* **8** (2017) 15856.
[6] J. Landman *et al.*, *Sci. Adv.* **4** (2018) eaat1817.
[7] S. Ouhajji *et al.*, *ACS Nano* **12** (2018) 12089.
[8] M. Vis *et al*., *to be published.*

L-11 **Tuesday, 11.06., 10^{20}-11^{00}**

The role and potential benefits of protein structural disorder in viral replication machinery: study and modeling from synchrotron SAXS data

E. V. Shtykova[1]*

[1]*FSRC «Crystallography and Photonics» RAS, Leninskiy Prospekt 59, 119333, Moscow, Russia*

Keywords: synchrotron radiation, small-angle X-ray scattering, proteins, structural disorder, viruses, modelling

*e-mail: viwopisx@yahoo.co.uk

Interrelation between the 3D structure and functional properties of proteins is one of the most important basic concepts in biochemistry. This means that in order to perform a defined function, the protein must have a definite amino acid sequence and be folded in a certain way. This idea, however, was revised about 2 decades ago when a myriad of proteins with partly or entirely disordered structure have been found. These proteins, called intrinsically disordered proteins (IDPs), exist as dynamic ensembles of conformations that do not have a stable folded structure, but nevertheless they carry out their biological functions, often very varied.

The concept of IDPs can be applied to explain the multifunctional character of viral matrix proteins' activity. The ID proteins can contribute to the rapid response of viruses to changing environmental conditions and, consequently, to their survival and evolution. The IDPs actualize the principle of "you cannot break what is already broken", which explains their exceptional ability to sustain exposure to extremely harsh environmental conditions. Moreover, a disorder in protein folding prevents binding of antibodies, therefore diminishing immune response.

The main method used to analyze the structure of the disordered proteins is bioinformatics, but among experimental approaches small-angle X-ray scattering (SAXS) is one of the most productive in structural studies of biological macromolecules with disordered regions, because (in contrast to the X-ray diffraction/ crystallography) this method allows one to study the objects in close to native solutions [1]. However, the applicability of SAXS to study the different viral proteins has long been limited as the analysis approaches were adapted from those developed for monodisperse systems of non-interacting particles. In addition to polydispersity, flexibility and intrinsic disorder of some samples led to difficulties in the SAXS data interpretation. The situation seriously changed when new methods and approaches in SAXS were developed including the ensemble optimization method (EOM) for quantitative analysis of protein flexibility [2] and various hybrid modeling, *e.g.* utilizing normal modes analysis [3].

This motivated us, relying on the data obtained by SAXS, to summarize our recent achievements in structural investigations of matrix proteins from taxonomically different enveloped viruses:(i) the Influenza A matrix protein M1 and (ii) the Newcastle disease virus M protein (M-NDV).

Structural analysis of M1 in solution demonstrates that M1 monomers co-exist with fraction of large clusters possessing a helical architecture similar to that observed in the authentic Influenza virions. Unlike the matrix protein M1, we observe that a measurable portion of the M-NDV protein self-associates into helical oligomers even at acidic pH, where the majority of the protein is dimeric.

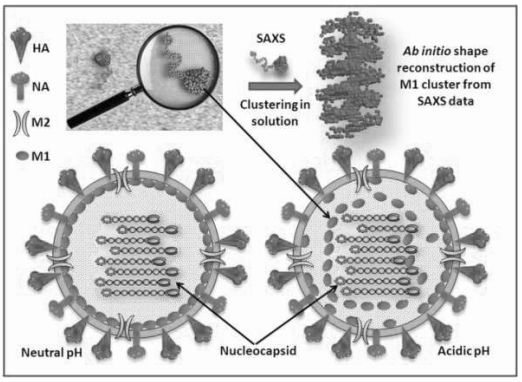

Figure 1. Scheme of the matrix scaffold disintegration for the nucleocapsid release: the case of the influenza A virus

By comparing M-NDV helices with self-assemblies of the M1 protein of influenza A virus, we can say that the latter fill the search volume while the former ones form hollow structures, located mainly along the walls of the hollow cylinder. Such a difference in the scaffold structures can be explained by the difference in the structure of the individual protein macromolecules. The low-resolution structural models of influenza M1 built from the SAXS data reveal that the protein is a structurally anisotropic monomer consisting of compact NM-domains and an extended and partially disordered flexible C-terminal domain, while SAXS data for M-NDV indicates that the protein, is predominantly a compact dimer in solution, in agreement with the crystalline state.

Matrix proteins, due to the presence of intrinsically disordered regions, contact at the same time the membrane and RNPs through these flexible IDPs ("arms"). We show that the arms can serve as a flexible linker between functional domains, which encourages binding and promiscuity, *i.e.* providing both virion stability and budding. However, being flexible and unstructured these regions can serve as a target for the development of antiviral strategy.

Acknowledgements: This work was supported by the Ministry of Science and Higher Education within the State assignment FSRC «Crystallography and Photonics» RAS.

[1] D. I. Svergun, M. H .J .Koch, P. A. Timmins, R. P. May. *International Union of Crystallography monographs on crystallography*, **19**, (Oxford University Press, 2013, 368)
[2] P. Bernado *et al.*, *J. Am. Chem. Soc.* **129** (2007) **5**656.
[3] A .Panjkovich, D. I.Svergun. *Phys. Chem. Chem. Phys.***18** (2016) 5707.

L-12 **Tuesday, 11.06., 11^{40}-12^{20}**

Comparison of bulk and microscale infrared characterisation of stratum corneum – key aspects of hyperspectral data processing

K. Banas[1]*, A. Banas[1], Ngai Mun Hong[2], G. Pastorin[2], S. Gupta[3] and M. H. B. Breese[1]

[1]*Singapore Synchrotron Light Source, National University of Singapore, 5 Research Link, Singapore 117603*
[2]*Department of Pharmacy, National University of Singapore Block S4A, Level 3 18 Science Drive 4, Singapore 117543*
[3]*Procter & Gamble Company 11 North Buona Vista The Metropolis Tower 2, The Metropolis, Singapore 138589*

Keywords: FTIR, ATR, spectral processing, stratum corneum

*e-mail: slskb@nus.edu.sg

Stratum corneum (SC) is the uppermost layer of the skin that protects the body from water loss and invasion of biological and chemical agents [1-2]. About 90% of SC are large, flat cells called corneocytes, but the barrier function is provided mainly by the intercellular lipid matrix that surrounds these cells. Traditional approach to characterize these lipids by Fourier Transform Infra-Red spectroscopy (FTIR) is based on macroscopic experiments by means of Attenuated Total Reflection (ATR) accessories [3-5]. With this study, we propose a novel way of measurement this kind of samples in order to obtain microscopic chemical information and to investigate the heterogeneity of the samples. In this case, special attention must be paid to hyperspectral data pre-processing methods in order to ensure the reliability of the research. Intensities of the selected IR peaks as well as integrals, ratios and peak shifts were evaluated. Discussion of the potential sources for discrepancies between the macroscopic and microscopic FTIR results is provided.

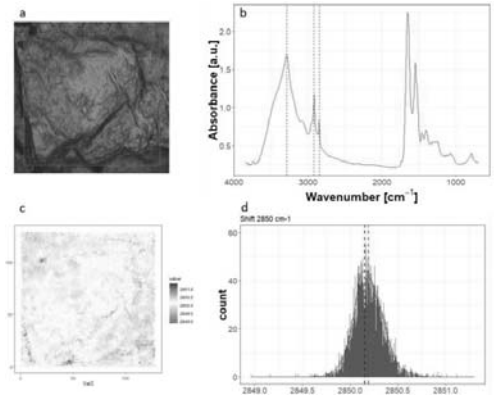

Figure 1. Infrared characterization of stratum corneum: a) visual overview of the region of interest, b) mean spectrum, c) mapped 2850 cm^{-1} band shift d) histogram of the 2850 cm^{-1} band shift

Acknowledgements: Singapore Synchrotron Light Source (SSLS) is a National Research Infrastructure under the National Research Foundation Singapore.

[1] P. Garidel, *Phys. Chem. Chem. Phys.* **4** (22) (2002) 5671–5677.
[2] C. Laugel, N. Yagoubi, A. Baillet, *Chem Phys Lipids*., **135**(1) (2005) 55–68.
[3] M. Boncheva, F. Damien, V. Normand, *Biochim Biophys Acta Biomembr.* **1778**(5) (2008) 1344–1355.
[4] J. Caussin, G. S.Gooris, J. A Bouwstra, *Biochim Biophys Acta Biomembr.* **1778**(6) (2008) 1517–1524.
[5] Y. Obata, S. Utsumi, H. Watanabe, M. Suda, Y. Tokudome, M. Otsuka, K. Takayama, *Int. J. Pharm.* **389** (1–2) (2010) 18–23.

L-13 **Tuesday, 11.06., 12^{20}-13^{00}**

Laser-Driven High-Order Harmonic Generation Sources - Technical Frontiers and Future Directions

P. Johnsson[1]*

[1]*Lund Laser Centre & Department of Physics, Lund University, P.O. Box 118, 221 00 Lund, Sweden*

Keywords: high-order-harmonic generation

*e-mail: per.johnsson@fysik.lth.se

High-order harmonic generation (HHG) sources driven by ultrashort laser pulses have, during the last decades, become indispensable tools for basic research in atomic, molecular and optical physics, with first promising applications also in e.g. liquids and nanosystems. This presentation will give an overview of the current trends in HHG source development, and elaborate on some future directions.

L-14 **Tuesday, 11.06., 14^{20}-15^{00}**

Synchrotron X-ray Diffraction Rocking Curve Imaging of the Defect Structure of GaN Substrates

L. Kirste[1]*, T. N. Tran Thi[2], T. Sochacki[3], M. Zając[3], A. N. Danilewsky[4], M. Boćkowski[3] and J. Baruchel[2]

[1]*Fraunhofer Institute for Applied Solid State Physics, Freiburg, Germany*
[2]*European Synchrotron Radiation Facility, Grenoble, France*
[3]*Institute of High Pressure Physics, Polish Academy of Sciences, Warsaw, Poland*
[4]*Crystallography, Institute for Geo- and Environmental Sciences, Freiburg, Germany*

Keywords: synchrotron X-ray diffraction, rocking curve imaging, gallium nitride

*e-mail: lutz.kirste@iaf.fraunhofer.de

For the realization of demanding GaN-based high frequency or high power electronic devices there is a need for substrates with low defect densities, since e.g. defects such as threading dislocations increase the leakage current, reduce the room temperature mobility and thereby limit the efficiency, performance and lifetime of these devices. Very often, the broadening of an HRXRD 'rocking curve' is used to quantify e.g. dislocation densities of GaN substrates. However, such rocking curves represent convoluted, projected and experimentally distorted images of the actual situation in reciprocal space and should be looked upon with suspicion unless the nature of the crystal defects present is well known. A more detailed picture of the defect structure can be obtained by X-ray topography. But even with this technique, it is often not possible to clearly identify the exact type of defect, since the defect density in GaN substrates with 10^4 cm^{-2} - 10^7 cm^{-2} is often too high and defect contrasts are integrated over the entire crystal volume [1]. A technique, which overcomes this disadvantage is synchrotron X-ray monochromatic rocking curve imaging (RCI). RCI enables the local determination of the effective misorientation, which results from lattice parameter variation and the local lattice tilt, and the local Bragg position. Maps of the integrated intensity, the FWHM and the peak position angle of the diffracted intensity, calculated from the ensemble of rocking curve images, provide quantitative values related to the local distortion of the crystal lattice [2].

In this work, we present a detailed analysis of defect structures of GaN (0001) substrate crystals grown by hydride vapor-phase epitaxy (HVPE) on foreign substrates, the ammonothermal method and HVPE GaN grown on ammonothermal GaN seeds. Beside standard laboratory X-ray diffraction methods, different synchrotron X-ray diffraction techniques were used for this study: Laboratory X-ray topography and synchrotron white-beam X-ray topography in large-area diffraction mode and section transmission mode was employed. Additional, synchrotron X-ray monochromatic rocking curve imaging (RCI) was used in different modes to get an insight into the defect structures of the GaN substrates within the submicron scale.

As an example, Fig.1 shows the FWHM reconstruction of a synchrotron X-ray monochromatic RCI measurement of a 350µm thick HVPE GaN (0001) substrate grown on foreign substrate ($11\bar{2}0$reflection). The spatial resolution for these measurements is 0.75 × 0.75 μm^2. For the investigated region of this wafer the FWHM varies locally from 5 arcsec - 40 arcsec. The lateral sizes of domains / grains are in the 10 - 100 µm range. From the peak position map (not shown here) it can be extracted that the sample is composed by a series of slightly misoriented grains (global misorientation 15-30 arcsec). The observations for this HVPE GaN sample can be interpreted by the formation of a cellular dislocation network. The grouped dislocations tend to be concentrated in and around the cellular walls with central regions tending to have less dislocation density.

With the combination of the results from the different X-ray diffraction techniques, models for the diverse defect structures of the GaN crystals grown by HVPE on foreign seeds, the ammonothermal method and HVPE on ammonothermal GaN are discussed.

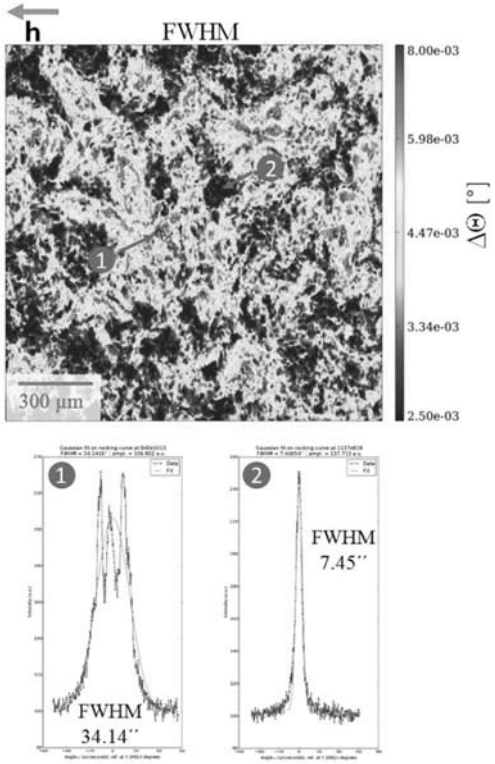

Figure 1. $11\bar{2}0$reflection RCI of a HVPE GaN substrate (upper picture: FWHM map, bottom pictures: examples of individual local rocking curves)

[1] L. Kirste *et al*., *ECS J. Solid State Sci. Technol.* **4** (8) (2015) 324-330.
[2] T. N. Tran Thi *et al.*, *J. Appl. Cryst*., **50** (2017) 561–569.

L-15 **Tuesday, 11.06., 15^{00}-15^{40}**

IR and THz spectroscopy with the FELIX free electron laser: From astrochemistry to condensed matter physics

B. Redlich[1]*, J. t Bakker[1], G. Berden[1], S. Brünken[1], P. Christianen[2], V. Claessen[1], H. Engelkamp[2], A. Kirilyuk[1], J. Martens[1], L. van der Meer[1], B. Murdin[3], J. Oomens[1] and A. Rijs[1]

[1]*FELIX Laboratory, Radboud University, Toernooiveld 7, 6525 ED Nijmegen, The Netherlands*
[2]*High Field Magnet Laboratory (HFML)Toernooiveld 7, 6525 ED Nijmegen, The Netherlands*
[3]*Advanced Technology Institute and SEPNet, University of Surrey, Guildford, GU2 7XH, United Kingdom*

Keywords: free-electron laser, infrared/THz spectroscopy

*e-mail: Britta.Redlich@ru.nl

The international user facility FELIX (Free Electron Lasers for Infrared eXperiments) at the Radboud University in Nijmegen, the Netherlands, offers a unique tuning range in the infrared and THz regime from 3 – 1500 micron (3300 – 6 cm^{-1} or 100 – 0.2 THz) to perform experiments in various areas of science. It comprises four free electron lasers– FLARE, FELIX1, FELIX-2 and FELICE – of which three beam are operated in parallel. The layout of the lasers is shown in figure 1 and more detailed information and specifications can be found here [1]. The facility offers 16 user laboratories to its international user community. Most of them equipped with advanced infrastructure such as (cryogenic) ion traps, molecular beam machines, degenerated and two-color non-linear optics endstations. Unique features such as the free-electron laser for intra-cavity experiments, FELICE, and the connection of the FELIX beam lines to the High Field Magnet Laboratory will be introduced.

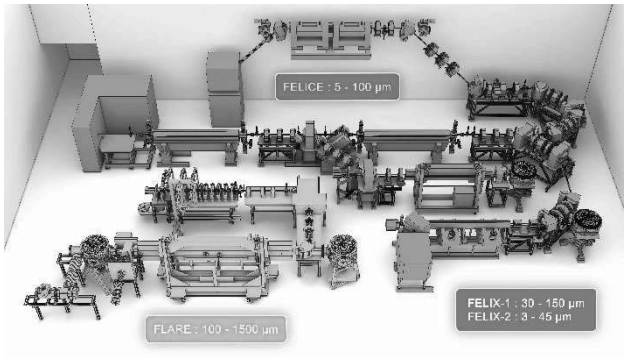

Figure 1. Overview of the layout and frequency ranges of the FELIX free electron lasers

Primary applications of the lasers at the FELIX Laboratory are found in areas benefitting either from the high brightness or the high fluence offered by the free electron lasers. Infrared and THz radiation can act as a spectrometric tool that probes important excitations like vibrations, electronic and magnetic transitions in condensed matter and molecules and thereby reveals information about 3D structures, functional and electronic properties.

Selected experiments from fields including time-resolved measurements in condensed matter systems, action spectroscopy of molecular systems in the gas phase and spectroscopy at 33 T some of which are depicted in figure 2 will be presented.

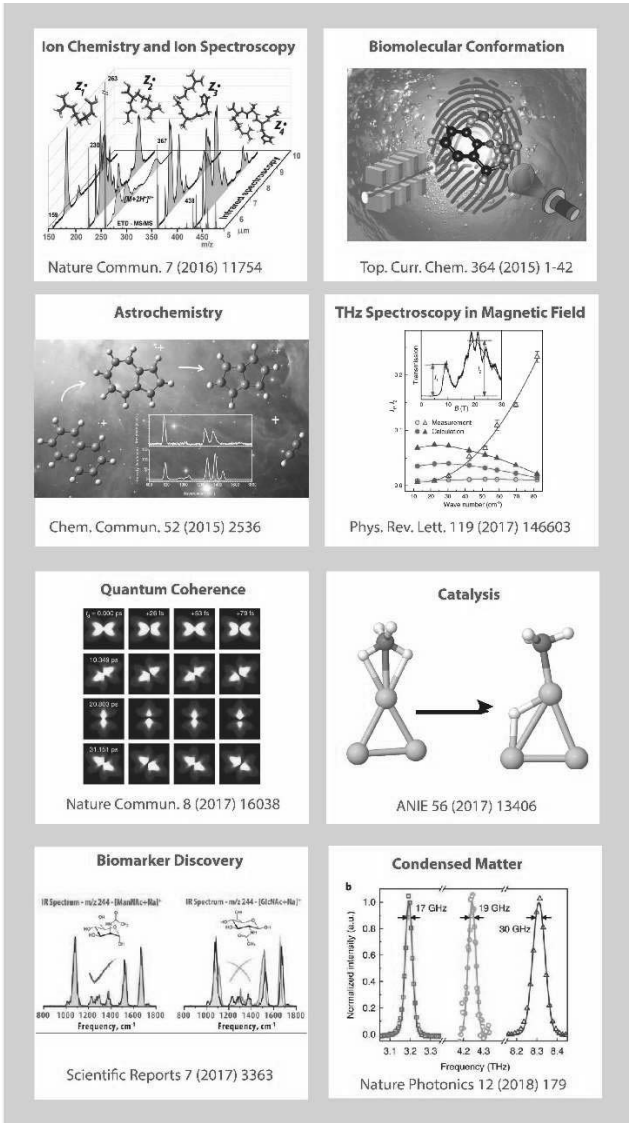

Figure 2. Selected scientific highlights of a broad range of applications of the FELIX laboratory

Acknowledgements:
We gratefully acknowledge the *Radboud University* and *Nederlandse Organisatie voor Wetenschappelijk Onderzoek* (NWO) for the support of the FELIX Laboratory.

[1] https://www.ru.nl/hfml-felix/
[2] https://www.youtube.com/watch?v=Bed2ZUDvKvc

L-16 **Wednesday, 12.06., 9^{00}-9^{40}**

Nanoscale characterisation of chemical speciation in CNT based composites - advantages and pitfalls of photothermal infrared spectroscopy in light of data processing

A. Banas[1]*, K Banas[1], A. Mikhalchan[2], A. Borkowska[3], M. Nowakowski[3], Cz. Paluszkiewicz[3], W. M. Kwiatek[3] and M. B. H. Breese[1]

[1]*Singapore Synchrotron Light Source, National University of Singapore, 117603 Singapore*
[2]*IMDEA Materials, C/Eric Kandel, 2, Tecnogetafe, 28906 Getafe, Madrid, Spain*
[3]*The Henryk Niewodniczanski Institute of Nuclear Physics, Polish Academy of Sciences, 31-342 Krakow, Poland*

Keywords: AFM-IR, Carbon nanotubes, polymers

*e-mail:slsba@nus.edu.sg

Nanostructural composites reinforced with carbon nanotube assemblies, such as CNT fibres and mats [1] are interesting materials for the multiple potential applications: from avionics to high-tech industry. Possibility to gain insight into the chemical composition of such materials may provide a way for their further development and improvement of manufacturing process. By combining infra-red spectroscopy (IR) and atomic force microscopy (AFM) it is possible to perform the chemical mapping with the spatial resolution down to 30 nm. The CNT nanocomposites were analysed by means of nanoIR2 system (Anasys Instruments, USA). Due to specific method of the detection of the infrared signal special attention must be paid during data-processing stage. Obtained results were carefully evaluated with the help of open source software suites: R environment [2], ImageJ [3] and Gwydion [4] in order to ensure interpretability and reproducibility of the collected data. Various modes of measurements were processed, visualised and correlated to gain a better understanding of the system under investigation. Particularly the problem of obtaining topography-free infrared absorbance signal is discussed and some possible solutions are suggested in this contribution.

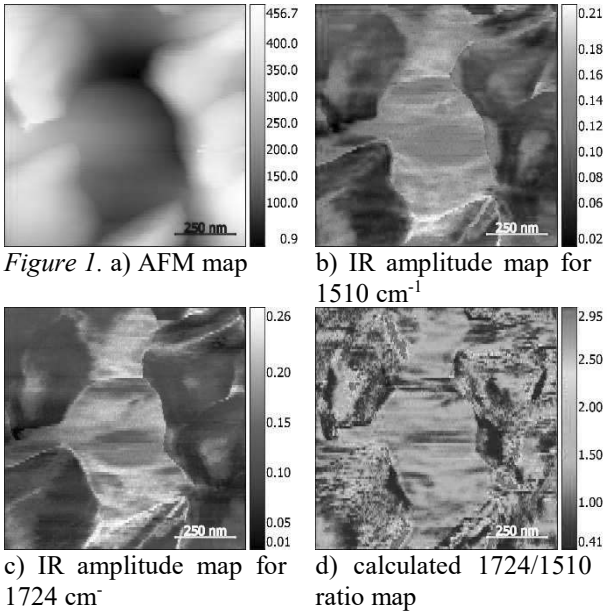

Figure 1. a) AFM map b) IR amplitude map for 1510 cm^{-1} c) IR amplitude map for 1724 cm^{-} d) calculated 1724/1510 ratio map

Fig. 1 illustrates: a) AFM map showing the local topography of the nanocomposite cross-section; b) and c) IR amplitude maps collected for 1510 and 1724 cm^{-1} vibrational bands; d) calculated ratio of the IR amplitudes indicating the polymer distribution.

Acknowledgements: This work was supported by NUS Univesity Strategic Funding for the Centre for Composite Engineering and Research under R-265-000-523-646. The part of the spectroscopy research was performed using equipment purchased in the frame of the project co-funded by the Malopolska Regional Operational Programme Measure 5.1 Krakow Metropolitan Area as an important hub of the European Research Area for 2007−2013, Project MRPO.05.01.00-12-013/15.

[1] Y. L. Li, I. A. Kinloch, A. H. Windle, *Science* **304** (5668) (2004) 276-278.
[2] R Development Core Team (2017). R: A language and environment for statistical computing. R Foundation for Statistical Computing, Vienna, Austria.
[3] C. A. Schneider, W. S. Rasband, K. W. Eliceiri, *Nat. Methods* **9**(7) (2012) 671-675.
[4] D. Necas, P. Klapetek, *Cent. Eur. J. Phys*. **10** (1) (2012) 181-188.

L-17 **Wednesday, 12.06., 9^{40}-10^{20}**

Establishment of XAS, XES and HERFD-XAS for sustainable chemistry applications

M. Bauer[1]*

[1]*Paderborn University, Warburger Str. 100, 33098 Paderborn, Germany*

Keywords: HERFD-XANES, XES, sustainability

*e-mail: matthias.bauer@upb.de

Environmental sustainability is defined as the rate of renewable resource harvest, environmental pollution and non-renewable resource depletion that can be continued indefinitely [1]. Contributing to a sustainable world is one of the important future tasks for the scientific community. As such, synchrotron radiation techniques are high impact tools to understand and further improve chemical reactions related to the field of sustainability. With this contribution, a connection will be established between solar energy conversion and environmental protection and recent developments in the fields of X-ray absorption (XAS) and X-ray emission spectroscopy (XES).

Solar energy can be converted into chemical energy by photocatalytic water or proton reduction. Here, the solar energy is converted into electrons employing a photosensitizer. The electrons are then used to reduce protons with the help of a catalyst. The nature and interaction of the catalyst with the protons is of outmost importance to understand and improve the catalytic systems [2]. Due to the limitations of EXAFS (Extended X-ray absorption fine structure) with respect to the sensitivity to hydrogen, recent photon-in/photon-out techniques in the form of high energy resolution fluorescence detected XAS (HERFD-XAS) and valence-to-core X-ray emission spectroscopy (VtC-XES) offer unique new opportunities.

Figure 1 presents the VtC-XES spectra of a hydride iron complex in comparison to a non-hydride reference. By application of (TD-)DFT calculations, signal C in the upper spectrum can be clearly assigned to donor orbitals dominated by the Fe-H contribution [3]. In this talk, further case studies of chemically relevant complexes and applications of XAS, HERFD-XAS and VtC-XES to in-situ investigations of water reduction reactions are presented together with extended theoretical X-ray spectroscopy. All these results suggest that the methodical combination of XAS, HERFD-XAS and VtC-XES is capable to investigate hydride complexes – or more general, hydride compounds – and their chemical fate under in-situ conditions. An outlook regarding ultrafast X-ray investigations of such reaction types and the application of a newly developed von Hamos spectrometer that enables two-colour experiments will finally close the topic.

While photocatalytic proton reduction relates to renewable resource harvest, X-ray spectroscopy at synchrotrons can also help to reduce environmental pollution, which will be demonstrated with the investigation of new catalysts for carbon monoxide removal from exhaust gases. Typically, such catalysts employ noble metals as active sites. However, in times of increasing noble metal demands, the need for alternative systems – preferably biocompatible and inexpensive – is obvious. Iron is a dream candidate for this purpose, but the nature of active sites in such CO oxidation catalysts is unknown. Nevertheless, on the way to make such catalysts compatible with noble metals, it is mandatory to elucidate the geometric and electronic structure of the active centers.

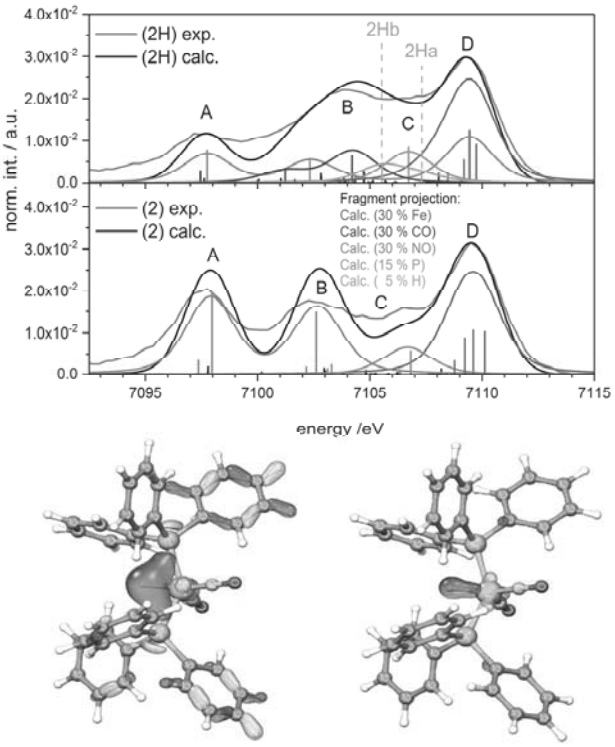

Figure 1. Comparison of experimental (grey) and theoretical (blue) VtC-XES spectra of an iron hydride (top) and the corresponding non-hydride (bottom) complex. The donor orbitals of the Fe-H contribution are shown below

The value of synchrotron techniques, focusing on X-ray absorption spectroscopy, will be demonstrated in the second part of this contribution. Here the combination of different techniques is of outmost important and will be discussed in the talk [4,5].

Acknowledgements: This work was supported by the German ministry for research and education (BMBF, grant No. 05K13UK1, 05K16PP1, 05K14PP1 and 05K18PPA) and the Deutsche Forschungsgemeinschatf (DFG, grant No. BA 4467/5-1 and BA 4467/8-1).

[1] H. Daly, *Beyond Growth* (1996).
[2] S. Fischer, A. Rösel, A. Kammer, L. Burkhardt, R. Schoch, H. Junge, M. Bauer, M. Beller, R. Ludwig, *Chem. Eur. J.* **24** (2018) 16052.
[3] L. Burkhardt, M. Holzwarth, B. Plietker, M. Bauer, *Inorg. Chem.* **56** (2017) 13300.
[4] R. Schoch, M. Bauer, *Chem. Sus. Chem*. **9** (2016) 1996.
[5] R. Schoch, H. Huang, V. Schünemann, M. Bauer, *Chem. Phys. Chem.* **15** (2014) 3768.

L-18 **Wednesday, 12.06., 11^{40}-12^{20}**

Probing the structure and dynamics of soft matter by synchrotron radiation

M. Sztucki[1]* and T. Narayanan[1]

[1]*European Synchrotron Radiation Facility, 71, avenue des Martyrs, CS 40220, 38043 Grenoble Cedex 9, France*

Keywords: synchrotron radiation, (ultra) small-angle X-ray scattering, micro-/nano-diffraction, soft matter

*e-mail: sztucki@esrf.eu

Small- and Wide-Angle X-ray Scattering (SAXS/WAXS) are well-established, non-invasive techniques for elucidating the microstructure from sub-nanometer to micron scales [1]. Typical systems investigated span over a wide range of soft matter such as polymers, liquid crystals, colloids, surfactants, etc. and their mixtures, and related (noncrystalline) biological systems such as proteins, nucleic acids, membranes, tissues, bones, etc. Modern synchrotron SAXS/WAXS instruments cover more than four orders of magnitude in length scales, corresponding to real-space dimension from the μm down to the Angstroms facilitating the investigation of hierarchical structures. Furthermore, the high photon flux and collimation provide high angular resolution and allow time-resolved experiments down to millisecond range, even with dilute samples. The scattering techniques can be combined with various sample environments (e.g., in-situ rheology, stopped-flow mixing, varying temperature, humidity or pressure) for in-situ experiments to follow real-time structural dynamics, crystallization/dissolution kinetics, or out-of-equilibrium dynamics. Sub-micron beams can also provide high real-space spatial resolution.

This presentation is aimed to give an overview of different possibilities offered by synchrotron scattering techniques illustrated by recent examples [1] and also of industrial relevance as many consumer products are based on soft matter technology where their macroscopic properties often depend on micro- and nano-structures extending over multiple size scales.

The performance of the scattering techniques has been considerably enhanced in the past years by developments of new instrumentation, advanced online data reduction and data analysis softwares. This will be illustrated in particular by the possibilities offered by the upgraded ID02 beamline at the ESRF [2]. This instrument combines Small Angle X-ray Scattering (SAXS), Ultra Small-Angle X-ray Scattering (USAXS) and Wide-Angle X-ray Scattering (WAXS) in a unique instrument, covering a wide scattering vector(q) range of 10^{-3} nm^{-1} ≤ q ≤ 50 nm^{-1} using 1 Å X-ray wavelength. The high angular resolution is achieved by a combination of high degree of collimation, long sample-to-detector distance (~31 m) and high-resolution detector. In addition, for anappropriate system, the equilibrium dynamics over these time and length scales may be probed by exploiting the coherence properties of the X-ray beam.

The ID13 beamline for scanning micro-/nano-beam SAXS/WAXS and single micro-crystal/fibre diffraction (μXRD) allows probing the local nanostructure of very small objects like micromechanical parts, polymer fibres, micro-fluidics, and biological specimens with an X-ray beam of 200 nm size.

Finally, new possibilities offered by the ESRF EBS (Extremely Brilliant Source) Upgrade program in 2019/2020will further enhance the performance of the beamlines and allow even more challenging experiments. In particular, the transverse coherence of the X-ray beam will be significantly increased by a factor 30 or so. Therefore, the coherent scattering experiments will take a major leap forward after the upgrade.

Acknowledgements: The ESRF is acknowledged for financial support and synchrotron beam time. Contributions of many colleagues at ESRF are gratefully acknowledged.

[1] T. Narayanan, H. Wacklin, O. Konovalov, R. Lund, *Crystallogr. Rev.* **2** (2017) 160.

[2] T. Narayanan, M. Sztucki, P. Van Vaerenbergh, J. Leonardon, J. Gorini, L. Claustre, F. Sever, J. Morse, P. Boesecke, *J. Appl. Cryst.* **51** (2018) 1511.

L-19 **Wednesday, 12.06., 11^{40}-12^{20}**

Anomalous x-ray scattering and DAFS spectroscopy of nanoparticles in metallic single crystals

V. Holý[1;2]*, J. Šmilauerová[3], E. Piskorska-Hommel[4]

[1]*Department of Condensed Matter Physics, Charles University, Ke Karlovu 5, 121 16 Prague, Czech Republic*
[2]*CEITEC at Masaryk University, Kotlářská 2, 611 37 Brno, Czech Republic*
[3]*Departmet of Material Physics, Charles University, Ke Karlovu 5, 121 16 Prague, Czech Republic*
[4]*Institue of Low Temperature and Structural Research, ul. Okólna 2, 50-422 Wrocław, Poland*

Keywords: anomalous x-ray diffraction, Ti alloys, diffuse scattering

*e-mail: holy@mag.mff.cuni.cz

Ti-based alloys like Ti(Mo) are technologically important materials used in aerospace, automotive industries, and medicine, due to their excellent mechanical properties [1]. During the martensitic transformation of the cubic β-Ti(Mo) to hexagonal ω phase, nanoparticles of the ω phase grow with the final size of a few nm, and the impurity atoms (Mo in our case) are expelled from the volumes of the growing ω particles. Consequently, the Mo atoms create Mo-rich clouds around the nanoparticles [2]; the aim of the presented work is to investigate these clouds by anomalous x-ray diffraction method (AXRD).

Anomalous effects in x-ray diffraction are caused by a steep energy dependence of the real and imaginary parts of the form factor of a chosen element in the vicinity of its absorption edge (usually K edge). This effect has been used for determination of elastic strain and chemical composition in various types of nanostructures, see Refs. [3,4], among others. We have measured x-ray diffuse scattering from single crystals of Ti(Mo 8%at) of cubic β phase after several annealing steps; the samples contain ω-Ti nanoparticles of various sizes. We used $(006)_\beta$ diffraction and measured the dependence of the diffusely scattered intensity on the photon energy around the MoK absorption edge at $E_K = 20.0$ keV. The measurements have been performed at beamline BM02, ESRF Grenoble.

Figure 1(a) shows the distribution of the diffusely scattered intensity in the plane of the two-dimensional detector taken at 19.9. keV, Fig. 1(b) displays the energy dependences of the intensities integrated from various regions of interest (ROIs) denoted by rectangles in panel (a). Interestingly, the energy dependences from various ROIs have completely different shapes; the curves from the ROIs with negative coordinates q_2 (i.e. smaller scattering angle) exhibit sharp maxima just below E_K, those with positive q_2 are rather rounded below E_K. We have performed extensive numerical simulations of the AXRD intensity taking into account anisotropic elastic deformation around the nanoparticles and from the comparison with the experimental data we were able to determine the size of the Mo-rich cloud and the Mo concentration profile.

The AXRD curves above E_K show tiny oscillations, caused by the DAFS effect (Diffraction anomalous fine structure) [5]. We have analyzed these oscillations and determined the Mo-Ti distances (i.e. the radius of the first coordination sphere around Mo) both in the cubic β phase and in the hexagonal ω nanoparticles.

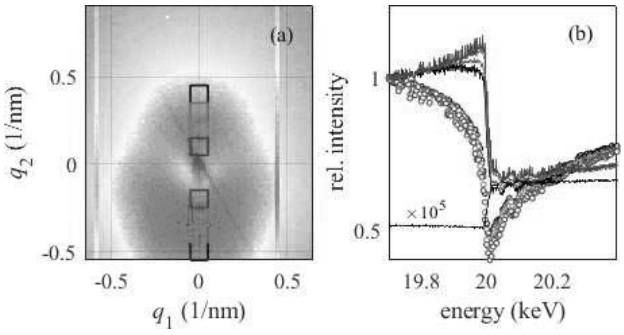

Figure 1 (a) Reciprocal-space distribution of diffuse scattering around the $(006)_\beta$ diffraction maximum in a β-Ti(Mo) single crystals with ω-Ti nanoparticles, photon energy 19.95 keV. The colors span over four decades; the axes q_1 and q_2 lie in the plane of a two-dimensional detector across and along the 2Θ direction, respectively. The rectangles denote the regions of interest (ROIs) from which the energy dependences were extracted. (b) The energy dependences of the intensities taken from various ROIs in panel (a), the colors correspond to the colors of the rectangles in (a). The full lines (open symbols) refer to the ROIs with negative (positive) q_2. The black line displays the energy dependence of the fluorescence. Both the fluorescence and the ROI signals exhibit rapid oscillations above the absorption edge; in the former case these oscillations are the pure EXAFS effect, while the ROI oscillations are due to the DAFS

Acknowledgements: This work was supported by the Czech Science Foundation (projects 16-12598S and 19-10799J), and by the project NanoCent financed by European Regional Development Fund (ERDF, project No. CZ.02.1.01/0.0/0.0/15.003/0000485). The assistance of H. Renevier (LMGP, Grenoble) is gratefully acknowledged.

[1]G. Lütjering, J. C. Williams, *Titanium*, Springer Verlag (2007).
[2] J. Šmilauerová *et al.*, *Acta Mater*. **100** (2015) 126.
[3] T. U. Schulli*et al.*, *Phys. Rev. Lett.* **90** (2003) 066105.
[4] D. M. Tobbens, S. Schorr, *Semicond. Sci. Technol.* **32** (2017) 103002.
[5] C. Lamberti, *Surf. Sci. Reports* **53** (2004) 1.

L-20 **Wednesday, 12.06., 12^{20}-13^{00}**

Influence of metal oxides surface stoichiometry on their physical and chemical properties – XAS and XPS studies

K. Lawniczak-Jablonska[1]*

[1]*Institute of Physics, Polish Academy of Sciences, Al. Lotnikow 32/46, 02-668 Warsaw, Poland*

Keywords: metal oxides, amorphous films, XAS, XPS

*e-mail: jablo@ifpan.edu.pl

Metal oxides are important materials in the modern nanotechnology e.g. [1]. They are used as dielectrics, protective coatings, a substrate for growing variety of structures and much more. Properties essential from point of view technologists depend on the morphology, structure and elemental composition of the oxide surface [2]. The overview of metal oxides studies performed applying x-ray photoelectron (XPS) and x-ray absorption (XAS) spectroscopy will be presented. Particular attention will be given to Ta_2O_5 and Al_2O_3 crystalline and amorphous oxides.

The crystalline compounds were studied as reference materials to estimate their stoichiometry and atomic order around metal atoms. Surprisingly, the detected composition and atomic order differ from that resulting from the crystal structure and chemical formula. The role of oxygen defects will be discussed as well differences observed between results from XAS (bulk) and XPS (surface) spectroscopy.

The main concern will be given to thin films of amorphous oxides. The example of thin films of amorphous tantalum oxide and sapphire will be presented. The a-TaO_x is known to exhibit an extremely large extent of oxygen nonstoichiometry, x. It has been widely exploited for highly integrated semiconductor devices as a high dielectric constant material because of its superior dielectric properties with high resistivity and the outstanding tolerance to the high voltage breakdown and high chemical resistance.

In contrast to crystalline insulating oxides, in which defect chemistry helps to understand the properties, polymerization reaction of MeO_x moiety has been employed to explain the large extent of oxygen nonstoichiometry observed in amorphousoxide [3]. In the case of a-TaO_x, there is still controversy about its MeO_x polyhedral distribution (TaO_7, TaO_6, and TaO5).

Presented EXAFS study aims to understand the structural variation of a-TaO_x and propose the model of polymerization of MeO_x.

Amorphous oxide films were grown on the crystalline or glass substrates with different thickness by atomic layer deposition. It was found that the stoichiometry of film depends on the type of substrate and thickness. Moreover, atoms bonding in amorphous films differ from crystalline materials (Fig. 1). The films are nonstoichiometric having over- or under-stoichiometric compositions. This fact strongly influences the properties of films such as chemical resistance or up-taking of elements during subsequent grown process what results with difference in formed nanostructures on such substrates.

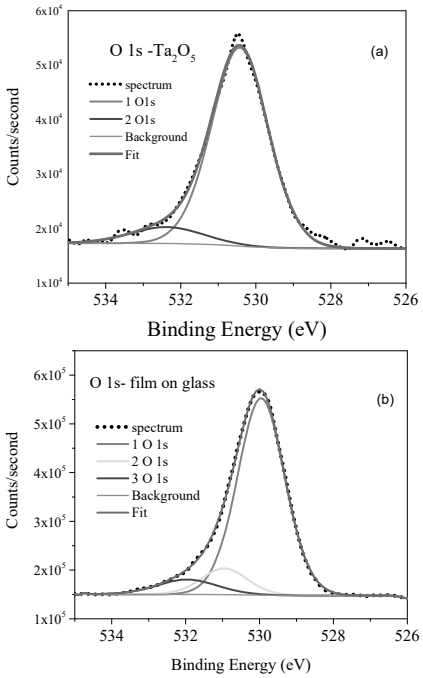

Figure 1. In crystalline Ta_2O_5 oxygen is bonded in two chemical states (a), in amorphous layer in three (b)

The presented studies demonstrate the example of necessity of detailed knowledge of surface composition, atomic structure and chemical bonding in know-how of modern nanotechnology.

Acknowledgements: Presented study have been performed in cooperation with A. Wolska, P. Kuzmiuk, Z. Zytkiewicz, M. Sobanska (IF PAN) and K. Kosiel (ITE), and results are the subject of separate publications.

[1] K. Kosiel *et al.*, *Nanotechnology* **29** (13) (2018) 135602.
[2] K. Kosiel *et al.*, *J. Vac. Sci. Technol. A* **36** (3) (2018) 031505.
[3] T. Tsuchiya *et al.*, *Phys. Chem. Chem. Phys*. **13** (2011) 17013.

L-21 **Thursday, 13.06., 9^{00}-9^{40}**

Combining femtosecond hard X-ray scattering and spectroscopy to study photochemical dynamics in solution: instrumentation and recent results

D. Khakhulin[1*], F. Alves Lima[1], M. Biednov[1], A. Galler[1], W. Gawelda[1;2], K. Kubicek[1], P. Zalden[1] and C. Bressler[1]

[1]*European XFEL, 22869, Schenefeld, Germany*
[2]*Adam Mickiewicz University, 61-614, Poznań, Poland*

Keywords: free-electron laser, X-ray scattering, X-ray spectroscopy, chemical dynamics

*e-mail: dmitry.khakhulin@xfel.eu

Recent development of optical pump/X-ray probe techniques at large scale facilities such as synchrotrons and X-ray free-electron laser (XFEL) sources enabled direct visualization of various fundamental ultrafast phenomena in solution photochemistry. Due to intrinsically much shorter pulses, the temporal resolution of such experiments at XFELs is over three orders of magnitude higher compared to that at conventional synchrotron sources, reaching the sub-100 fs domain – the fundamental timescale of elementary steps in photochemical dynamics.

In particular, understanding photochemistry of transition metal complexes is currently of high interest since they often are the major players in many fundamental photochemical processes that define e.g. biochemical reactivity and photovoltaic/photocatalytic functionality. In these reactions photoexcitation typically triggers ultrafast charge and spin changes of the metal center which intrinsically drives dramatic rearrangements in the structure of the molecule and its solvation shell.

Taking advantage of combining structurally and electronically sensitive probes, namely time-resolved X-ray scattering/diffraction [1], X-ray emission [2] and absorption [3] spectroscopies in one experiment [4,5], it has become possible to accurately monitor intrinsically coupled ultrafast electronic and structural transformations during e.g. ultrafast spin transitions and ligand exchange reactions in solvated iron complexes. A few examples of such studies performed at synchrotrons and XFEL sources are presented in this contribution.

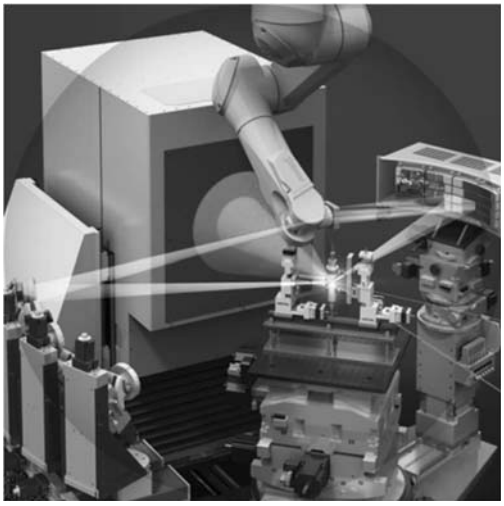

Figure 1. Schematic representation of the combined time-resolved X-ray methodologies at the FXE instrument

The methodology of combining simultaneous structural and electronic observables is applied for experiments at the Femtosecond X-ray Experiments (FXE) instrument of the European XFEL, which came online only about 1.5 years ago. The new European XFEL source is capable of MHz pulse repetition rate thus providing a 100-fold increase in average flux over other XFELs and can deliver high X-ray photon energies up to 20-25 keV. We report on the progress of the FXE instrument commissioning over the past year, describe current capabilities of the setup as well as the first experimental results.

[1] H. Ihee *et al.*, *Science* **309** (2005) 5738.
[2] G. Vankó *et al.*, *Angew. Chem.* **122** (2010) 6046.
[3] Ch. Bressler *et al.*, *Science* **323** (2009) 489.
[4] Ch. Bressler *et al.*, *Faraday Discuss.* **171** (2014) 169.
[5] S.E. Canton *et al.*, *Nat. Comm.* **6** (2015) 6359.

L-22 **Thursday, 13.06., 9^{40}-10^{20}**

A low energy X-ray spectroscopy beamline for SOLARIS

J. Hormes[1;2*], W. Klysubun[3], H. Lichtenberg[4], J. Göttert[4] and A. Prange[4]

[1]*Institute of Physics, Bonn University, Nussallee 12; D-53115 Bonn, Germany*
[2]*Center for Advanced Microstructures and Devices (CAMD), Louisiana State University, 6980 Jefferson Hwy.; Baton Rouge, LA 70806, USA*
[3]*Synchrotron Light Research Institute (SLRI) Synchrotron Light Research Institute, 111 University Avenue, Suranaree Sub-district, Muang, Nakhon Ratchasima 30000, Thailand*
[4]*Hochschule Niederrhein, University of Applied Science, Reinarzstraße 49, D-47805 Krefeld, Germany*

Keywords: X-ray spectroscopy, synchrotron radiation

*e-mail: Hormes@LSU.edu

SOLARIS is the new Polish 3rd generation synchrotron radiation facility in Cracow operated under the auspices of the Jagiellonian University. With an electron energy of 1.5 GeV SOLARIS is a low energy storage ring and with a characteristic energy Ec ~ 2 keV of the synchrotron radiation from the bending magnets (radius 3.81 m) SOLARIS is specifically suitable for low energy X-ray spectroscopy experiments. As a rule of thumb, experiments are possible up to at least ~ 5x Ec i.e. ~ 10 keV so that the K-edge of elements up to Z=31 (Ga) and the L-III edges of Z=74 (W) (plus of course the M-III and M-V edges of many elements) can be reached.

The Hochschule Niederrhein University of Applied Science is in the process of building at SOLARIS a beamline for X-ray absorption (XAS) and X-ray fluorescence (XRF) experiments that will cover the energy range from ~ 1 keV up to ~ 12 keV with an energy resolution ΔE/ E ~ 10-4. In phase 1 this beamline will be "simple" high flux beamline without any additional optical elements (mirrors, lenses, etc.). The front-end of the beamline will be built commercially according to SOLARIS standards by FMB (Berlin). The other components of the beamline (with the exception of the X-ray monochromator) will be developed and built in a collaboration between SOLARIS (Poland), Hochschule Niederrhein (Germany) and Synchrotron Light Research Institute (Thailand). The basic set-up of the beamline will be very similar to beamline BL8 of SLRI [1]

The central part of the beamline is a vacuum double crystal monochromator that will be built at the Institute of Physics of Bonn University. This monochromator is a modified Lemmonier design covering the Bragg angle range between ~150 and ~650 with a fixed monochromatized exit beam [2]. Though this monochromator is "just" an HV system (basis pressure ~ 5 x 10-6 Torr) the beamline will have no windows between the storage ring and the monochromator allowing measurements down to the Na-K-edge. The UHV required in the front end of the beamline will be ensured by a special "differential ion pump" that can uphold up to 4 orders of magnitude of pressure difference [3]. For covering the full energy range targeted (at least) 4 sets of crystals will be used: Beryl ($10\bar{1}0$), multilayer/ADP-combination, InSb (111) and Ge(220). Time for changing crystals and restarting experiments is less than 1 hour. Measuring techniques that will be available are: transmission mode with 3 "standard" ionization chambers, fluorescence mode using a multi-element Si-drift detector and electron yield mode for surface sensitive experiments.

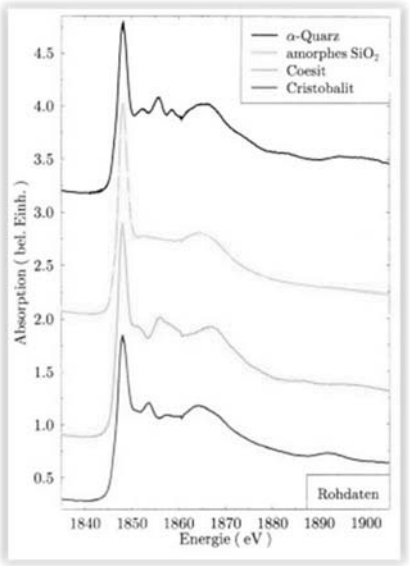

Figure 1. Si-K-XANES spectra

Figure 1 shows as a typical example for the performance of the planned beamline the Si-K-XANES spectra of various SiO_2 modifications measured with InSb (111) crystals and the same monochromator that will be used at SOLARIS.

[1] W. Klysubun, P. Sombunchoo, W. Deenan, C. Kongmark, *J. Synchrotron Rad.* **19** (2012) 930–936.
[2] M. Lemmonier, O. Collet,C. Depautex, J. M. Esteva, C. Raoux, *Nucí. Instrum. Methods* **152** (1978) 109.
[3] https://www.xia.com/Datasheets/DP3_flyer_150408.pdf.

L-23 **Thursday, 13.06., 10^{20}-11^{00}**

Synchronization between the petawatt-class optical laser and XFEL (SACLA)

H. Tomizawa[1;2]*

[1]*Japan Synchrotron Radiation Research Institute, Kouto 1-1-1, Sayo, Hyogo 679 – 5198, Japan*
[2]*RIKEN, SPring-8 Center, Kouto 1-1-1, Sayo, Hyogo 679 – 5148, Japan*

Keywords: petawatt-class laser, synchrotron radiation, x-ray free-electron laser, femtosecond synchronization

*e-mail: hiro@spring8.or.jp

SACLA [1] X-ray Free Electron Laser(XFEL) has been constructed and operated next to the largest 3rd-generationsynchrotron radiation source at SPring-8. XFELs have had a significant impact in broad scientific areas because of their unique properties: high brilliance, short pulse-duration, and high spatial coherence. There is the synergy experimental facility at the meeting point of both SACLA and SPring-8 (see Figure 1). We are planning synergy experiments utilizing both x-ray sources at this unique facility.

Besides, the third "extreme" light source was constructed in this facility: petawatt-class optical laser systems synchronized to XFEL. These light sources are a complementary trinity to discover the dynamical nature of a variety of materials under different conditions. Experimental research using high power optical lasers combined with XFELs open new frontiers in high energy density (HED) sciences. The capabilities of pump/probe methods are dramatically improved due to the brightness of the XFEL pulses with an ultrafast duration (<10 fs).

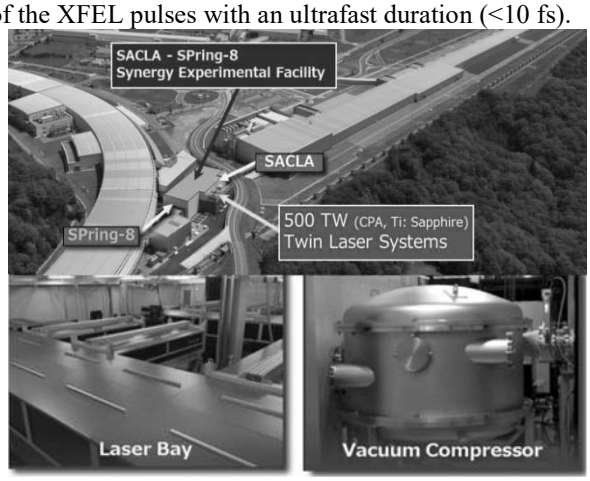

Figure 1. The synergy experimental facility with petawatt-class laser systems (500 TW x2)

Currently, an experimental platform for HED sciences with a twin 500 TW Ti:Sapphire laser system was completed for experiments synchronized with the XFEL at research objectives. Thanks to alternative seeding from one of the common frontends, two optical laser pulses are delivered simultaneously with the maximum power of 500 TW in each into a target chamber located in an experimental hutch 6 (EH6) at SACLA's 2nd hard x-ray beamline (BL2).

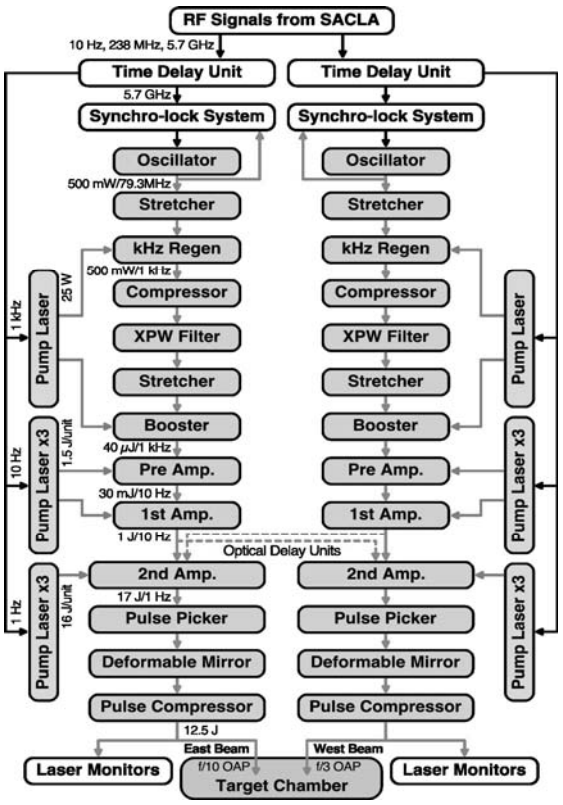

Figure 2. The petawatt-class twin optical laser system synchronized to XFEL (SACLA)

One of the most important key technologies for pump/probe methods is high-resolution timing delay units between the petawatt-class laser and XFEL pulses (see Figure 2). The laser timing system consists of a timing clock and re-clocked trigger delay systems. The laser oscillator is synchro-locked directly to the SACLA accelerator basic RF (C-band: 5712 MHz) with BOM-PD (MenloSystems GmbH). The fluctuations of arrival timing between the petawatt-class laser and XFEL pulses have been investigated using a GaAs-based femtosecond-resolution timing monitor at an interaction point in BL2. The timing fluctuation in 3 min (i.e. 1800 events), namely the jitter, is ∼ 20 fs r.m.s., which is shorter than the pulse duration of the petawatt-class laser [2].

The optimizations of laser pulse characteristics are strongly required for user experiments. Hitherto, laboratory lasers have been tuned and aligned for each requirement manually by laser experts. Automatic laser tuning requires sophisticated algorithms; a hill-climbing method extended with a fuzzy set theory to align the laser path automatically [3]. We are installing Advanced Tactical Aligner (ATA) [4] based on a metaheuristic algorithm in the frontends of this petawatt laser system.

The status and future perspective of the developments of this facility will be reported in the presentation. The synergy user experiments utilizing extreme light sources will be openly discussed.

[1] T. Ishikawa *et al*., *Nat. Photonics*. **6** (2012) 540.
[2] T. Yabuuchi, *et al., J. Synchrotron Rad.* **26** (2019) 585.
[3] H. Tomizawa, *Rad. Phys. Chem*. **80** (2011) 1145.
[4] H. Tomizawa and T. Kojima, Application Date: March 3 2010; Japanese Patent No.554583

L-24 **Thursday, 13.06., 11^{40}-12^{20}**

The laser plasma wakefield accelerator as versatile radiation sources for applications

D. A. Jaroszynski[1]*, M. P. Anania[1;2], C. Aniculaesei[1;3], G. Battaglia[1], E. Brunetti[1], S. Chen[1], S. Cipiccia[1;4], B. Ersfeld[1], D. Reboredo Gil[1], D. W. Grant[1], P. Grant[1], G. K. Holt[1], M. S. Hur[5], L. I. Inigo Gamiz[1], T. Kang[5], K. Kokurewicz[1], A. Kornaszewski[1], W. Li[1], A. Maitrallain[1], G. G. Manahan[1], R. McArthur[1], A. Noble[1], L. R. Reid[1], M. Shahzad[1], K. Sivanathan[1], R. Spesyvtsev[1], A. Subiel[1;6], M. P. Tooley[1], G. Vieux[1], S. M. Wiggins[1], G. H. Welsh[1], S. R. Yoffe[1] and X. Yang[1,7]

[1]University of Strathclyde, Glasgow G4 0NG, Scotland, UK, [2]INFN, Frascati, Italy, [3]Center for Relativistic Laser Science, IBS, Gwangju 61005, Rep. of Korea. [4]Diamond Light Source, Oxfordshire OX11 0DE, [5]School of Natural Science, UNIST, Ulsan, 689-798, Rep. of Korea, [6]National Physical Laboratory, Teddington, Middlesex, TW11 0LW, UK, [7]Capital Normal University, and Beijing Advanced Innovation Center for Imaging Technology, Beijing, China

Keywords: laser-plasma interactions, betatron radiation, undulator radiation, femtosecond and attosecond pulses, synchrotron radiation, free-electron laser, ion channel laser,

*e-mail: d.a.jaroszynski@strath.ac.uk

Plasma waves excited by intense, ultra-short laser pulses have been shown to produce not only high energy particle beams, but also high brightness incoherent electromagnetic radiation. We show that diverse radiation sources with unique properties can be developed using the laser wakefield accelerator (LWFA) [1]. High quality, sub percent energy spreadsbeams have been measured for 100-300 MeV energies [2-4], and there is good evidence that this can be extended to GeV by controlling injection.

A unique property of the LWFA is that it produces ultra-short duration electron bunches. Durations as short as 1 fs have been measured [5], which is orders of magnitude shorter than possible from conventional accelerators. Furthermore, by controlling self-injection using a plasma density gradient applied over a short length, the bunch duration can be further reduced to attoseconds, for 10s to 100s pC bunches [6], which allows the bunch charge to be adjusted. These ultra-short bunches are potential sources of pulsed XUV and X-ray radiation, which could be useful as time-resolved tools for applications requiring ultra-short probes [7].The high energy (100s MeV – GeV) self-injected LWFA beams are also bright intrinsic sources of XUV, X-ray and MeV gamma-ray photons with high transverse coherence, which makes them useful for phase contrast imaging [10].

An unexpected source of high charge, but low energy electron bunches, arises from the non-injected plasma electrons in the LWFA, which are emitted at oblique angles. These high charge (10s – 100s nC), relatively low energy (1-10 MeV) beams have durations of 100s fs to ps [8], which makes them potentially useful for pulsed radiolysis, single shot imaging of macroscopic objects, and as sources of THz radiation [8,9].

We present experiments that demonstrate visible [11] to XUV (currently 60 – 120 nm) undulator radiation with pulse durations as short as 20 fs [12]. Ultra-short duration pulses are possible because the LWFA bunches have durations of the order of a femtosecond [5], energy spreads less than 1 % [2, 3] and emittances of the order of 1 π mm mrad [13]. We show that by extending the electron beam energy to 1 GeV, 1-2 fs duration XUV pulses with peak powers of several MW per pC can be produced. We also show that the beam quality [2-4, 14] is sufficiently high to potentially realise a compact free-electron laser (FEL) [7, 14, 15]. Furthermore, the charge can be increased by controlling injection [6]. By increasing the energy to GeV levels [10], a compact, narrow-bandwidth synchrotron source [11, 12] with peak powers in excess of 1 GW may be possible, without the need to build an FEL. This would make LWFA driven synchrotrons very useful sources of ultra-short duration XUV pulses. Furthermore, by reducing the bunch length to attosecond durations, LWFA based radiation sources may become next generation tools for scientists [5, 6].

The undulator can be replaced by an ion channel, further reducing the size of incoherent [10] and coherent [16] X-ray sources. With the expected advances in laser stability and increases in laser repetition rates, these ultra-short pulse radiation sources would become affordable and therefore widely used, which may change the way science is done [17, 18].

Acknowledgements: We acknowledge support of the U.K. EPSRC (grants no. EP/J018171/1, EP/J500094/1 and EP/N028694/1), LASERLAB-EUROPE (grant no. 654148), EuPRAXIA (grant no. 653782), and the Extreme Light Infrastructure (ELI) Project.

[1] S. P. D. Mangles *et al.*, *Nature* **431** (2004) 535.
[2] S. M. Wiggins *et al.*, *Plasma Phys. Control. Fusion* **52** (2010).
[3] S. M. Wiggins *et al.*, Conference on Lasers and Electro-Optics (CLEO) and Quantum Electronics and Laser Science Conference (QELS) (2010).
[4] G. H. Welsh *et al.*, *J. of Plasma Physics* **78** (2012) 399.
[5] M. R. Islam *et al.*, *New J. Phys.* **17** (2015).
[6] M. P. Tooley *et al.*, *Phys. Rev. Lett.* **119** (2017).
[7] D. A. Jaroszynski *et al.*, *Philos. Trans. Royal Soc. A* **364** (2006) 710.
[8] X. Yang *et al.*, *Sci. Rep.* **7** (2017).
[9] X. Yang, E. Brunetti, D.A. Jaroszynski, *New J. Phys.* **20** (2018).
[10] S. Cipiccia *et al.*, *Nat. Phys.* **7** (2011) 867.
[11] H. P. Schlenvoigt *et al.*, *Nat. Phys.* **4** (2008) 130.
[12] M. P. Anania *et al.*, *App. Phys. Lett.* **104** (2014).
[13] E. Brunetti *et al.*, *Phys. Rev. Lett.* **105** (2010).
[14] D.A. Jaroszynski, and G. Vieux, in 10th Workshop on Advanced Accelerator Concepts C. E. Clayton & P. Muggli, Eds., pp. 902-913, Mandalay Beach, Ca (2002).
[15] D. A. Jaroszynski *et al.*, *Phys. Rev. Lett.* **71** (1993) 3798.
[16] B. Ersfeld *et al.*, *New J. Phys.* **16** (2014).
[17] D. A. Jaroszynski *et al.*, Proc. 40th Int. Conf. IRMMW-THz, H2E-1 (2015).
[18] D. A. Jaroszynski *et al.*, Proc. SPIE 11042, XXII International Symposium on High Power Laser Systems and Applications, 110420Y (2019).

L-25 **Thursday, 13.06., 12^{20}-13^{00}**

Attosecond High Harmonic Sources at ELI-ALPS and the opportunities

S. Kahaly[1]*

[1]*ELI-ALPS, ELI-Hu Kft., Dugonics tér 13, H-6720 Szeged, Hungary*

Keywords: attosecond pulses, ultrafast laser, high harmonic generation, atomic and molecular physics, laser plasma, strong field science

*e-mail: subhendu.kahaly@eli-alps.hu

The emergence of coherent attosecond (*as*) XUV sources [1,2] has allowed unprecedented spatio-temporal resolution in photonics studies of ultrafast processes [3]. These are the shortest known electromagnetic pulses produced in a controlled way on a laboratory scale. The interactions generating *as* pulses span a wide range of laser matter parameter space and take place through high harmonic generation in a nonlinear medium. The prerequisite drive laser peak intensities can range from moderately strong ($I\lambda^2 \sim 1\times10^{13\text{-}14}$ W.cm^{-2}μm^2,λ being the central wavelength) for atomic gases to ultrastrong ($I\lambda^2 \geq 1.37\times10^{18}$ W.cm^{-2}μm^2) values in solid density plasmas. This demands state of the art ultrafast intense femtosecond lasers to drive such processes. The nonlinear medium where the generation of *as* pulses can take place, depending on the interaction regime, includes all the four phases of matter (gas, liquid, solid and plasma forms with different dimensionalities). This demands sophisticated target designs. In addition, the requirement of generating attosecond pulses at high repetition rate puts stringent conditions on replenishable target development. The intense laser evolution took place over several decades culminating in half of the Nobel Prize award for physics in 2018 being given for the "method of generating high-intensity, ultra-short optical pulses". Novel target design is a continuously evolving phase.

ELI-ALPS, the Hungarian pillar of the Extreme Light Infrastructure project in Europe, benefits from all these parallel scientific developments and houses state of the art high repetition rate lasers that drive different sophisticated attosource beamlines [4,5,6] based on high harmonic generation (HHG) process [2]. The complexity of the multi-parameter laser matter interaction space demands optimal and clever experimental designs for brighter and shorter attosecond pulses. It also necessitates a complete insight on the competing HHG processes.

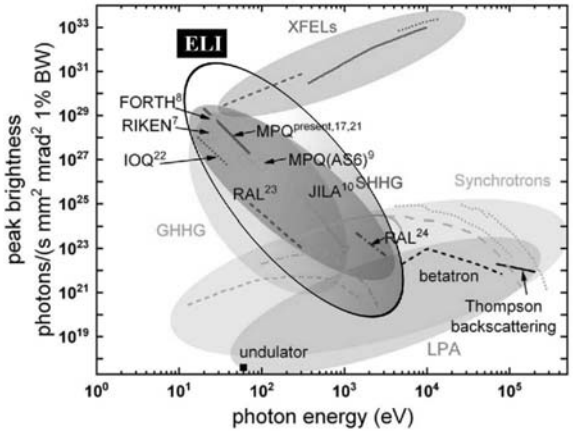

Figure 1. Peak brightnesses of contemporary x-ray sources: gas and solid based high harmonic sources (GHHG and SHHG), XFELS (FLASH, LCLS, SACLA etc.), synchrotrons (BESSY, NSLS, PETRA, etc.) and laser plasma accelerator sources (LPA) from [7]. The black semi transparent region fills the ELI-ALPS expected parameter space, which would provide both, isolated and trains of attosecond pulses

The figure 1 summarizes the peak brightnesses of the contemporary x-ray sources [7]. In this figure only RIKEN and MPQ dots pertain to isolated bright attosecond pulse category. ELI-ALPS attosecond HHG sources would potentially span the several orders of magnitude in peak brightness and photon energies.

In this presentation I would talk about the diverse attosecond high harmonic sources that are in the process of implementation at ELI-ALPS and would be available for user experiments soon. While stressing the uniqueness of these sources I would also talk about the application possibilities and scientific opportunities that such sources would provide.

Acknowledgements: ELI-ALPS is supported by the European Union and co-financed by the European Regional Development 1360 Fund (GINOP-2.3.6-15-2015-00001).

[1] M. Reduzzi *et.al.*, *J. Electron Spectros. Relat. Phenomena* **204** (2015) 257.
[2] S. Chatziathanasiou, *Photonics* **4** (2017) 26.
[3] F. Krausz, M. Ivanov, *Rev. Mod. Phys.* **81** (2009) 163.
[4] S. Mondal *et al.*, *J. Opt. Soc. Am. B* **35** (2018) A93.
[5] S. Kühn *et.al*., *J. Phys. B At. Mol. Opt. Phys.* **50** (2017) 132002.
[6] D. Charalambidis *et al.*, *Progress in Ultrafast Intense Laser Science XIII, Springer Series in Chemical Physics (ed. Yamanouch, K.)* (Springer, Cham, (2017) 181–218.
[7] O. Jahn *et.al.,Optica.* **6** (2019) 280.

L-26 **Thursday, 13.06., 14^{20}-15^{00}**

Automation and the DB system in the MX beamlines of Photon Factory

T. Senda[1]*

[1]*Structural Biology Research Center, Photon Factory, Institute of Materials Structure Science, High Energy Accelerator Research Organization (KEK), 1-1 Oho, Tsukuba, Ibaraki 305-0801, Japan.*

Keywords: synchrotron radiation, protein crystallography, automation, pipeline

*e-mail: toshiya.senda@kek.jp

The 3D structure of the protein at atomic resolution is essential information to study cell functions. On the basis of the 3D structure of a target protein, we can modulate its *biochemical* function by mutations. To analyze the *biological* function(s) of the protein, the mutant protein should be introduced into cells and resultant phenotype should be examined under appropriate conditions. In many cases, not only the structure-based mutational analysis but also other techniques of molecular/cell biology are required to obtain concrete results. Since this type of the experimental approach is becoming common in today's biology, the field of the structure biology is still expanding. But, since many non-structural biologists such as cell biologists and molecular biologists need to have 3D structure information of proteins, it is critically important in synchrotron facilities to develop an easy-to-use system for the 3D structure determination to support today's biological science. In addition, pharmaceutical companies need a high throughput system to obtain a lot of 3D structures of protein-compound complexes to design compounds. To meet the needs form academia and industry, Structural Biology Research Center (SBRC) in KEK has developed automated systems from crystallization to structure determination.

Automated crystallization screening system (PXS)

PXS is all-in-one type fully automated robot for crystallization screening of proteins [1]. PXS performs sitting-drop type crystallization screening and it takes less than 30 minutes to try 800 crystallization conditions. Since the robot can handle 0.1-0.2μL of protein solution, less amount of protein sample is required than before. The resultant crystallization plate is automatically stored in an incubator (20°C or 4°C) and images of each droplet are taken following a programmed schedule. The images of the droplets stored in the server computer can be accessed *via* a specific web system from anywhere in the world. Importantly, the crystallization plate can directly be mounted to a diffractometer in BL-17A of Photon Factory for *in situ* data collection [2].

Automated centering system (SIROCC)

We have developed an automated crystal-centering system, SIROCC. Each MX beamline in PF has a crystal mounting robot that can mount a crystal from UNIPACK in the liquid nitrogen bath. After mounting the crystal, SIROCC takes several photos of the mounted crystal on the diffractometer and centers the loop region of the cryo-loop. Then, the grid scan using X-ray is performed for precise centering. Based on the diffraction images obtained by the grid scan, the crystal is precisely centered at the position of the X-ray for data collection.

PReMo

After the centering, automated data collection can be performed based on the conditions given by users. The collected data are automatically processed and scaled. All these procedures are controlled by PReMo[3]. PReMo not only controls the data collection procedures but also has a DB function; PReMo stores all experimental parameters and results of MX data collection in PF. Users therefore can search conditions of earlier experiments and their results. In addition to the statistics of earlier data collections, images of crystals are also stored. These data are critically important to optimize conditions of data-collection, cryo-protection etc. Importantly, data from the PXS are also managed by PReMo (PXS-PReMo). The data of the crystallization screening is integrated with *in situ* data collection system. In future, further integration would be achieved for optimal data collection.

COMPASS

BL-1A of PFis a unique BL that can use long wave length X-ray (2.7-3.3 Å) for native SAD phasing. Because of installation of a He chamber and a pixel array detector, it becomes to be possible to collect high quality native SAD data in a routine manner. While it is possible to determine the crystal structure using the native SAD method, a combination of the molecular replacement (MR) and native SAD methods is powerful and useful. Since many protein structures are already determined, importance of the MR method is increasing. However, the MR method needs a lot of computer analyses for structure validation to remove phase biases. It is therefore useful to incorporate experimental phases derived from the native SAD method into the MR method. At the same time, while determination of the substructure (determination of the position of sulphur atoms in the crystal) is frequently a bottleneck of the native SAD method, initial phases from MR make it much easier to determine the sub-structure. Since we had confirmed the effectiveness of the MR-native SAD method, we have constructed a pipeline for the MR-native SAD method. This pipeline can automatically solve the crystal structure of proteins by the MR-native SAD method in a few hours, if diffraction data for native SAD is available. The pipeline will be opened to academic users in this fiscal year.

SBRC has many collaborations with cell biologists, bioinformaticians, OMICS researchers etc. The effectiveness of the above described automated system becomes evident in these collaborations. Next challenge is an integration of data stored in PReMo to guide user experiments. In future, we would like to develop a cloud-based PReMo system to integrate experimental knowledge of all users.

[1] Hiraki *et al., Acta Crystallogr.* **D62** (2006) 1058.
[2] Yamada *et al., AIP Conf. Proc.* **1741** (2016) 050023.
[3] Yamada *et al., J Phys: Conf. Ser.* **425** (2013) 012017.

L-27 **Thursday, 13.06., 15^{00}-15^{40}**

From molecular switching to material transformation: revisiting the spin crossover with ultrafast pump-probe techniques

E. Trzop[1]*, M. Lorence[1], E. Collet[1], M. Cammarata[1], R. Bertoni[1], C. Mariette[1], A. Volte[1], H. Cailleau[1], M. Servol[1], M. Wulff [2] and M. Levantino[2]

[1]*Univ Rennes, CNRS, IPR (Institut de Physique de Rennes) - UMR 6251, F-35000 Rennes, France*
[2]*European Synchrotron Radiation Facility, ID09, B.P.220, F-38043 Grenoble Cedex, France*

Keywords: spin crossover, molecular switching, pump-probe techniques, synchrotron radiation

*e-mail: elzbieta.trzop@univ-rennes1.fr

The recent advances of the ultra-fast techniques open the way to today's challenges in the 'Ultrafast Control of Materials' [1,2]. One feat in particular has been draining a lot of effort, namely the control of materials with an ultrashort laser pulse.

The materials switching with a laser pulse can severely change their macroscopic properties (electric conductivity, magnetism, colour, etc.), whereby emerging cooperativity and coherence of different degrees of freedom underpin the resulting phase transitions of various sorts. However, the pertinent time scales for photo-switching processes in materials have been rather difficult to characterize.

The pioneering investigations dealt mainly with the electron/phonon dynamics immediately following the femtosecond excitation or the kinetics of recovery to the thermally stable states. Time-resolved X-ray diffraction and ultrafast VIS-IR spectroscopy reveal that the degrees of freedom triggered by a femtosecond laser pulse in a spin-crossover (SCO) material follow a sequence in the out-of-equilibrium dynamics [3-8]. Those steps dissected in time, provided a mechanistic picture of a material transformation driven under different regimes.

Acknowledgements: This work was supported by CNRS, University of Rennes 1 (France) and ELASTICA project (ANR-16-CE30-0018).

[1] G.R. Fleming, M.A. Ratner, *Physics Today* **61(7)** (2008) 28.
[2] D. N. Basov, R.D. Averitt, D. HSIEH, *Nat. Mat.* **16** (2017) 1077.
[3] M. Lorenc *et al.*, *Phys. Rev. B* **103** (2009) 028301.
[4] M. Lorenc *et al.*, *Phys. Rev. B* **85** (2012) 054302.
[5] E. Collet *et al.*, *Phys. Chem. Chem. Phys.* **14(18)** (2012) 6192.
[6] R. Bertoni *et al.*, *Nature Materials* **15** (2016) 606.
[7] C. Enachescu *et al.*, *Phys. Rev. B* **95** (2017) 224107.
[8] S. Zerdane *et al.*, *Chem. Sci.* **8** (2017) 4978.

L-28 **Thursday, 13.06., 15^{40}-16^{20}**

Macromolecular Xtallography Raw Data Repository MX-RDR

M. Gilski[1;2]*

[1]*Department of Crystallography, Faculty of Chemistry, A. Mickiewicz University, Umultowska 89b, 61-614 Poznan, Poland*
[2]*Center for Biocrystallographic Research, Institute of Bioorganic Chemistry, Polish Academy of Sciences, Noskowskiego 12/14, 61-704 Poznan, Poland*

Keywords: raw diffraction data, data repositories, big data, raw data deposition

*e-mail: mirek@amu.edu.pl

The rapid development of computer technology in the past three decades has opened up new opportunities and challenges for researches. It became possible not only to perform very fast and complex calculations but also to process and analyze a huge amount of data. The results of such calculations and analysis often are the basis of scientific reports and publications. Unfortunately, the vast majority of raw experimental data, in the best case, are stored (for short period of time only) on the local archive systems and due to disk-space limitations are discarded or irreversibly lost for other reasons.

The crystallographic community has always been at the forefront of sharing experimental data. The Protein Data Bank (PDB) established in 1971 with only seven X-ray crystallographic structures of proteins experienced an almost exponential growth up to over 150,000 currently stored structures and became the first open access digital data resource in the biological sciences. Since 2008, deposition of the processed diffraction data (intensities or structure-factor amplitudes) has been mandatory for all determined structures and that fact hugely stimulated progress in development of refinement software. In the same way depositing raw diffraction images could stimulate the improvement of integration and processing software. Raw diffraction data sets are several orders of magnitude larger than the reduced sets of structure factors but recent technology development allows to manage and store such data. Despite the continuous growth of data-storage technology, the fraction of publicly available data sets is still quite low.

Reasons for archiving raw data include: verification or support the validity of deductions from an experiment, safeguard against error or fraud, possibility of reanalysis with future improved algorithms and software tools, example materials for teaching and learning, and provision of mechanism for long-term preservation of experimental results.

In 2018, as part of EU funded project, coordinated by Interdisciplinary Centre for Mathematical and Computational Modelling (ICM) of the University of Warsaw, which aimed to create an open access discipline dedicated raw data repositories, works on Macromolecular Xtallography Raw Data Repository (MX-RDR) has begun. The project will develop tools to create a set of crystallographic metadata by combination of all information extracted from diffraction images, obtained from a PDB deposit and/or user input. Each data set will be characterized by rich metadata, both to facilitate their management and long-term curation, and to allow effective scientific reuse.

Acknowledgements: This work was supported by Operational Programme Digital Poland, POPC.02.03.01-00-0036/18-0.

L-29 **Friday, 14.06., 9^{00}-9^{40}**

Charge correlations and the Fermi surface reconstruction in cuprate superconductors

W. Tabiś[1;2]*, I. Biało[1;2] and N. Barišić[2;3]

[1]*AGH University of Science and Technology, Faculty of Physics and Applied Computer Science, 30-059 Krakow, Poland*
[2]*Institute of Solid State Physics, TU Wien, 1040 Vienna, Austria*
[3]*Department of Physics, Faculty of Science, University of Zagreb, HR-10000 Zagreb, Croatia*

Keywords: cuprates, X-ray scattering

*e-mail: wtabis@agh.edu.pl

A major difficulty in understanding high-T_c systems is the complexity of the materials, the presence of strong electron-electron interactions, and their rich phase diagrams. Synchrotron X-ray scattering is a powerful tool allowing exploration of the electronic and structural degrees of freedom of complex materials. Furthermore, high magnetic fields play an important role in studying the high-T_c phenomenon, because such fields weaken the superconducting state and enable us to explore the competing states. One of such states is the spontaneous self-organized charge modulation, so called the charge density wave (CDW) order. Although its presence has been demonstrated within the CuO_2 plane of each family of cuprate superconductors [1], the extent of the CDW order as a function of doping, temperature, or magnetic field remains controversial.

First, I will present the resonant X-ray scattering experiments in the model cuprate $HgBa_2CuO_{4+\delta}$ (Hg1201). The systematic doping and temperature dependent study, performed at BESSY II, Canadian Light Source and Swiss Light Source, allowed us to establish the region of the phase diagram where the static CDW order exists [2,3]. The combined results are presented in Figure 1.

The following resonant inelastic X-ray scattering (RIXS)study of the underdoped Hg1201 (T_c = 70 K) allowed us to detect dynamic CDW correlations at about 40 meV at T = 250 K, above the charge-density-wave (CDW) order

temperature $T_{CDW} \approx 200$ K. At $T = T_c$, both short-range quasi-static as well as dynamic CDW correlations are observed. The latter now extends to much higher energy, with a new characteristic scale of about160 meV. The paramagnon dispersion along [1,0], across the two-dimensional CDW wavevector $\boldsymbol{q}_{CDW}$, is unaffected by the CDW correlations and consistent with magnetic excitations measured by inelastic neutron scattering. Such coexistence of static and dynamic CDW correlations is furthermore consistent with theoretical predictions [4].

Complementary electronic transport measurements were performed in magnetic fields up to 70 T at the National High Magnetic Field Laboratory, LNCMI in Toulouse. The Hall effect and magnetoresistance studies allowed us to investigate the changes of the Fermi surface topology in the underdoped cuprates. The results are consistent with the picture of the Fermi surface reconstruction by the CDW order at elevated magnetic fields.

The combined results allow us to draw a universal electronic phase diagram of the cuprates.

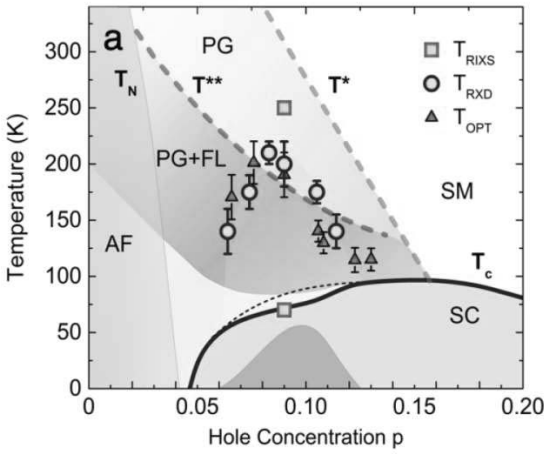

Figure 1. Phase diagram of Hg1201 [3]. Solidblue line: Doping dependence of the superconducting (SC)transition temperature $T_c(p)$. Dark gray region: Deviation (not to scale) of T_c from estimated parabolic doping dependence (dashed blue line). T^*: Pseudogap (PG) temperature, estimated from deviation of T-linear resistivity in the strange-metal (SM) state. T^{**}: Temperature below which Fermi-liquid (FL) behavior is observed in the PG state [2]. T_{RXD}- Onset of short-range CDW correlations estimated from RXS [2, 3]. T_{OPT}- Characteristic temperature observed in time-resolved optical reflectivity measurements [5]. T_{RIXS}: Temperatures at which the RIXS was measured in Hg1201 sample (T_c = 70 K, p ~ 0.086).

Acknowledgements: This work was supported by FWF project P27980-N36 and the European Research Council (ERC Consolidator Grant No725521).

[1] R. Comin, A. Damascelli, *Annu. Rev. Condens. Matter Phys.* **7** (2016) 369.
[2] W. Tabis *et al*., *Nature Commun*. **5** (2014) 5875.
[3] W. Tabis *et al*., *Phys. Rev. B* **96** (2017) 134510.
[4] S. Caprara *et al.*, *Phys. Rev. B* **95** (2017) 224511.
[5] J. P. Hinton *et al*., *Sci. Rep.* **6** (2016) 23610.

L-30

Characterization and measurement of magnetic materials using X-Ray and Threshold Photoemission Electron Microscopy

T. Giela[1]*, D. Wilgocka-Ślęzak[2], N. Spiridis[2] and J. Korecki[2;3]

[1]CERIC-ERIC, S.S. 14 - km 163,5 in AREA Science Park 34149 - Basovizza, Trieste, Italy
[2]Jerzy Haber Institute of Catalysis and Surface Chemistry, Polish Academy of Sciences, ul. Niezapominajek 8, 30-239 Kraków, Poland
[3]AGHUniversity of Science and Technology, Faculty of Physics and Applied Computer Science, Al. Mickiewicza 30, 30-059 Kraków, Poland

Keywords: X-Ray Absorption Spectroscopy, Magnetic Circular Dichroism, Threshold Photoemission, Photoelectron Emission Microscopy

*e-mail: tomasz.giela@ceric-eric.eu

Magnetic Circular Dichroism (MCD) is a direct and effective way for the characterization and measurement of magnetic materials. The effect is widely used in synchrotron-based X-Ray methods because of easily accessible circular polarization, a broad range of available energies and great intensity of synchrotron radiation. The effect can be used in Photoemission Electron Microscopy (PEEM) to study the magnetic domain patterns of magnetic samples.

In contrast to X-PEEM which targets the core level electrons, one can try to focus on valence band and utilize the threshold photoemission processes. Threshold Photoemission (TP) is inherently spin polarized and can be further enhanced using circularly polarized light [1]. High asymmetry values measured for magnetic samples open a venue for exploiting the effect in PEEM microscopy to mimic the advantages of synchrotron-based X-PEEM [2].

During the talk, the new method of TP-MCDPEEM will be presented as an alternative for standard X-PEEM that could be realized adopting simple laboratory illumination sources. A novel approach of using tunable UV light source coupled with an augmented optical system to match the binding energies of valence electrons proved the feasibility of the method but also highlighted certain challenges.

The presentation will be a comprehensive comparison of X-PEEM and TP-MCDPEEM techniques. It will give simple examples of experimental results using both methods. Finally, it will be concluded by the remarks about the pros and cons of applying Threshold Photoemission for obtaining magnetic contrast and will provide an insight into the possible future of the method.

Acknowledgements: This work was supported by Foundation for Polish Science in the frame of TEAM project: "Atomic and molecular level devising of functional nanostructures for magnetic and catalytic applications" (TEAM/2008-2/3). The PEEM and LEEM microscopes were obtained within SPINLAB project (contract nr POIG.02.02.00-00-020/09-00). The research was carried out in the frame of "Harmonia" project od National Science Center (contract nr UMO-2012/06/M/ST4/00032). The research was carried out in The Swiss Light Source at the Paul Scherrer Institute and in cooperation with AGH University of Science and Technology.

[1] R. Feder, J. Henk, B. Johansson, *Solid State Commun.* **108** (10) (1998) 713-716.
[2] T. Nakagawa, T. Yokoyama, *J. Electron. Spectros. Relat. Phenomena* **185** (10) (2012) 356-364.

O-01 **Sunday, 09.06., 17^{40}-18^{00}**

Core-level spectroscopy triggered by femtoseconds X-ray pulses

J. Szlachetko[1]*, K. Tyrala[1], J. Czapla-Masztafiak[1], K. Wojtaszek[1],W. Blachucki[2],C. Milne[3], J. Sa[4], Y. Kayser[5], A. Wach[1] and W. M. Kwiatek[1]

[1]*Institute of Nuclear Physics Polish Academy of Sciences, Krakow, Poland*
[2]*Institute of Physical Chemistry, Polish Academy of Sciences, Warsaw, Poland*
[3]*Paul Scherrer Institut, 5232 Villigen PSI, Switzerland*
[4]*Department of Chemistry, Uppsala University, 752 37 Uppsala, Sweden*
[5]*Physikalisch-Technische Bundesanstalt, Abbestr. 2-12, 10587 Berlin, Germany*

Keywords: x-ray free-electron laser, nonlinear interaction, core-level excitations

*e-mail: jakub.szlachetko@ifj.edu.pl

Introduction of X-ray sources delivering femtosecond long pulses opened new possibilities in exploration of the area of X-ray science and allowed for tracking of matter transformations in physical, chemical and biological systems at exceptional time-scales [1]. However, studies of complex systems with X-rays have always been associated with concerns about the destructive nature of the incidence beam. Radiation damage manifest itself through different effects like change of electronic structure, bond breaking, Coulomb explosion as well as structural changes. The strength of X-ray damage may be reduced with number of experimental approaches, such as sample circulation or sample cryocooling. To this point, the most significant development for suppressing the radiation damage is relying on the shortening of the X-ray pulse duration down to tens of femtoseconds, which pioneered the growth of the so called “probe-before-destroy” approach.

We report on X-ray interaction with metal-center molecular solution at times scales shorter than atomic movements (<50fsec) [2, 3]. Ultra-short X-ray spectroscopy measurements showed significant damage of electronic structure of atoms while still preserving the molecule atoms’ positions. Investigation of the X-ray induced processes revealed that the main contribution to the radiation damage results from the photo-generated solvated electrons. Interaction of these electrons with molecule leads to electronic structure modifications and this process is found to be much faster than direct absorption of photons by metal-center. This phenomenonshould be considered as main radiation damage mechanism in samples embedded in, e.g., solutions or in matrices.

Acknowledgements: Partial support of National Science Center (NCN, Poland) under grant no. 2017/27/B/ST2/01890 is acknowledged.

[1] K. Tyrała, C. Milne, K. Wojtaszek, A. Wach, J. Czapla-Masztafiak, W. M. Kwiatek, Y. Kayser and J. Szlachetko, *Phys. Rev. A* (2019) accepted.
[2] Y. Kayser, C. Milne, P. Juranić, L. Sala, J. Czapla-Masztafiak, R. Follath, M. Kavcic, G. Knopp, J. Rehanek, W. Błachucki, D. Zhu, R. Alonso-Mori, R. Abela, J. Sá and J. Szlachetko, *in review* (2019).
[3] W. Błachucki, Y. Kayser, J. Czapla-Masztafiak, M. Guo, P. Juranić, M. Kavčič, E. Källman, G. Knopp, M. Lundberg, C. Milne, J. Rehanek, J. Sá and J. Szlachetko, *Struct. Dyn.***6** (2019) 024901.

O-02 **Sunday, 09.06., 18^{00}-18^{20}**

Extended Abstract

Review of Health Research at the Canadian Light Source

P. Grochulski[1]*

[1]*Canadian Light Source Inc.,44 Innovation Boulevard, Saskatoon, SK S7N 2V3, Canada*

Keywords: synchrotron radiation phase contract imaging (SR-PCI), macromolecular crystallography, Fourier-transform infrared spectroscopy (FTIR), X-ray absorption spectroscopy (XAS), scanning transmission X-ray microscopy (STXM)

*e-mail: pawel.grochulski@lightsource.ca

The Canadian Light Source (CLS) is a 3rd generation synchrotron facility that started its operation in 2006. Currently it is composed of 18 functional beamlines, with an additional five being commissioned. Health is one of the strategic sectors of the CLS, besides agriculture, environment and advanced materials. From 2017 through 2019, researchers from across Canada published more than 200 health-related papers and deposited more than 410 structure coordinates in the Protein Data Bank (PDB). Their work was mostly performed at the Biomedical Imaging and Therapy Facility (BMIT), Canadian Macromolecular Crystallography Facility (CMCF) and the Mid-Infrared Spectroscopy (Mid-IR) beamline, but also at the Very Sensitive Elemental and Structural Probe Employing Radiation from a Synchrotron (VESPERS), Soft X-ray Microcharacterization Beamline (SXRMB) and Soft X-ray Spectromicroscopy (SM) beamlines. Their research covers diseases ranging from cystic fibrosis, hearing loss, porosity and bone remodeling, developing vaccination for malaria, and Alzheimer's as well as making strides in cancer research and the development of new antibiotics and other novel pharmaceuticals.

For years, scientists have hypothesized that in cystic fibrosis, a mutation to a gene called CFTR interferes with the production of airway surface liquid (ASL). The ASL consists of a mucus layer that traps bacteria, dust and other particles and a thinner liquid layer on which the mucus “floats” as it is swept out of the lungs by tiny hair-like cilia. In addition, the ASL also has bactericidal properties, not only trapping potential disease-causing microbes, but also inactivating and killing them. Applying synchrotron-based x-ray phase contract imaging (SR-PCI) at BMIT, for the first time allowed measurement and comparison of the thickness of the ASL layer in wild-type and cystic fibrosis (CF) swine [1]. The conclusion of this work is that CF swine’s airways do not respond to inhaled pathogens, therefore allowing infection and inflammation. Building on this work, the team studied the inhaled hypertonic saline (HTS) treatment that is used to improve health in patients with cystic fibrosis [2]. The understanding was that the HTS treatment generates an osmotic gradient drawing water into the airways, increasing ASL volume. On the other hand, there was evidence that HTS may also stimulate active secretion of ASL by airway epithelia through the activation of sensory neurons. The study

concluded that the HTS-triggered ASL secretion pathway is partially mediated by the stimulation of airway neurons, and that the osmotic gradient accounts for only ~50% of the effect.

According to the Canadian Health Measures Survey, about 20 % of adults aged 19 to 79 years have at least mild hearing loss in one or both ears, while close to 47 % of adults aged 60 to 79 years have some level of hearing loss. Damage to the middle ear is a common contributor to hearing loss. High-resolution visualization of middle-ear soft-tissue commonly uses imaging techniques such as micro-computed tomography (CT) and optical microscopy that require extensive sample preparation, including processing or staining using contrast agents to achieve sufficient soft-tissue contrast. Work done at BMITprovided superior visualization of soft-tissue microstructures over conventional micro-CT images [3]. Additional work has also included obtaining detailed 3D maps of the human cochleain an intact temporal bone [4]. Results suggest that SR-PCI has the potential to replace histology as the gold standard for evaluating intracochlear structural integrity in human specimens. An SR-PCI experiment with 3D reconstruction was performed to analyze the complex anatomy of the cranial nerves and vessels in the acoustic-facial cistern in the human internal acoustic canal [5]. The SR-PCI reproduced, for the first time, the variable 3D anatomy of the humaninternal acoustic canal, including cranial nerve complexes, anastomoses, acoustic-facial cistern in unprocessed and un-decalcified specimens. A thorough knowledge of the gross and microanatomy of the human internal acoustic canal is essential in vestibular schwannoma removal, cochlear implant surgery, vestibular nerve section, and decompression procedures.

Porosity in bone is associated with bone fragility and fracture risk, and is an indicator of osteoporosis progression. However, bone degeneration has traditionally been linked with a deficit of spongy bone. The significant role of cortical porosity in quantifiably marking bone loss and fragility has been recently recognized. Studies performed atBMIT beamlines compared the traditional method of cortical porosity assessment with high-resolution peripheral quantitative computed tomography (HR-pQCT) and synchrotron radiation micro-CT based measurements (SR-μCT) [6]. Results indicate that HR-pQCT imaged porosity assessed with the density inhomogeneity method with optimized equations showed the best agreement with SR-μCT-derived porosity. Bone acts as a reservoir for many trace elements, therefore understanding the extent and pattern of elemental accumulation in the skeleton is important from diagnostic, therapeutic and toxicological points of view. For example, related work from the VESPERS beamline, using X-ray absorption spectroscopy, indicate that tungsten accumulated in bone acquired from drinking water was no longer in the originally-administrated form, but rather resembled the heteropolytungsten species, phosphotungstate [7]. Other studies using BMIT looked at bio-distribution of strontium and barium in the developing and mature skeletons of rats [8]. They concluded that barium and strontium can be used as surrogates for calcium to study the pathological changes in animal bone diseases. Effects of pharmaceutical compounds on bone micro-architecture and bone remodeling can also be studied with high spatial sensitivity and precision.

Malaria is a global health priority, with an estimated 216 million cases worldwide in 2016 alone. The *Plasmodium falciparum* (*Pf*) parasite is responsible for most malaria-related mortalities. Developing a vaccine is one promising means of fighting this disease. For example, disrupting the *Pf* life cycle as the parasite circulates between humans and *Anopheles* mosquitoes has the potential to reduce infections. When a mosquito bites someone with malaria who produces appropriate antibodies, the transmission rate of the disease is subsequently greatly reduced. Transmission-blocking vaccines are based on this principle; therefore, they are the target proteins for this type of vaccine development. One of the target molecules, Pfs48/45, isa gametocyte surface protein critical for parasite development and transmission, and its targeting by monoclonal antibody (mAb) 85RF45.1 leads to the potent reduction of parasite transmission. The 3-D structure ofthe 85RF45.1 Fab-Pfs48/45 6C complex was determined using data collected at the CMCF [9]. The structure describes potent epitope I, and showed how mAb 85RF45.1 recognizes an electronegative surface with nanomolar affinity. Another molecule, Pfs25,is also a leading malaria transmission-blocking vaccine antigen. Pfs25 vaccination is intended to elicit antibodies that inhibit parasite development when ingested by *Anopheles* mosquitoes during blood meals. Six crystal structures of Pfs25 in complex with antibodies elicited by immunization via Pfs25 virus-like particles in human immunoglobulin loci transgenic mice were determinedat CMCF [10]. The molecular characterization of inhibitory antibodies provides information on the natural disposition of Pfs25 on the surface of ookinetes and provides structural blueprints for designing the next-generation of immunogens. Another study determined the molecular mechanism underlying the clonal selection and affinity maturation of human B cells expressing protective antibodies against the circumsporozoite protein of the malaria parasite *Pf* (PfCSP) [11]. The molecular details reveal that the repetitive nature of PfCSP facilitates direct homotypic interactions between two PfCSP repeat-bound monoclonal antibodies, improving antigen affinity and B cell activation.

The hospital environment tends to drive the development of an increasing number of bacterial strains that are resistant to antibiotics. There is no doubt antibiotic resistance is one of the biggest dangers to hospital care worldwide. Each year in the U.S., at least 2 million people become infected with bacteria that are resistant to antibiotics, as has been confirmed by the Centers for Disease Control and Prevention. Those so-called superbugs include methicillin-resistant *Staphylococcus aureus* (MRSA). MRSA strains are resistant to a variety of antibiotics, including the classic penicillin and cephalosporin classes of β-lactams, making treatment difficult.It has been observed that resistance can be mediated by the trans-peptidase penicillium-binding protein 4 (PBP4). Mutations in PBP4 and its promoter were identified in a laboratory-generated mutant strain, CRB, which exhibits high-level resistance to β-lactams,

including resistance to the new-generation cephalosporins active against methicillin-resistant strains of *S. aureus*. To understand PBP4's role in the resistance, crystal structures of PBP4 of apo and acyl-enzyme intermediate forms complexed with three late-generation β-lactam antibiotics (ceftobiprole, ceftaroline and anaftcillin, were determined [12]. Structural and kinetics effects of PBP4 mutations present in the CRB strain were also characterized. With ceftobiprole, the missense mutations impaired the K_m value 150-fold, decreasing the proportion of inhibited PBP4. Whereas, ceftaroline resistance appeared to be mediated by other factors, possibly including mutations in thePBP4 promoter. Located within the transpeptidase active-site-cleft, the two substitutions have different effects depending on the drug. The conclusion of the studies is that *S. aureus* CRB strain has at least two PBP4-mediated resistance mechanisms. Resistance to another class of antibiotic, the macrolides, is the subject of another study [13]. The work describes crystal structuresof two clinically relevant macrolide kinases that confer resistance to erythromycin and related antibiotics.Their complex structures with six different macrolides rationalize the broad substrate spectrum and reveal an extended flexible interdomain linker to be critical for antibiotic binding. Most commonly, resistance emerges through the action of enzymes that chemically modify antibiotics, transferring chemical groups from donor molecules to an acceptor group on the antibiotic to render it inactive. Therefore, a different lab studied another class of antibiotics, aminoglycosides, which are effective against many bacterial pathogens, by probing plasticity of aminoglycoside binding to antibiotic kinase APH(2")-Ia [14]. APH(2″)-Ia preferentially binds 4,5-disubstituted and 4,6-disubstituted aminoglycosides by using the neamine rings in a conserved pocket. Additional rings linked to this core neamine element are accommodated in various orientations in the spacious binding cleft of the enzyme. In cases where this type of binding is obstructed, the enzyme can bind compounds in alternative binding modes, though more weakly. Some of these alternative binding modes may facilitate low levels of phosphorylation on additional sites of the aminoglycoside, such as the 5″ position of lividomycin.Structures of the enzyme cocrystallized with the N1-substituted aminoglycosides amikacin and arbekacin indicate that these nonnatural aminoglycosides can still be bound by the enzyme and explain the low-level background phosphorylation at the 2″ position. These binding interactions may provide a means for the enzyme to evolve mutations that shift the resistance spectrum toward new compounds, such as the S376N mutant with elevated arbekacin phosphorylation.

A large portion of the beamtime at the CMCF beamlines is devoted to development of new pharmaceuticals. Industrial researchers use ~25% of the available beamtime via industrial contracts. In addition, many academic researchers are involved in this important research. For example, work on the crystal structure of a human enzyme called acid ceramidase (aCDase, ASAH1),which hydrolyzes lysosomal membrane ceramide into sphingosine, the backbone of all sphingolipids, to regulate many cellular processes [15]. Abnormalities in aCDase are associated with Farber disease, spinal muscular atrophy with progressive myoclonic epilepsy, Alzheimer's, diabetes, and cancer. Structural mapping of disease mutations revealed that most would destabilize the protein fold. These results provide key information for rational design of aCDase inhibitors and recombinant aCDase for new therapeutics. In another search for new analgesic and anti-inflammatory medicines that are both effective and safe, the 3D structure determination of N-acylethanolamine acid amidase (NAAA) - an intracellular enzyme that degrades the lipid mediator palmitoylethanolamide was performed [16]. Animal studies have shown that inhibition causes profound analgesic and anti-inflammatory effects. The results illustrate the sequential steps leading to the activation of NAAA at lipid membranes, and reveal how current inhibitors block this enzyme.An illustration of cancer research performed at the CMCF beamlinesis work related to melanoma [17]. Research unraveled the prenylation–cancer paradox in multiple myeloma with novel geranylgeranyl pyrophosphate synthase (GGPPS) inhibitors. These results provide the first proof-of-principle that GGPPS is a valuable therapeutic target in oncology and more specifically for the treatment of multiple myeloma. Another example of cancer research was work performed at the Mid-IR and SXRMB beamlines, looking into biochemical alternations in cancer-associated fibroblasts by using novel correlative spectroscopy [18]. Their studies highlighted new avenues for future research into the microenvironment of breast tumors.

In recent decades, a tremendous amount of evidence has strongly suggested a crucial role for the human microbiota in health and disease. The microbiota has the potential to increase energy extraction from food, and improve nutritional status. It also provides a physical barrier against foreign pathogens and is essential in the development of the intestinal mucosa and immune system of the host. The human microbiota consists of 10-100 trillion symbiotic microbial cells living with each person, primarily comprising bacteria in the gut. Work performed at the CMCF determined the basis of an agarose metabolic pathway acquired by human intestinal symbionts [19]. While bacteria that live in the oceans predominantly catalyze bioconversion of agarose, agarases have been discovered in micro-organisms that inhabit diverse terrestrial ecosystems, including human intestines. The team defined the structure–function relationship of the agarolytic pathway from the human intestinal bacterium *Bacteroides uniformis* (Bu) NP1. Using recombinant agarases from Bu NP1 to completely depolymerize agarose, they demonstrated that a non-agarolytic Bu strain can grow on GAL released from agarose. This relationship underscores that rare nutrient utilization by intestinal bacteria is facilitated by the acquisition of highly specific enzymes that unlock inaccessible carbohydrate resources contained within unusual polysaccharides. Intriguingly, the agarolytic pathway is differentially distributed throughout geographically distinct human microbiomes, reflecting a complex historical context for agarose consumption by human beings.

The formation of amyloid-β (Aβ) plaques are a manifestation of Alzheimer's disease. Work performed using STXM on the SM beamline explored a model of unsaturated anionic neuronal membranes at high concentrations of Aβ25–35, the transmembrane segment of the Aβ peptide. In particular, three membrane-active components; melatonin, acetylsalicylic acid and curcumin, which have been speculated to have an effect on Alzheimer's disease, were investigated [20]. The findings show that membrane-modulating drugs can affect the size of Aβ25–35 aggregates in anionic membranes.

Finally, an example of work toward elucidating biosynthetic pathawys of enzymes was the development of a strategy to trap biosynthetic acyl-enzyme intermediates by incorporating 2,3-diaminopropionic acid into recombinant proteins, via expansion of the genetic code [21]. This method will facilitate the study of diverse acyl-enzyme complexes. Work on structure-function relationship of *Lactococcus lactis* prolidase confirmed a twelf-residue loop structure from one subunit over the active site of the other subunit [22]. It showed the loop can form two states ("open" and "closed") and provided support for allosteric site by the loop and Arg293.

In conclusion, from 2017 through 2019, researchers from across Canada using beamlies at the Canadian Light Source published more than 200 health-related papers and deposited more than 410 structure coordinates in the Protein Data Bank.The results presented in this review come from a limited selection of papersthat covers dieseases ranging from cystic fibrosis, hearing loss, osteoporosis,and Alzheimer's, as well as making steps in cancer research and the development of new antibiotics and other novel pharmaceuticals.

Acknowledgements: The Canadian Light Source is supported by the Canada Foundation for Innovation, Natural Sciences and Engineering Research Council of Canada, the University of Saskatchewan, the Government of Saskatchewan, Western Economic Diversification Canada, the National Research Council Canada, and the Canadian Institutes of Health Research.

[1] X. Luan *et al.*, *Nat. Communications* **8** (2017) 786.
[2] X. Luan *et al.*, *Sci. Rep.* **9** (2019).
[3] M. Elfarnawany *et al.*, *Hear Res.***354** (2017) 1.
[4] J. Iyer *et al.*, *Biomed Opt Express* **9** (2018) 3757.
[5] X. Mei *et al.*, *J. Anat.* **234** (2019) 316.
[6] N. Soltan *et al.*, *Bone* **120** (2019) 439-445
[7] C. VanderSchee *et al.*, *Com. Chemistry* **1** (2018) 1.
[8] A Panahifar *et al.*, *JBMM* (2018) 1.
[9] P. Kundu *et al.*, *Nat. Communications* **9** (2018) 4458.
[10] S. Scally *et al.*, *Nat. Communications* **8** (2017) 1568.
[11] K Imkeller *et al.,Science* **360** (2018) 1358.
[12] J. Alexander *et al.*, *J. Biol. Chem*. **293** (2018) 19854.
[13] D. Fong *et al.*, *Structure* **25** (2017) 750.
[14] S. Caldwell, A. Berghuis *Ant. Agents and Chemother.* **62** (2018).
[15] A. Gebai *et al.*, *Nat. Communications* **9** (2018) 1621.
[16] A. Gorelik *et al.*, *PNAS* **115** (2018).
[17] C. Lacbay *et al.*, *J. Med. Chem*. **61** (2018) 6904.
[18] S. Kumar *et al.*, *Chemistry Open* **6** (2017) 149.
[19] B. Pluvinage *et al.*, *Nat. Communications* **9** (2018) 1043.
[20] A. Khondker *et al.*, *Sci. Rep.* **8** (2018) 12467.
[21] N. Huguenin-Dezpt *et al.*, *Nature* **454** (2019) 112.
[22] O. Kgosisejo *et al.*, *Biochim. Biophys. Acta*, **1865** (2017) 473.

O-03 **Sunday, 09.06., 18^{20}-18^{40}**

Introducing monochromatic Microbeam Radiation Therapy (m-MRT) modality

T. W. Wysokinski[1]* and D. Sherin[2]

[1]*Canadian Light Source, Saskatoon, S7N 2V3, Canada*
[2]*Saskatoon Cancer Centre, Saskatoon, S7N 4H4, Canada*

Keywords: monochromatic microbeam radiation therapy, synchrotron radiation

*e-mail: wysokinski@alumni.sfu.ca

The classical microbeam radiation therapy (MRT) is based on the spatial fractionation of a high peak dose-rate (≥2000 Gy/s) and low energy (~100 keV) pink-beam X-rays, using a single shot or interlaced geometry [1]. It is an extension of classical grid therapy method used to spare the skin from high entrance dose in orthovoltage radiation therapy [2].

Monochromatic microbeam radiation therapy (m-MRT) is an extension of the classical MRT technique and expands this therapy method into a low dose-rate (1-10 Gy/s) regime with dose rates comparable to clinical standards, using high brilliance monochromatic beams.

Microbeam radiotherapy requires a spatially collimated beam divided into sub-millimeter beamlets and a high precision positioning sytem that can deliver vertical or rotational movement, or both, with resolution in the range of micrometers. Specifically a combination of vertical and rotational scanning that would reduce the entry dose irradiation, while delivering a high dose to the tumour volume, is of specific interest for X-ray based therapy methods. There are several on-going programs to assess the advantage and feasibility of using both monochromatic and polychromatic beamlets [3-6].

Spiral microbeam radiation therapy (spiralMRT), offers similar spatial fractionation properties as interlaced MRT, combining spatially fractionated entrance beams and homogeneous dose distribution [3]. SpiralMRT can deliver homogeneous dose distributions to a target volume, while using spatially fractionated entrance beams. The valley dose of spiralMRT entrance beams is up to 40% lower than the corresponding tomotherapy dose, thus indicating a better normal tissue sparing. The optimum photon energy is around 150 keV to 200 keV [3].

Synchrotron radiation rotational radiotherapy method for breast cancer treatment was modelled and evaluated to assess the skin sparing effect in terms of centre-to-periphery dose ratio at different energies in the range 60–175 keV. Monte Carlosimulations showed that the technique assures a tumour-to-sk.in absorbed dose ratio from about 7:1 (at 60 keV photon energy) to about 10:1 (at 175 keV), sufficient for skin sparing during radiotherapy [5].

We will present here several models of application of m-MRT which were developed and tested at the Canadian Light Source. Those included: a step-and-shoot, bi-directional interlaced irradiation as well as a spiral m-MRT method. All those methods were tested at BMIT Facility at the Canadian Light Source [6] which provides access to high energy and high dose monochromatic X-rays and high accuracy, high load, positioning system.

As part of this study, the tumor fragments and cells samples were irradiated ex-situ and then analyzed to assess the damages induced by m-MRT irradiation. Eight patient derived xenografted (PDX) tumor fragments were irradiated and implanted in live NOD Severe Combined Immuno-deficient (SCID) gamma (NSG) mice to assess the effect of irradiation on tumor growth comparing to the control. The pilot studies showed that the m-MRT treatment of cancerous tissue slowed down the tumor growth in (NSG) mice as compared to untreated controls [7]. Further studies were carried on to investigate how the cancer cells respond to the irradiation treatment in vivo in the live animals [in prepration].

Acknowledgements: Research described in this paper was performed at the BMIT facility at the Canadian Light Source, which is supported by the Canada Foundation for Innovation, Natural Sciences and Engineering Research Council of Canada, the University of Saskatchewan, the Government ofSaskatchewan, Western Economic Diversification Canada, the National Research Council Canada, and the Canadian Institutes of Health Research.

[1] M.AGrotzer *et al*., *Physica Medica* **31**(2015) 564-567.
[2] J.A. Laissue *et al*., *Z. Med. Phys*. **22** (2012) 90-99.
[3] M. Donzelli *et al.*, *Phys. Med. Biol.* **64** (2019) 065005.
[4] F.A. Dilmanian *et al*., *Sci. Rep.* **9:1198** (2019) 1-15.
[5] F. Di Lillo *et al.*, *Physica Medica* **41** (2017) 20-25.
[6] T.W. Wysokinski *et al.*, *Nucl. Instrum. Methods Phys. Res. A* **775** (2015) 1-4.
[7] T. W. Wysokinski *et al.*, *CMBES Proceeding* **39** (2016).

O-04 **Sunday, 09.06., 18^{40}-19^{00}**

XUV coherence tomography with nanoscale resolution driven by broadband XUV sources

S. Skruszewicz[1;2]*, S. Fuchs[1;2], M. Wünsche[1;2], J. Nathanael[1,2], J. J. Abel[1;2], J. Reinhard[1;2], F. Wiesner[1;2], C. Rödel[1;2] and G. G. Paulus[1;2]

[1]*Institute of Optics and Quantum Electronics, Friedrich Schiller University Jena, Germany*
[2]*Helmholtz Institut Jena, Jena, Germany*

Keywords:, nanoscale 3D imaging, broadband XUV sources, synchrotron radiation,

*e-mail: slawomir.skruszewicz@uni-jena.de

Optical coherence tomography (OCT) is a well-established method to retrieve three-dimensional, cross-sectional images of biological samples in a non-invasive way using near-infrared radiation. The axial resolution of OCT is on the order of the coherence length $l_c \sim \lambda_0^2/\Delta\lambda$which depends on the central wavelength and the spectral width $\Delta\lambda$of the light source. As a consequence, the axial resolution only depends on the spectrum rather than the geometrical properties of the radiation. OCT with broadband visible and near-infrared sources typically reaches axial (depth) resolutions on the order of a few micrometers. Since its invention in the early 1990s by Huang et al. [1], OCT has become a well-established and standard diagnostic method in medicine especially for investigating the retina*in vivo* [2]. In recent years the capabilities of OCT has been employed in metrology and in material characterization e.g. inspection of LED's [3], solar cells [4] and the conservation of cultural heritage objects [5].

In this contribution, we present the extreme ultraviolet (XUV) coherence tomography (XCT) [6], utilizing short coherence length of broadband XUV and soft X-ray (SXR) radiation delivered by synchrotron and table-top sources. Powerful capabilities of XCT can be demonstrated when employedfor investigation of samples in theirnative spectral transmission windows. For instance, in the silicon transmission window (30-99 eV) a coherence length of about 12 nmhold promise for applicationof XCT in the growing sector of semiconductor metrology. In the water window (280-530 eV), in turn, the coherence length as short as 3 nm paves the road towards applications in life sciences.

Since broadband beam splitters in the XUV range are extremely complicated and fragile, XCT utilizes a variant ofthe Fourier-domain OCT scheme that completely avoids such optics. In XCT, the reflection from a capping layer of the sample serves as a reference wave [6]. This scheme enables realization of a robust and intrinsically stable experimental apparatus where broadband XUV radiation [7, 8] is directly focused onto the sample without further splitting. The reflected beam, i.e.the superposition of all backscattered partial waves from every layer in the sample, is spectrally analyzed by an XUV spectrometer. The structural information encoded in spectral modulations is extracted via the Fourier-transformation. Lateral resolution is provided by conventional imaging and scanning of the sample.

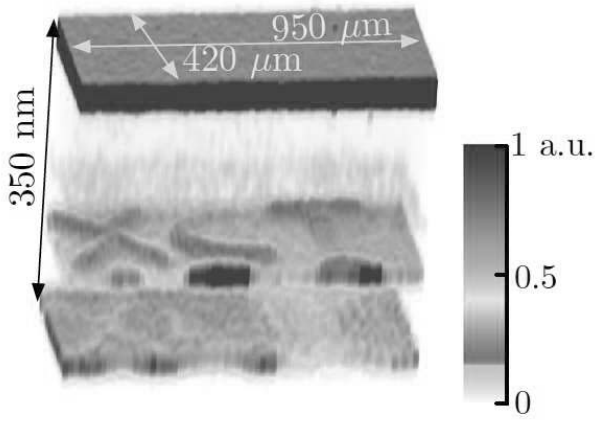

Figure 1. Reconstructed 3D PR-XCT measurement of a structured sample consisting of two gold layers and an additional thin silicon dioxide layer buried in silicon. The demonstrated axial resolution is 24 nm

Fig. 1 shows a 3D-tomogram of a non-destructive XCT scan of sample consisting of two laterally structured gold layers of nanometer thickness buried in a silicon matrix. An axial resolution demonstrated in the experiment is about 24 nm. Remarkably,the XCT revealsa high material sensitivity by resolvinga thin Silicon dioxide layer (blue) localized at depth of about 160 nm has been detected. This nanometer thin layerhas been developed during the production process of the sample. Such contaminationremains elusive for the SEM and remains barely visible in the TEM image. The XCT tomograms are analyzed by the phase-retrieval algorithm capable of extracting material information buried inside of the sample.

[1] D. Huang, *Science* **254** (1991) 1178.
[2] W. Drexler, J. G. Fujimoto, *Optical Coherence Tomography* (Springer International Publishing Switzerland, 2015).
[3] W. Walecki, *Phys. Status Solidi C: Conf.* **2** (2005) 984.
[4] L. Thrane, *Sol. Energy. Mat. Sol*, **97** (2012) 181.
[5] P. Targowski, *Appl. Phys. A* **106** (2012) 265.
[6] S. Fuchs, *Sci. Rep.* **6** (2016) 20658.
[7] S. Fuchs, *Appl. Phys. B* **106** (2012) 789.
[8] M. Wünsche, *Opt. Express* **25** (2017) 6936.

O-05 **Monday, 10.06., 12^{20}-12^{40}**

Integrative Structural Characterization of Biopharmaceuticals by Small-Angle X-Ray Scattering (SAXS)

G. Richter[1]*, F. Zhang[1], A. Moser[2], N. Weiner[3], P. Kotnik[2], S. Krahulec[3] and T. Madl[1;4]

[1]Gottfried Schatz Research Center for Cell Signaling, Metabolism and Aging, Institute of Molecular Biology & Biochemistry, Medical University of Graz, Neue Stiftingtalstrasse 6, 8010 Graz, Austria.
[2]Anton Paar GmbH, Anton Paar Strasse 20, 8054 Graz, Austria
[3]Boehringer-Ingelheim RCV GmbH & Co KG, Dr. Boehringer-Gasse 5-11, 1121 Vienna, Austria
[4]BioTechMed-Graz, Graz, Austria

Keywords: SAXS, proteins, biopharmaceuticals, structural characterization, automation

*e-mail: gesa.richter@medunigraz.at

In the development of new drugs for the treatment of human diseases, bio-pharmaceutical products have been experiencing a veritable boom for years. Most biopharmaceuticals, including seemingly simple, well-characterized and specified recombinant proteins, contain considerable heterogeneity, the drug actually being a complex mixture of molecular subtypes with a number of variations in structural aspects. The requirements for biopharmaceuticals put the current analysis methods to the test. In contrast to generics for which "only" bioequivalence has to be proven, a biopharmaceutical drug must prove that it corresponds to the biological counterpart both in its mode of action and in its structural composition. Current biophysical and biochemical methods may cover some of the evidence, but at present there is no methodology for high throughput in the biopharmaceutical environment to provide essential information on correct spatial structure and folding since biopharmaceuticals are typically highly sensitive, complex large molecules.
Small-angle X-ray scattering (SAXS) has emerged in recent years as a key method for the structural analysis of biomolecules, such as proteins, DNA, and RNA, and has the potential to close this gap. In particular, the development of laboratory SAXS systems facilitates their use in basic biological research and industrial application.
We will present our innovative laboratory SAXS pipeline for automated structural analysis of biomolecules and pharmaceuticals, thereby opening up new, broad application areas in the pharmaceutical industry. This pipeline enables the determination of the spatial structure and correct folding of biomolecules, integrates the SAXS technology into the existing industrial setup, and establishes the SAXS technology as a key method in the bio-pharmaceutical industry. In addition, the innovative SAXS technology will also provide new opportunities and applications in basic, industrial, and other industrial applications with a focus on structural analysis of biomolecules worldwide.

Acknowledgements: This work was supported by the Austrian Science Foundation (P28854, I3792, DK-MCD W1226 to TM), the President's International Fellowship Initiative of CAS (No. 2015VBB045, to TM), the National Natural Science Foundation of China (No. 31450110423, to TM), the Austrian Research Promotion Agency (FFG: 864690, 870454), the Integrative Metabolism Research Center Graz, the Austrian infrastructure program 2016/2017, the Styrian government (Zukunftsfonds) and BioTechMed/Graz. E.S. was trained within frame of the PhD program Molecular Medicine.

O-06 **Monday, 10.06., 12^{40}-13^{00}**

Synchrotron X-ray diffraction investigation of graphene on liquid copper

M. Jankowski[1*], F. La Porta[2], S. Fava[2], A. Manikas[3], J. M. de Voogd[4], G. J. C. van Baarle[4], C. Galiotis[3], I. Groot[5],G. Renaud[1], O. Konovalov[2] and A. Saedi[5]

[1]CEA/INAC-MEM, 38000 Grenoble, France
[2]ESRF−The European Synchrotron, 71 Avenue des Martyrs, 38000 Grenoble, France
[3]Foundation of Research and Technology-Hellas (FORTH/ICE-HT) and Dept. of Chem. Eng., University of Patras, Patras 26504, Greece
[4]Leiden Probe Microscopy (LPM), Leiden, The Netherlands
[5]Leiden Institute of Chemistry, Gorlaeus Laboratories, Leiden University, P.O. Box 9502, 2300 RA Leiden, The Netherlands

Keywords: X-ray diffraction, graphene, liquid metal

*e-mail: maciej.jankowski@esrf.fr

The aim of the LMCat (liquid metal catalysis) EU Horizon 2020 project is to deliver an instrumentation and methodology allowing to study in situ and in operando the growth of 2D materials (2DMs) on liquid metal surfaces.

The current approach to graphene (Gr) synthesis generally relies on CVD growth on solid substrates, mainly copper. Despite recent progress and fine-tuning of growth procedures there are significant obstacles in transferring the current knowledge towards mass production of good quality sheets over large-scales. The main showstoppers are slow procedures of 2DMs separation from solids, their environmental unfriendliness, and low quality of produced layers. All these factors significantly impact process costs, speed, and waste production.

In this contribution we will present the first experimental results of graphene growth on liquid copper in a newly developed CVD reactor, dedicated to the study of chemical reactions on LMCats. By combining in situ synchrotron X-ray diffraction and optical microscopy, supported by ex situ Raman spectroscopy, we are capable to resolve in real-time the growth dynamics and atomic

structure of graphene during its growth on liquid copper. Contradictory to solid, this later is an atomically smooth, isotropic and mobile medium, which allows to produce graphene crystals of extremely high-quality and large sizes limited only by the liquid bath surface. A myriad of interesting growth scenarios was observed which allowed to fine-tune the fabrication procedures and to identify key factors impacting the growth of individual flakes, their self-assembly and further association into a single layer with a coherent atomic structure

The obtained results are indispensable for establishing the methodology for the continuous production of graphene sheets on LMCats and pave a new way for the future cost-effective and large-scale fabrication of 2DMs.

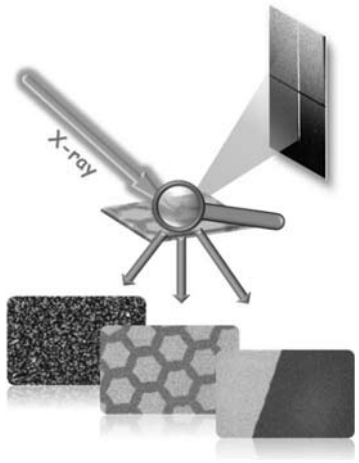

Figure 1. Diffraction rod of 2D Gr crystal on liquid-Cu recorded using synchrotron X-ray diffraction (top), optical microscope snapshots recorded during the growth of Gr (bottom)

[1] N. Taccardi *et al.*, *Nat. Chem.* **9** (2017) 862–867.
[2] P. Kula *et al.*, *App. Mech. Mat.***510** (2014) 8–12.
[3] D. Geng *et al.*, *PNAS* **109** (2012) 7992-7996.

O-07 **Monday, 10.06., 15^{40}-16^{00}**

Successful Experimental Quantitative Charge Density Feasibility Study of Grossular Under High Pressure

K. Woźniak[1]*, R. Gajda[1], M. Stachowicz[1], A. Makal[1], S. Sutuła[1] and P. Fertey[2]

[1]*Department of Chemistry, University of Warsaw, Pasteura 1, 02093 Warszawa, Poland*
[2]*Synchrotron SOLEIL, L'Orme des Merisiers Saint-Aubin, BP 48 91192 Gif-sur-Yvette Cedex, Paris, France.*

Keywords: Charge density, synchrotron radiation, grossular

*e-mail:kwozniak@chem.uw.edu.pl

We would like to present results of our high resolution X-ray data collection conducted on the CRISTAL beamline at the SOLEIL synchrotron (Paris, France) and refinement of experimental charge density under pressure. We studied single crystal of a natural mineral grossular - $Ca_3Al_2(SiO_3)_4$, which crystallizes in the space group Ia-3d of the cubic crystal system. We wanted to check if it is possible to determine an experimental electron density of a single crystal under pressure. The beamline parameters such as beam wavelength (0.41 Angstrom) and a special type of Diamond Anvil Cell (DAC) with the opening angle 110 deg. let us collect data with the resolution up to 0.35 Angstrom (with 100% completeness up to 0.39 Angstrom). We then used CrysAlis(Pro) for data reduction, Olex2 for structure solution and refinement, Jana2006 and XD program packages for multipole refinement, and WinXPro for visualization of different types of maps. We have compared our results with experimental charge densities obtained for grossular at ambient conditions and those obtained for pyrope - $Mg_3Al_2(SiO_3)_4$ (isostructural with grossular), measured at low temperature, 30K (Destro at al., 2017) [1]. In the case of our measurements for grossular, the calculated properties of the charge density at the (3, -1) BCPs as well as the net atomic charges are comparable. We think that thanks to the new type of DACs with wider opening angle and access to synchrotron radiations for some types of high symmetry compounds charge density distribution can be determined experimentally. Up to our knowledge this is the first successful determination of quantitative charge distribution in crystal under high pressure. We will present detailed results of our investigations.

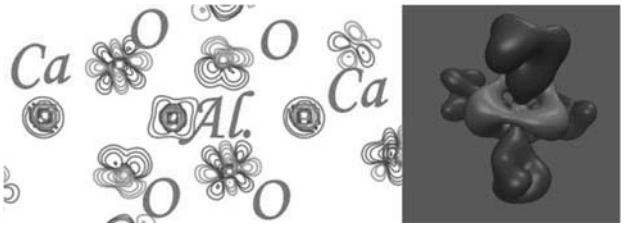

Figure 1. (left) Redistribution of electron density at O and Al ions under high pressure, and (right) the 3D SiO_4 deformation electron density maps at ambient conditions - isosurfaces: blue colour +0.1 e/A^3, red colour -0.1e/A^3

Acknowledgements: This work was supported by the Foundation for Polish Science (FNP) within the "Core Facility for Crystallographic and Biophysical Research to support the development of medicinal products" project.

[1] R. Destro, R. Ruffo, P. Roversi, R. Soave, L. Loconte and L. L. Presti, *Acta Cryst.* **B73** (2017) 722-736.

Monday, 10.06., 16^{30}-16^{40}

SOLARIS Special Session

How to apply for a beamtime at Solaris Synchrotron?

A. Górkiewicz[1]*

[1]*SOLARIS National Synchrotron Radiation Centre, Jagiellonian Univeristy, Czerwone Maki 98, 30-392 Kraków, Poland*

*e-mail: alicja.gorkiewicz@uj.edu.pl

SOLARIS is a Polish national research centre providing scientists with synchrotron radiation. The SOLARIS Centre is open for all interested scientists, both from Poland and abroad.

The beamtime is split into two 6-months allocation periods corresponding to spring and autumn calls for proposals. The spring call (deadline for proposal submission: 1st of April) is for experiments to be performed from September of the same year till February the following year. The autumn call (deadline for proposal submission: 1st of October) is for experiments to be performed from March till August of the following year.

Beamtime applications are submitted through the user portal Digital User Office (DUO).

Proposals are evaluating according to the following criteria:

- Innovative range of research areas;
- Precise scientific hypotheses;
- Clearly defined methodology and anticipated research results;
-Convincing grounds for purposefully using the synchrotron radiation;
- Proposer's scientific achievements;
-Timely presentation of reports on the earlier measurements performed at SOLARIS.

O-08 **Monday, 10.06., 16^{40}-17^{00}**

SOLARIS Special Session

SOLARIS operation status

A.I. Wawrzyniak[1]*

[1]*SOLARIS National Synchrotron Radiation Centre, Jagiellonian Univeristy, Czerwone Maki 98, 30-392 Kraków, Poland*

Keywords: synchrotron, emittance, storage ring

*e-mail: adriana.wawrzyniak@uj.edu.pl

Solaris is a third generation light source operating since 2015 in Krakow, Poland. The project was started in 2010 as a green filed project with unique cooperation between JU and the MAX-Lab in Lund, Sweden. Between 2015 and 2018 the synchrotron as well as two beamlines were commissioned. During commissioning phases the good performance of the Solaris storage ring has been reached [1-3]. The beam optics was brought close to the design one. The measured storage ring parameters with respect to the theoretical values are presented in Table 1.

Table 1. Solaris storage ring parameters

Parameter	Designed	Measured
Energy	1.5 GeV	1.45 ±0.05 GeV
Max. Current	500 mA	500 mA
Harmonic numer	32	32
Natural emittance (bare lattice)	5.982 nmrad	6.5 nmrad
Coupling	1 %	0.83 %
Tune νx, νy	11.22, 3.15	11.22, 3.15
Corrected chromaticity ξx, ξy	+2,+2 ; +1, +1	+1.4, +1.6;+0.9,+0.9
Energy loss/turn	114.1 keV	103.7 ±12.3 keV
Momentum acceptance	4%	3.7± (0.3)%
Synchronous phase	168°	167.4° ± 2.7°
Synchrotron tune	0.00239	0.00228
Physical acceptance horizontal/vertical	18 /4 mmrad	15.68/3.77 mmrad
Lifetime	13h	10h

The evolution of the $I\tau$ product with respect to the integrated current from the start-up of the storage ring up to now is shown in Fig. 1. The degradation of the lifetime after few shutdowns periods are mostly connected with the installation of the new vacuum chambers (ID straight sections; frontends; bending magnet section; diagnostic beamline) and/or some leaks and their repairs at RF section.

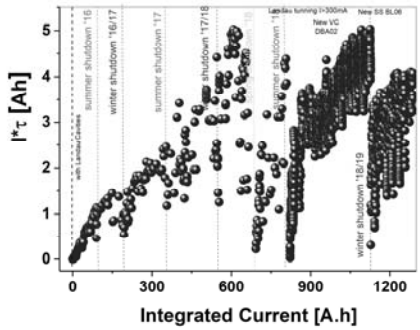

Figure 1. The $I\tau$ product versus integrated current in the storage ring

Since 1st of October 2018 Solaris storage ring is in the user operation mode. In 2018 the SOLARIS storage ring has run more than 1328 h for beamlines commissioning and users. The total beam availability of 90.4% was reached. About 376 h have been dedicated to the optimization of the accelerators for the users. The average operating current was 270 mA. The mean time before failure (MTBF) in 2018 was 16.3h whereas the mean time to recover (MTTR) 1.5 h. During the presentation the current status of Solaris storage ring will be given.

Acknowledgements: The author would like to acknowledge whole SOLARIS team for the excellent work during installation, commissioning and operation of the synchrotron.

[1] A.I. Wawrzyniak et al, "First Results of Solaris Synchrotron Commissioning", IBIC2015, Melbourne, Australia, Sep 2015.
[2] A.I. Wawrzyniak*, A. Kisiel, A. Marendziaket al, ProceedingsofIPAC2017, WEOCA01, Copenhagen Denmark (2017), 2490.
[3] A.I. Wawrzyniak et al, "Solaris a new class of low energy and high brightness light source", *Nuclear Inst. and Methods in Physics Research* B **411** (2017) 4.

O-09 **Monday, 10.06., 17^{00}-17^{20}**

SOLARIS Special Session

The first experimental results from PEEM/XAS beamline at Solaris

M. Zając[1]*, P. Dróżdż[2], K. Freindl[3], T. Giela[4], J. Korecki[2;3], E. Madej[3], M. Sikora[5], N. Spiridis[3], J. Stępień[5], M. Ślęzak[2], T. Ślęzak[2] and D. Wilgocka-Ślęzak[4]

[1]*National Synchrotron Radiation Centre Solaris at Jagiellonian University, ul. Czerwone Maki 98, 30-392 Kraków, Poland*
[2]*AGHUniversity of Science and Technology, Faculty of Physics and Applied Computer Science, Al. Mickiewicza 30, 30-059 Kraków, Poland*
[3]*Jerzy Haber Institute of Catalysis and Surface Chemistry, Polish Academy of Sciences, ul. Niezapominajek 8,30-239 Kraków, Poland,*
[4]*CERIC-ERIC, S.S. 14 - km 163,5 in AREA Science Park 34149 - Basovizza, Trieste, Italy*
[5]*AGH University of Science and Technology, Academic Centre for Materials and Nanotechnology, Al. Mickiewicza 30, 30-059 Kraków, Poland*

Keywords: synchrotron radiation, soft x-ray absorption spectroscopy, photoelectron emission microscopy

*e-mail: mar.zajac@uj.edu.pl

The PEEM/XAS beamline has been optimized for the soft X-ray photon energy range (150-2000 eV) with the bending magnet as a synchrotron radiation source. The chosen optical design based on the plane grating monochromator working in the collimated light (cPGM) has been optimized by the Optical Group from Elettra. The cPGM is equipped with two switchable gratings to ensure energy resolution ($\Delta E/E$) of the order $2.5x10^{-4}$ or better in the full energy range and available linear horizontal and elliptical polarization [1].

The Photoemission Electron Microscope (PEEM) is a primary end station of the beamline. Exchangeable with the microscope we use a separate end station for X-ray absorption spectroscopy measurements. It is dedicated to experiments in the field of biology, chemistry, catalysis, material science and physics. The beamline is operated in cooperation between AGH (Faculty of Physics and Applied Computer Science and Academic Centre for Materials and Nanotechnology), Jerzy Haber Institute of Catalysis and Surface Chemistry PAS and Jagiellonian University. Both stations comprise several vacuum chambers including dedicated chambers for sample preparation and characterization under UHV conditions. The dimensions of the photon beam at the sample in PEEM and XASare100 μm (H) x 50 μm (V) and 2 mm (H) x 2 mm (V), respectively [1].

This contribution reports on the present performance of the PEEM/XAS beamline and on selected results obtained during first experiments. The measured beamline parameters and characteristics will be summarized. The results of several accomplished experimentswill be presented, and among others the recently explainedantiferromagnet (AFM) / ferromagnet (FM) magnetic moment structure in an exchange bias CoO/Fe(110) system [2]. Finaly, the conclusions drawn from the first beamtime periodeswill be summarized for the perspective feasibility and limitations of future experiments.

Acknowledgements: Authors would like to thank A. Bianco, E. Busetto and I. Cudin from Synchrotron Elettra, Trieste for beamline optical design optimization and support during design period and also J. Raabe from Swiss Light Source at Paul Scherrer Institute for help in solving of many technical aspects.

[1] https://synchrotron.uj.edu.pl/en_GB/linie-badawcze/peem-xas
[2] M. Ślęzak *et al., Sci. Rep.* **9**, (2019) 889 https://doi.org/10.1038/s41598-018-37110-8

O-10 **Monday, 10.06., 17^{20}-17^{40}**

SOLARIS Special Session

SOLCRYS - new SAXS/XRD beamline for NCPS Solaris

T. Kołodziej [1], D. Paliwoda[1], A. Wawrzyniak, and M. Kozak[1;2*]

[1]*National Synchrotron Radiation Centre SOLARIS, Jagiellonian University, Czerwone Maki 98, 30-392 Kraków, Poland*
[2]*Department of Macromolecular Physics, Faculty of Physics, Adam Mickiewicz University, Uniwersytetu Poznanskiego 2, 61-614 Poznan, Poland*

Keywords: NCPS Solaris, beamline, small-angle X-ray scattering, SAXS, protein crystallography

*e-mail: ma.kozak@uj.edu.pl

A combination of macromolecular crystallography (MX) and small angle X-ray scattering (SAXS) techniques with single-particle cryo-electron microscopy (cryo-EM) allows the complex study of the structure of biological macromolecules (protein complexes, viruses or nucleic acids) [1-3]. Currently, at the National Synchrotron Radiation Center "Solaris" in Krakow, an electron cryo-microscope is installed and also work has begun on the construction of the SOLCRYS beamline, operating by the use of hard X-ray radiation, for diffraction studies and SAXS, in particular for the needs of macromolecular crystallography and material sciences. This beamline will be located in a new, extended part of the experimental hall. The project assumes that the efficient X-ray source (up to 25 keV) for SOLCRYS beamline will be a superconducting multipole wiggler operating at 4 Tesla. The synchrotron radiation beam will be divided into two independent branches.

The first one will be used for diffraction studies especially for the needs of protein crystallography and will enable also powder diffraction studies. This station will be used both for standard PX experiments and for MAD studies. The numerical simulations of X-ray optics for PX branch, carried out using the ray-tracing method, allowed estimation of the expected X-ray photon flux ($\sim10^{13}$ph/sec) and the beam size of about 50-60 μm (calculation without transfocator and aperture). The end station will be equipped with the microgoniometer,

robotic autosampler and high-end semiconductor detector suited for the diffraction measurements of crystals of biological macromolecules. The second end station will offer measurements using the small-angle X-ray scattering technique, in particular bioSAXS studies of biomacromolecules in solution.

This project is carried out in cooperation with the Joint Institute for Nuclear Research (Dubna, Russia).

[1] S. C. Shoemaker, N. Ando, *Biochemistry* **57(3)** (2018) 277.
[2] A. Doerr, *Nat. Methods* **13** (2016) 23.
[3] J. Lengyel, E. Hnath, M. Storms, T. Wohlfarth, *J. Struct. Funct. Genomics.* **15(3)** (2014) 117

O-11 **Monday, 10.06., 17^{40}-18^{00}**

SOLARIS Special Session

X-ray optics for SOLCRYS beamline at SOLARIS

T.Kołodziej[1]*, D. Paliwoda[1] and M. Kozak[1]

[1]*National Synchrotron Radiation Centre SOLARIS, Jagiellonian University, Czerwone Maki 98, 30-392 Kraków, Poland*

Keywords: synchrotron radiation, crystallography, beamline design, optical simulations, ray tracing

*e-mail: t.kolodziej@uj.edu.pl

Significant number of users of synchrotron radiation for crystallographic research and growing interest of this kind of studies in Poland calls for the development of competitive beamline for such purposes at the new Polish synchrotron radiation facility.

SOLCRYS beamline at National Synchrotron Radiation Centre SOLARIS is one of the upcoming beamlines, dedicated to crystallographic research. The SOLCRYS beamline will be built thanks to the cooperation of the Jagiellonian University with the Joint Institute for Nuclear Research in Dubna (Russian Federation). The beamline is designed to operate in hard x-ray regime (5 – 25 keV photon energies). Since the machine is the low energy storage ring (1.5 GeV electron beam energy), various insertion devices, including superconducting wiggler are considered as potential sources of hard x-ray photon beams.

Construction of the beamline will have to meet a number of technical challenges, e.g. the length of the beamline (~45 m from the source) requires extension of the experimental hall, and since this will be first hard x-ray beamline at SOLARIS, adjustment of the infrastructures (e.g. cryogenic cooling of the optics, etc.) has to be prepared.

The beamline will consist of two branches. First one ("PX" branch) will be dedicated to macromolecular crystallographic research, protein crystallography, single crystal diffraction (also under extreme conditions), etc. The second one ("SAXS" branch) will be dedicated to small-angle x-ray scattering, especially for biological samples. Two separated endstations are supposed to operate simultaneously. Different scopes are considered for the beam-sharing, including cooled fixed mask (an idea similar to beamline BL14.1-3 at Bessy II, HZB [1]), or side-bounce mirror in the front-end section (outcoupling portion of the ID beam to one of the endstations).

Different specifics of the techniques exploited at two endstations call for different parameters of the beam delivered to the users, in the meaning of the flux, spot size, beam divergence and energy resolution. While at the PX branch we aim at the flux and focus, at the SAXS endstation desired shape and smallest achievable divergence of the beam is the goal. This calls for different optical layouts of two branches, regarding collimating the beam onto the monochromator for the best usage of the single crystal's Darwin width of the reflection, and focusing the beam on the sample position. Additionally, to maximize the flux at the SAXS branch, wide bandwidth monochromator based on the multilayer optics interchangeable with standard crystal monochromator is considered. Alternative options for the beam conditioning, like usage of the compound refractive lenses, Kirkpatrick-Baez mirrors, etc. will be discussed.

To evaluate the performance of the whole optical setup the optical simulations (geometrical ray tracing) have to be conducted. It was done with the use of the most popular codes: XOP/Shadow [2] and OASYS/ShadowOui [3]. Codes allow to model the performance of the complete beamline, from the generation of the radiation in the insertion device to the propagation of the x-ray beam through the optical system with the assumption of the realistic parameters of the elements (slope errors of the mirrors, reflectivity of the surfaces, etc.)

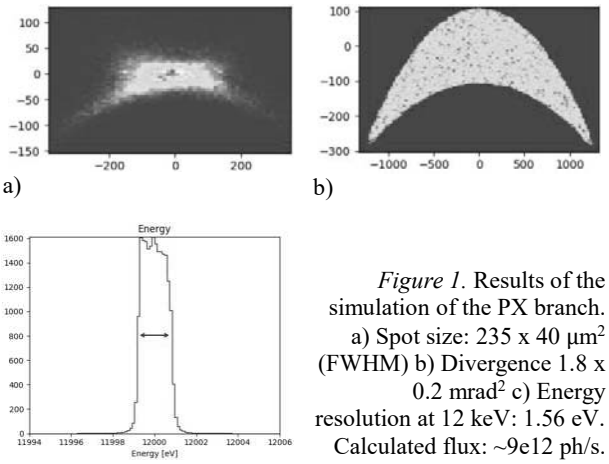

Figure 1. Results of the simulation of the PX branch. a) Spot size: 235 x 40 μm^2 (FWHM) b) Divergence 1.8 x 0.2 mrad^2 c) Energy resolution at 12 keV: 1.56 eV. Calculated flux: ~9e12 ph/s.

Possible equipment for the endstations including latest developments in the detectors, goniometers, sample changing robots, high pressure cells, etc. will be also presented.

[1] M. Gerlach, U. Mueller, M. S. Weiss,*Journal of large-scale research facilities* **2** (2016) A47.
[2] M. Sánchez del Río, R. J. Dejus. *SPIE proceedings* 8141 (2011).
[3] L. Rebuffi, M. Sanchez del Rio, *J. Synchrotron Rad.* **23** (2016) 1357–1367.

O-12 **Monday, 10.06., 18^{00}-18^{20}**

SOLARIS Special Session

XMCD beamline status

B. Wolanin[1]*, T. Sobol[1;2] and J. Szade[1;2]

[1]*National Synchrotron Radiation Centre SOLARIS, Jagiellonian University, Czerwone Maki 98,30-392 Kraków, Poland*
[2]*University of Silesia, Bankowa 12,40-007 Katowice, Poland*

Keywords: synchrotron radiation, free-electron laser, Solaris beamline, XMCD

*e-mail: barbara.wolanin@uj.edu.pl

The future XMCD beamline is based on the former beamline I1011 from MaxLab, Lund. In 2016 the I1011 beamline was transported to Solaris National Synchrotron Radiation Centre for reinstallation. Elliptically polarizing undulator will be implemented as a light source. The undulator can deliver linearly polarized radiation in the horizontal and vertical directions and left- and right handed circularly or elliptically polarized radiation.

The concept of the new XMCD beamline assumes the coexistence of two measurements branches with three experimental stations: octupole, PEEM (Photoemission Electron Microscope) and STXM (Scanning Transmission X-ray Micorscope). It also assumes the following parameters: energy range of 100 – 2000 eV, energy resolution $3x10^3$ – $1.5x10^4$, photon flux on the sample ~10^{12} ph/s/0.1%bw, spot on the sample: 104µm x 370µm for octupole, 5µm x 30 µm for PEEM, 500µm x 500µm for STXM.

The octupole end station will be dedicated to measurements of magnetic circular dichroism in the absorption of X-ray. The signal willbe measured by total electron yield or using total fluorescence yield.

The PEEM end station with standard equipment, will allow for preparation of the new samples/systems and for their modification in situ. The main advantage of the PEEM method is the ability to use different energy of excitations and to tune the energy to the characteristic edge of the absorption. The use of this technique provides information about sample topography, chemical contrast and magnetic contrast.

The STXM end station will provide chemical analysis in nanoscale because of connectionspectrometry with microscopy.

Acknowledgements: Reinstallation of the XMCD beamline is supported by Polish Ministry of Science and Higher Education.

O-13 **Monday, 10.06., 18^{20}-18^{40}**

SOLARIS Special Session

PHELIX – a new beamline at SOLARIS synchrotron

M. Szczepanik-Ciba[1]*, T. Sobol[1], and J. Szade[1;2]

[1]*National Synchrotron Radiation Centre SOLARIS in Kraków, Poland*
[2]*University of Silesia in Katowice, Poland*

Keywords: synchrotron radiation, beamline

*e-mail: magdalena.szczepanik-ciba@uj.edu.pl

PHELIX is a new beamline at National Synchrotron Radiation Centre SOLARIS in Kraków, using soft X-rays, the source of which is an Elliptically Polarizing Undulator APPLE II type with permanent magnets. This type of insertion device gives the opportunity to obtain variable polarization of light: from linear at any angle to elliptical. The maximum predicted size of the excited area on the sample is smaller than 100 µm × 100 µm with the resolving power (RP) at least 10 000 over the entire energy range (available range 30-1500 eV) and for all polarizations. The beamline itself will be shortly ready for the commissioning stage.

The PHELIX end-station will enable a wide range of spectroscopic and absorption studies (TEY and TFY modes) under UHV conditions, characterized by different surface sensitivity. A hemispherical photoelectron energy analyzer with the energy resolution of 1 meV enables to collect standard high-resolution spectra, to map the 3D band structure and detect the spin in three dimensions. Applying VLEED-type spin detector gives rise to the scattering probability of the electrons by a factor of ten comparing to the Mott detector. This, along with about two to four times higher sensitivity for spin polarization, results in a few tens times higher efficiency than for the Mott detector. The analysis chamber is equipped with additional sources of radiation (X, UV) allowing preliminary measurements without a beam.

The PHELIX end-station also allows to perform samples preparation with precise control of their thickness. A preparation chamber contains effusion cells and electron beam evaporators (EBVs), a LEED diffractometer, leak valves with different gases and a sample heating stage with the possibility to elevate the temperature up to 2000°C. The system is also equipped with an additional preparation chamber designed for reaction with gases (up to 800 mbar) and with a crystal cleaver chamber allowing to expose atomically smooth surfaces under ultra-high vacuum conditions.

The beamline is suitable for investigations of new materials for spintronics and magnetoelectronics, topological insulators, thin films and multilayers systems, surface of bulk compounds, surface magnetism, spin polarized surface states, chemical reactions taking place on the surface, biomaterials, etc.

Acknowledgements: The construction of the beamline is supported by the Polish Ministry of Science and Higher Education upon the decision 6582/IA/SP/2015**.**

O-14 **Monday, 10.06., 18^{40}-19^{00}**

SOLARIS Special Session

UARPES –high resolution photoelectron spectroscopy beamline at NSRC Solaris - Current state

N. Olszowska[1]* and J. J. Kołodziej[2]

[1]*NSRC Solaris, Czerwone Maki 98, 30-392 Kraków, Poland*
[2]*Institute of Physics, Jagiellonian University, Łojasiewicza 11, 30-348, Kraków, Poland*

Keywords: ARPES, photoemission, band structure, quantum materials, low dimensional solids

*e-mail: natalia.olszowska@uj.edu.pl

Angle-Resolved Photoelectron Spectroscopy (ARPES) technique allows for measurements of fundamental quantities, i.e. energy and momentum, describing a photoelectrons states outside of a solid sample. From this one can deduce the band (electronic) structure of the solid *E(k)*. The knowledge about the band structure is nowadays extensively employed for tailoring of functional materials and heterostructures for quantum-, opto-, spin- and magneto- electronic devices.

The beamline name UARPES arises by adding the letter *U* standing for *Ultra* to the usual acronym ARPES to indicate that the research installation is constructed for the efficient angle resolved photoelectron spectroscopy studies with the ultimate energy and angular resolution. Due to wide photon energy range and the full control over the UV beam polarization it facilitates the measurements of the full 3D band structure, i.e. $E(k_x, k_y, k_z)$, identification of surface and bulk states, and studies of some particular electron states by their selective excitation.

The UARPES installation has been designed to provide UV radiation in energy range 8-100 eV with photon flux on the sample > 5×10^{11} photons/s at full resolving power. It was assembled (2015)in result of a collaboration of Solaris (conceptual design, the backbone construction, and coordination), Elettra Sincrotrone Trieste (radiation source and the beamline),and Prevac (the endstation).

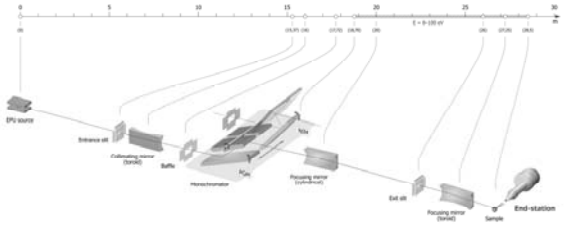

*Figure 1.*UARPES layout

The UARPES layout is presented in Fig. 1. It consistsof EPU (elliptically polarising undulator) as a source, baffles, collimating mirror, diffraction gratings, focusing mirror exit slit, refocusing mirror and the endstation.

The EPU, manufactured by Kyma S.r.l., is of the Apple II type.It is quasiperiodic to reduce unwanted harmonic contributions and provide a spectrally pure excitation beam. This feature is of a crucial importance for ARPES since high background levels and multiplied electron bands due to the undulator harmonics may be devastating for many experiments. The undulator works both in parallel and antiparallel modes to provide UV beams of every possible polarization (linear at any angle, circular left and right, elliptical).

UARPES beamline adopts a dual solution for a monochromator, including the PGM (Plane Grating Monochromator) and NIM (Normal Incidence Monochromator) availablealternatively. At the moment only PGM with 600 l/mm grating has been calibrated ands works correctly.The available energy range is 16.5-140 eV (higher than the designed range). The designed NIM range is 8-40 eV. Resolving power is up to 20 000 over the full energy range, giving for examplethe resolution around 1 meV at the lowest photon energies.

The heart of the endstation is a hemispherical (radius = 180 mm) electron spectrometer VG SCIENTA DA-30L which can measure the 3D photocurrent map $I(\phi,\theta,E)$ natively.Its angular resolution is 0.1° (corresponding to the k-vector resolution 0.002-0.01 $Å^{-1}$) and the energy resolution is 1.8 meV. The spectrometer works in two angular dispersive modes ± 7°, ± 15° recording 750 angular and 1000 energy channels in parallel. For automatic sequential measurements its software remotely controlsthe 5-axes cryogenic manipulator (three translation and two rotation axes). The sample temperature can be stabilized in the range 7-500 K (using LHe/LN_2 and a heater). The endstation is also equipped witha LEED diffractometer (OCI MCP-LEED)for surface structure studies.

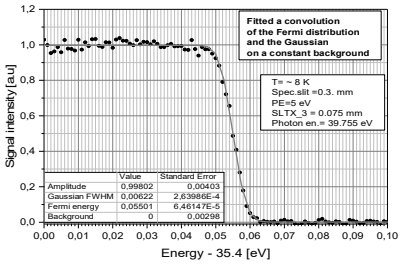

Figure 2. The Fermi step at 8 K on polycrystalline gold and fitted a convolution of the Fermi distribution and the Gaussian. The Gaussian width 6.0 meV for hν = ~40 eV and the exit slit opening 0.075 mm fully confirms that the beamline has reached the design parameters

The beamline has reached the designed performance – see Fig 2. The UV beam at the sample is~200 μm in diameter. In the users' opinion (2018 -)both the resolution and the fluxare very good and comparable to the state-of-the-art ARPES beamlines worldwide.

In the UHV preparation chamber the samples can be bombarded with Ar^+ ion beam and heated up to 1500°C. The chamber has two separable and retractable ports for connecting users' devices, for example effusion cells, easily (in future it will be upgraded to 4 ports). The preparation processes can be monitored by quartz crystal microbalance and RGA. In situ sample cleaving and exfoliation are also available. The prepared samples can be studied using MiniLEED and Auger RFA spectrometer. Up to 12 samples may be stored in UHV in queue to be measured.

O-15 **Tuesday, 11.06., 15^{40}-16^{00}**

X-ray absorption spectroscopy using laser plasma soft X-ray sources

P. Wachulak[1], T. Fok[1], A. Bartnik[1], K. Janulewicz[1] and H. Fiedorowicz[1]*

[1]*Instituteof Optoelectronics, Military University of Technology, Urbanowicza 2, 00-908 Warsaw, Poland*

Keywords: X-ray absorption spectroscopy, NEXAFS, EXAFS, laser plasma soft X-ray sources

*e-mail: henryk.fiedorowicz@wat.edu.pl

In the paper laboratory systems for X-ray absorption spectroscopy (XAS) measurements based on laser plasma soft X-ray sources are presented. Soft X-rayradiation in the wavelength between 3.5 nm and 5.5 nm, corresponding to the photon energy range of about 220-670 eV, is emitted from a laser plasma produced as a result of the interaction of nanosecond laser pulses with a gas puff target. Commercially available Nd:YAG laser systems (EKSPLA) generating 4 ns pulses with energy up to 0.8 J or 1 ns pulses with energy up to 10 J at 10 Hz repetition rate are used to irradiate the targets formed by pulsed injection of working gas (Kr) in an additional annular stream of He gas under high-pressure using a double-nozzle set up (the double-stream gas puff target approach [1]).

Various laboratory systems for XAS measurements with the use of these sources have been developed at the Institute of Optoelectronics MUT. Compact, desk-top system for near-edge X-ray fine structure (NEXAFS) spectroscopy was presented [2]. Soft X-ray spectra have been measured using a grazing incidence grating with 2400 lines/mm (Hitachi) coupled to a CCD camera. 2-D elemental mapping of the PET polymer sample modified with EUV photons was demonstratedusing the NEXAFS spectromicroscopy technique and the compact XAS system [3]. Single-shot NEXAFS spectroscopy was also presented using the XAS system with the10 J laser [4]. It makes possible to perform time-resolved NEXAFS studies on a ns time-scale. Moreover, measurements of titanium L-edge EXAFS have been recently performed with the use of the compact XAS system [5]. The developed laboratory XAS systems and the results of the NEXAFS and EXAFS studies are presented.

Acknowledgements: This work was supported by National Science Centre (NCN) (UMO-2015/17/B/ST7/03718, UMO-2015/19/B/ST3/00435) and the European Union's Horizon 2020 research and innovation program Laserlab-Europe IV (654148) .

[1] H. Fiedorowicz, A. Bartnik, R. Jarocki, R. Rakowski, M. Szczurek, *Appl. Phys. B* **70** (2000) 305-308.
[2] P. Wachulak, M. Duda, A. Bartnik, A. Sarzyński, Ł. Węgrzyński, M. Nowak, A. Jancarek, H. Fiedorowicz, *Opt. Express* **26** (2018) 8260.
[3] P. Wachulak, M. Duda, A. Bartnik, A. Sarzyński, Ł. Węgrzyński, H. Fiedorowicz, *Spectrochim. Acta B* **145** (2018) 107-114.
[4] P. Wachulak, M. Duda, A. Bartnik, T. Fok, Z. Wang, Q. Huang, A. Sarzyński, A. Jancarek, H. Fiedorowicz, *Materials* **11** (2018) 1303.
[5] P. Wachulak, T. Fok, A. Bartnik, H. Fiedorowicz, Measurements of titanium L-edge EXAFS using a laboratory system based on a laser plasma soft X-ray source (2019) – submitted.

O-16 **Tuesday, 11.06., 16^{00}-16^{20}**

Nanometer resolution optical coherence tomography (OCT) using a compact laser plasma soft X-ray source

K. A. Janulewicz[1]*, P. Wachulak[1], J. A. Arikkatt[1], A. Bartnik and H. Fiedorowicz[1]

[1]*Institute of Optoelectronics, Military University of Technology, gen. W. Urbanowicza 2, 00-908 Warsaw, Poland*

Keywords: soft X-rays, X-ray tomography, X-ray imaging

*e-mail: karol.janulewicz@wat.edu.pl

Optical coherence tomography (OCT) is a well-established interferometric imaging technique providing high resolution cross-sectional views of objects (tomograms). The axial resolution of OCT is limited to about 1 μm when using infrared and optical wavelengths. An obvious way to improve the resolution is to shorten the wavelength of the probing light. Optical coherence tomography using broad bandwidth radiation in the nanometer spectral range (extreme ultraviolet and soft X-rays) has been proposed and demonstrated recently. This variant of OCT, referred to as XCT, allows for a reduction of the axial resolution from micrometers to a few nanometers. The XCT imaging with an axial resolution better than 8 nm was demonstrated using extreme ultraviolet and soft X-rays from a synchrotron. Tomographic imaging with an axial resolution of about 22 nm has been recently demonstrated using extreme ultraviolet from a laser-driven light source based on high-order harmonic generation (HHG). In this paper we present preliminary studies on XCT using broadband soft X-ray radiation from a compact laser plasma light source. The laser plasma was formed by the interaction of a nanosecond laser pulse with a gaseous target in a double-stream gas puff target approach. The laser plasma source was optimized for efficient soft X-ray emission from the krypton/helium gas puff target in the spectral range from 1.5 nm to 5 nm, containing the 'water-window' spectral range from 2.3 nm to 4.4 nm, particularly useful for imaging of microbiological objects. The coherence parameters of the soft X-ray radiation allowed to perform the XCT measurements of a bulk multilayer structure with 10 nm period and 40 % bottom layer thickness to period ratio, with an axial resolution of about 2 nm and detect multilayer interfaces up to a depth of about 100 nm. The experimental data are in agreement with OCT simulations performed on ideal multilayer structure. In the paper, detailed information about the source, its optimization, the optical system, XCT measurements and the results are presented and discussed. Planned works aimed at obtaining 3-D images using a compact laser plasma soft X-ray source will be shown.

Acknowledgements: This work was supported by Polish NCN within the Beethoven project.

O-17 **Tuesday, 11.06., 16^{20}-16^{40}**

Ultra-fast core-level dynamics in semiconducting WSe_2

M. Dendzik[1]*, R. P. Xian[1], D. Kutnyakhov[2], S. Dong[1], F. Pressacco[3], D. Curcio[4],S. Agustsson[5], M. Heber[2], J. Hauer[1], W. Wurth[2;3], G. Brenner[2], Y. Acremann[6], P. Hofmann[4], M. Wolf[1], L. Rettig[1], and R. Ernstorfer[1]

[1]*Fritz Haber Institute of the Max Planck Society, Faradayweg 4-6, 14915 Berlin, Germany*
[2]*DESY Photon Science, Notkestr. 85, 22607 Hamburg, Germany*
[3]*CFEL, Hamburg University, Luruper Chausee 149, 22761 Hamburg, Germany*
[4]*Aarhus University, 8000 Aarhus C, Denmark*
[5]*JGU Mainz, Staudingerweg 7, 55128 Mainz, Germany*
[6]*ETH Zurich, Otto-Stern-Weg 1, 8093 Zurich, Switzerland*

Keywords: free-electron laser, core-level spectroscopy

*e-mail: dendzik@fhi-berlin.mpg.de

The development of femtosecond XUV sources such as the Free-Electron Laser FLASH [1] combined with recent improvements of electron detection (momentum microscopy [2]) enables studying ultra-fast processes governing the excitations of core-level electrons. Here we present a study of femtosecond dynamics of W4f core levels in semiconducting WSe_2. We find that pumping A-exciton at 800 nm induces changes of both position and shape of observed spectra. In particular, we find a distinct change of the symmetric Lorentzian line profile into a metal-like Doniach-Šunjić asymmetric line shape. We follow the time evolution of induced changes and compare it with the dynamics of valence electrons [3].

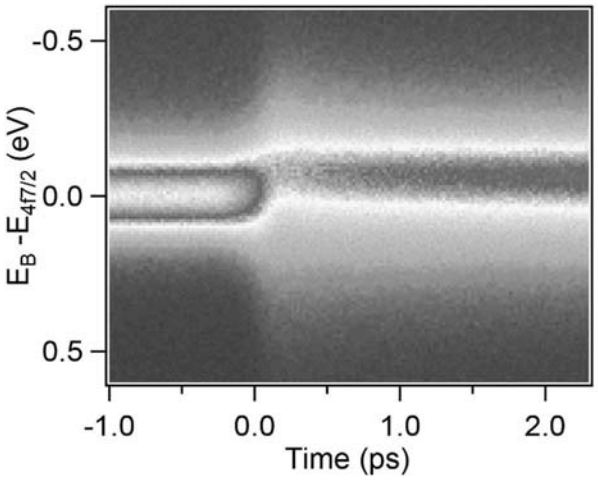

Figure 1. Time-resolved W 4f core-level spectrum. Photoemission intensity is represented with a false-color scale and plotted against the pump-probe time delay

[1] W. Ackermann *et al*., *Nat. Photonics* **1** (2007) 336.
[2] S.V.Chernov *et al.*, *Ultramicroscopy* **159** (2015) 453.
[3] R. Bertoni *et al.*, *Phys. Rev. Lett.* **117** (2015) 277201.

O-18A **Thursday, 13.06., 16^{50}-17^{10}**

Photon beams and experimental stations at the PolFEL free electron laser facility

R. Nietubyć[1], W. Bal[2], A. Bartnik[3], P. Czuma[1], H. Fiedorowicz[3], K. Janulewicz[3], P. Krawczyk[1], N. Pałka[3], J. Poznański[2], J. Sekutowicz[1;4], M. Staszczak[1], J. Szewiński[1], K. Szamota –Lenaderssson[1], P. Wachulak[3] and P. Zagrajek[3]

[1]*Narodowe Centrum Badan Jądrowych, Swierk, Soltana 7, Otwock-Świerk, Poland*
[2]*Institute of Biochemistry and Biophysics, Pawińskiego 5a, 02-106 Warsaw*
[3]*Institute of Optoelectronics, Military University of Technology, Kaliskiego 2, 00-908 Warsaw*
[4]*Deutsches Elektronen Synchrotron DESY, Notkestrasse 85, 22-607 Hamburg Germany*

Keywords: free electron laser, beamlines

*e-mail: r.nietubyc@ncbj.gov.pl

PolFEL, free electron laser proposal was last year accepted, the realisation of which proceeds in the prospect of entirely superconducting accelerator for continues wave (cw) and long pulses (lp) operation. Besides the photon beams provided to the experimental end stations, the gain of the accelerator physics and engineering capabilities are a desired benefit of this project. The striving to attain VUV ranged beam in spite of limited electrons energy brings forth the need of a challenging, short period undulator design and impels to minimize an electron beam emittance. We dedicate an augmented efforts to achieve these crucial characteristics while the matured solution will be utilized for the less critical systems.

PolFEL will be furnished with three undulators chains settled in the two accelerator branches. The full energy branch including four Rossendorf-like acceleration cryomodules and a bunch compression inserted in a midway, will provide and electron beam with energy up to 130 MeV in cw mode and up to 180 MeV in lp mode, milliseconds, to the chain of 16, Halbach-type. 0.7 m long undulators modules, having 1.8 cm period. Outcoming radiation will ranged from 5 μm down to 180 nm in the fundamental wavelength and to 60 nm in the third harmonic one. Pulse energies will range from 5 μJ to 20 μJ and from 50 nJ to 200 nJ, respectively. Such modular undulators will be constructed for all chains, differing in period, gap length. Low energy branch will split off the linac between the second cryomodule and bunch compressor. It will provide the electrons with energies up to 60 and 80 MeV in cw and lp modes, respectively. The IR undulator will be settled there, and consisted of 6 modules having 4 cm long period. The radiation wavelength will cover the spectral range from 5 μm up to 50 μm and will be emitted in pulses of energy reaching 20 μJ. THz radiation in the range of so called "terahertz gap" i.e. 0.3 THz – 5 THz will be generated with a superradiant undulator settled at the same branch, next to IR chain. It will consist of 4 modules of 17.5 cm in period and will emit pulses of energy between 1 μJ and 3 μJ.

Two photon beamlines will be constructed adjoined to the VUV and IR or THz undulators chains. In both of them the photon diagnostic setups followed with an experimental stations capable for the rudimental experiments will be installed. Such equipped beamlines will stay ready for the development specific to particular spectroscopic, imaging and surface modification applications risen. Accompanying, synchronised optical laser beams will be provided to each FEL endstation for the temporary resolved pump and probe experiments.

The VUV beamline emptied down to 10^{-9} mbar will be separated from the accelerator with a differential pumping stage and a safety valve system. It will be composed of steering mirrors chamber, gas attenuator, gas monitor for the absolute photon flux, beam focusing system and the experimental – interaction chamber. The arrangement will be accompanied with the diagnostic tools monitoring parameters of the VUV ($h\nu \approx 20$ eV, $\lambda \approx 60$ nm) photon beam. The installed instrumentation and the pump-probe setup will allow for time-resolved photoionization and photoemission experiments as well as for investigations of the laser-solid matter interactions on the femtosecond time scale.

The THz beamline will be first monitored to determine wavelength, energy, and pulse duration. It is planned to divide the beam into a few reconfigurable research stations to carry out pump-probe experiments, to measure reaction of the short high-energy THz pulses with matter including low-temperature and high-magnetic field experiments, to characterize THz devices e.g. detectors, to study superconductivity phenomena, and to analyze absorption and emission in gases, liquids, molecules, solids.

The stopped-flow instrument will be used to study fast reactions of biomolecules monitored with fluorescence and light scattering detection in UV-Vis range. The THz radiation will be adapt to spectroscopic measurements of biological samples.

Femtosecond x-ray pulses in the kiloelectronvolt range will be generated in Compton backscattering process employing the accelerated electron beam and photon beam form auxiliary optical laser.

Acknowledgements: The PolFEL project received funding from the European Regional Development Fund in the framework of the Smart Growth Operational Programme, Measure 4.2: Development of modern research infrastructure of the science sector, for which we want to express our gratitude. We are also grateful to all Consortium Members and Industry for their contributions to the project.

O-19A **Thursday, 13.06., 17^{10}-17^{30}**

The structure evolution of the self-regenerative doubly doped CeO

E. Piskorska-Hommel[1]*, D. Kowalska[1], P. Kraszewski[1] and M. Kurnatowska[1]

[1]*Institute of Low Temperature and Structure Research, Polish Academy of Sciences, W. Trzebiatowski Institute, Wrocław, Poland*

Keywords: XAFS, cerium oxides, catalysts

*e-mail: e.piskorska@intibs.pl

Worldwide regulations on emission require from automotive manufacturers cleaner and efficient work devices. The exhaust system in particularly its part, commonly referred to as catalysts is responsible for the emission reducing.The main catalysts task is to reduce the harmful exhaust components.Catalytic converters can be two types reduce and oxidizing catalysts.The first one only reduces the content of nitrogen oxides in the exhaust gases, the second reduces only the content of carbon monoxide and hydrocarbons. Due to the growing requirements of emission standards, single catalytic reactors are replaced by systems of several reactors. They are so-called three-way reactors (TWC), reduce nitrogen oxides (NO_x), oxidizing hydrocarbons (HC) and carbon monoxide (CO) simultaneously. Cerium oxide (CeO_x) is known and widely used in the three-way catalytic converter as an oxygen storage medium and thermal stabilizer [1, 2].

Redox reactions of material regulate its catalytic activity. The understanding the redox kinetics of catalysts is important to gain comprehensive knowledge about catalytic properties and control their geometric structure, oxidation states, and metal-support interaction. We successfully synthesized homogeneous, easily reducible oxide with high capacity of oxygen storage; and 3 nm crystallite size CeO mixed oxides [3]. In situ X-ray Absorption Fine Structure (XAFS) investigations of the Pd local structure have been performed for the doubly doped cerium oxides $Ce_{1-x-y}Yb_yPd_xO_2$ and for $Ce_{1-x}Pd_xO_2$under redox condition as a function of the temperature. The absorption edge position and the shape of the XANES spectrum are sensitive to coordination chemistry and it can provide information on, e.g., the oxidation states of the elements under inspection. The EXAFS oscillations are created due to the scattering of internal photoelectrons on neighbor, therefore, the analysis of these oscillations is a source of information of the local structure in the vicinity of the absorbing atoms. In the present case, this allows to probe changes of the bond lengths and of the atomic coordination of Pd atoms. The properties of the XAFS analysis provide unique information about the interaction between ceria and noble metals as well as explain the influence of the ytterbium on the properties of the ceria mixed oxide doped with palladium.

Pd dispersed on CeO_2 significantly increases catalytic activity of the catalysts[3] and is a good candidate for the TWCs due to the high hydrogenation activity and CO removal.The ytterbium (Yb) doping effects on cerium oxide crystallites during heating at high temperatures in a reducing and oxidizing atmosphere [4]. Moreover, Yb doping ceria is implementing stable oxygen defects in the lattice.

In the reported paper the detailed Pd local structure analysis will be presented.

Acknowledgements: The authors acknowledge the Synchrotron SOLEIL for provision of synchrotron radiation facilities.We would like to thank dr. Andrea Zitolo for assistancein using beamline SAMBA. This work was financially supported by the National Science Center in Poland (grant 2015/19/D/ST5/00722). Supported by the Foundation for Polish Science.

[1] S. Hosokawa, M. Taniguchi, K. Utani, H. Kanai, S. Imamura, *Appl. Catal., A* **289** (2005) 115–120.

[2] F.L. Normand, L. Hilaire, K. Killi, G. Krill, G. Maire,*J. Phys. Chem.* **92** (1988) 2561- 2568.

[3] M. Kurnatowska, E. Piskorska-Hommel, P. Kraszkiewicz, M.J. Winiarski, *Mater. Chem. Phys.***229** (2019) 49-55.

[4] M. A. Małecka, J. J. Delgado, L. Kepinski, J. J. Calvino, S. Bernal, G. Blanc, X. Chen,*Catal. Today* **187** (2012) 56.

O-20A **Thursday, 13.06., 17^{30}-17^{50}**

Structural insight into thymidylate synthase inhibition by N^4-OH-dCMP

P. Maj[1]*, P. Wilk[2;3], A. Jarmuła[1], A. Dowiercial[1] and W. Rode[1]

[1]*Nencki Institute of Experimental Biology PAS,Pasteura 3, 02-093 Warszawa, Poland*
[2]*Helmholtz-Zentrum Berlin, Macromolecular Crystallography, Albert-Einstein-Str. 15, 12489 Berlin, Germany*
[3]*Structural Biology Core Facility, Malopolska Centre of Biotechnology, Gronostajowa 7A, 30-387 Kraków, Poland*

Keywords: protein crystallography, thymidylate synthase, inhibition

*e-mail: p.maj@nencki.gov.pl

Reaction catalyzed by thymidylate synthase (TS; EC 2.1.1.45) is the sole *de novo* source of dTMP, one of the precursors in DNA biosynthesis. TSis a molecular target for chemotherapyaimed at cancerand several types of infections.

FdUMP, the active form of several drugs, is a time- and cofactor-dependent inhibitor of TS. It blocks TS activity by participating in the formation of a covalently-bound ternary complex (PDB ID: 5FCT) with the enzyme and the cofactor (me THF) [1]. N^4-OH-dCMP is another time- and cofactor-dependent TS inhibitor, suggestingits molecularinhibition mechanismto be the same as that of FdUMP.

However, structural data showedthat N^4-OH-dCMP acts differently. Crystal structure of mouse TS cocrystallized with N^4-OH-dCMP and meTHF (PDB ID: 4EZ8) revealed a covalently-bound complex of TS with the inhibitor (the pyrimidine ring is apparently reduced) and a non-covalently bound DHF molecule [2]. meTHF underwent conversion to DHF with parallel reduction of the inhibitor's C(5) atom and release of the methylene groupto an unknowndestination, but not to the C(5) atom (as is the case in both the physiological reaction with dUMP and mechanism-based binding with FdUMP). The latter observation is further supported by analogous crystal structure of *Trichinella spiralis* TS (PDB ID: 5M4Z) showing that N^4-OH-dCMP mode of action remains the same irrespective of the enzyme specific origin. Of note, 5M4Z structure is missing DHF molecules that were most likely released from the active sites before the crystallization.N^4-OH-dCMP apparently uncouples two parts of TS catalytic reaction that usually occur simultaneously, *i.e.* (i) methylene group transfer from meTHF to the C(5) atom of the pyrimidine ringand (ii)reduction of the methylene group and oxidation of the remaining tetrahydrofolate do DHF. Still, the two structures leave a gap in our understanding of N^4-OH-dCMP inhibition mechanism – they cannotpinpoint a direct cause preventing the transfer of the methylene group.Crystal soaking technique was employed,by soakingcrystals of mouse binary TS-N^4-OH-dCMP complex in meTHF solutions. Applying correct soaking conditions yielded a structure with the cofactor molecule in a previously unobserved form. Imidazolidine ring underwent opening in such a manner that the single-carbon group remained bound covalently to the N(10) atom. This is in contrast with the mechanism of both the physiological reaction and the mechanism-based FdUMP binding when the single-carbon group istemporally or stably bound to the N(5) atom.The unusual imidazolidine ring opening results in a much larger distance between the single-carbon group and the C(5) atom of the inhibitor's pyrimidine ring, directly eliminating the possibility of a covalent interaction (Figure 1). Mediocre resolution (2.13Å) of the structure (PDB ID: 6F6Z) does not allow identification of more subtle structural features of ligands, *e.g.* oxidation state of the single-carbon group. However, the ring opening described above, as well as the lack of covalent bound between N^4-OH-dCMP and catalytic cysteine residue are evident.

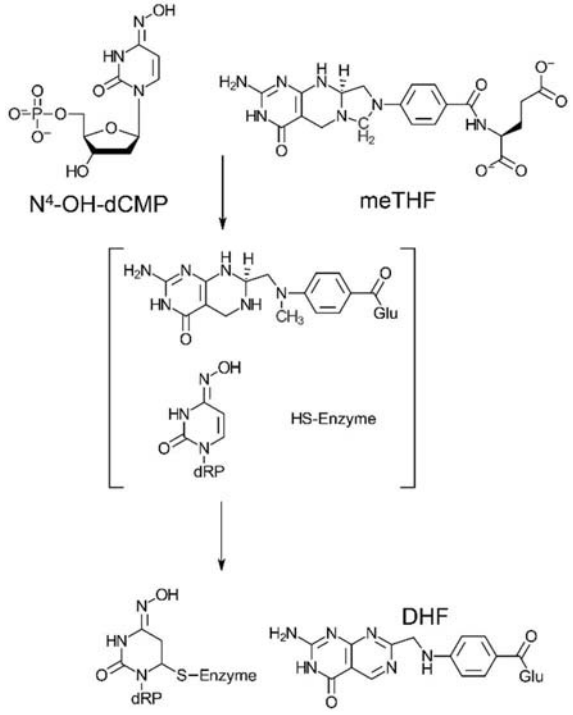

Figure 1. TS inhibition caused by N^4-OH-dCMP

Intermediate reaction step captured by 6F6Z structure shows why the single-carbon group is not transferred from meTHF to the C(5) atom of the pyrimidine ring. However, further fate of the single-carbon (methylene) group, the exact mechanism causing the unusual imidazolidine ring opening, and the mechanism of N^4-OH-dCMP pyrimidine ring reduction and formation of covalent bond with catalytic cysteine residue all require additional experiments and explanation.

Acknowledgements: This work was supported by National Science Centre grant No. 2016/21/B/NZ1/00288.

[1] A. Dowiercial *et al.*,*Struct. Chem.* **28** (2016) 667-74.
[2] A. Dowiercial *et al.*, *Pteridines* **24** (2013) 93-8.

O-21A **Thursday, 13.06., 17^{50}-18^{10}**

Cr $K\beta_{1,3}$ RXES reveals heterogeneity of Cr binding site types in various artificial lipid membranes

M. Nowakowski[1]*, A. Wach[1], J. Szlachetko[1], J. Czapla-Masztafiak[1], A. Kalinko[2], W. Caliebe[3] and W. M. Kwiatek[1]

[1]*Institute of Nuclear Physics Polish Academy of Sciences, PL-31342 Krakow, Poland*
[2]*University of Paderborn, Warburger Str. 100, 33098 Paderborn, Germany*
[3]*Deutsches Elektronen-Synchrotron, Notkestraße 85, 22607 Hamburg, Germany*

Keywords: synchrotron radiation, RXES, chromium, lipid membranes

*e-mail: michal.nowakowski@ifj.edu.pl

Hexavalent chromium (Cr(VI) compounds) is highly reactive, toxic and cancerogenic factor that has ability to pass through lipid membranes [1]. In contrary, Cr(III) is stable, considered as a much safer type of chromium than Cr(VI) and in comparison to Cr(VI), its membrane permeability is negligible. In case of natural cellular membranes it was proven, that Cr(VI) is being transported with the use of the anion exchange mechanism in anionic membrane transporters [2][3][4]. However, this mechanism does not explain high permeability ratio of Cr(VI) through cellular membranes, because free radicals generated during reduction from Cr(VI) to lower oxidation states in presence of common organic reductors should quickly damage anionic channels disabling ionic transport. This may be explained by our hypothesis [5] of permeation of Cr(VI) through pure lipid membrane with simultaneous Cr(VI) reduction accompanied by permanent binding of Cr to membrane content.

In current research we have determined the exact Cr binding sites in artificial lipid membranes by the use of RXES technique applied to DMPC and DMPC:DOPE liposomes in 1:1 and 1:10 ratios measurements. The experiment was conducted at P64 beamline in Hasylab, DESY. Measurements were taken at 10 K on dried liposomal samples, which were previously subjected to interaction with Cr(VI). By analysing changes in Cr $K\beta_{1,3}$ line, Cr K-edge pre-edge features visible on ΔRXES maps and by performing DFT based geometry study, we have proposed and confirmed model of two coexisting Cr chemical neighbourhoods. Two distinguished binding sites were present in hydrophilic part of membrane as well as inside hydrophobic part. This supported our hypothesis about creation of hydrophilic channels inside lipid membranes.

Our research complements and supports previous results [5]. Beyond that, data obtained suggests that Cr poisoning is in fact more complex process, which include acute and chronic phases. This finding is a first step of developing more accurate treatment of Cr intoxication.

Acknowledgements: Authors would like to acknowledge National Science Centre, Poland (NCN) for support under grant no. 2016/23/N/ST4/01601 .

[1] A. K. Das, *Coord. Chem. Rev.* **248** (2004) 81.
[2] J. Alexander, J. Aaseth, *Analyst* **120** (1995) 931.
[3] N. Farkas, M. Pesti, J. Belagyi, *Biochim. Biophys. Acta - Biomembr.* **1611** (2003) 217.
[4] N. S. Raja, K. Sankaranarayanan, A. Dhathathreyan, B. U. Nair, *Biochim. Biophys. Acta - Biomembr.* **1808** (2011) 332.

O-22A **Thursday,13.06., 18^{10}-18^{30}**

Extended Abstract

X-ray studies of charge correlations in cuprates under extreme conditions

I. Biało[1;2]*, W. Tabiś[1;2] and N. Barišić[2;3]

[1]*AGH University of Science and Technology, Faculty of Physics and Applied Computer Science, 30-059 Krakow, Poland*
[2]*Institute of Solid State Physics, TU Wien, 1040 Vienna, Austria*
[3]*Department of Physics, Faculty of Science, University of Zagreb, HR-10000 Zagreb, Croatia*

Keywords: uniaxial pressure, pulse magnetic field, resonant ResonantX-ray scattering, X-ray absorption spectroscopy

*e-mail: izabela.bialo@fis.agh.edu.pl

After more than thirty years since the high temperature superconductivity (high-Tc) was discovered, it is still unclear what is the mechanism driving this phenomenon. The charge correlations, which coexist and compete with the superconducting phase, may hold the key to understand this important issue.

With decreasing the temperature, close to the transition temperature (Tc),a rich variety of correlations appear (electronic-nematic fluctuations, spin or charge waves). The delicate balance among the coexisting effects makes it hard to identify the principal interactions between themand observe them experimentally.In our research, we usedsome of the most powerful synchrotron techniques incombination with extreme conditions (uniaxial pressure and high magnetic pulse fields) to investigate the interaction between superconductivity and one of the ordered phase – the Charge Density Wave (CDW) order.First, I will present the most recent design and development of the instrumentations for synchrotron beamlines. Furthermore, I will discuss our study of the CDW correlations in selected cuprates, using X-ray absorption spectroscopy under pulsed magnetic fields up to 28 T and resonant X-ray scattering under uniaxial pressure.

The CDW correlations are described as charge modulationswithin thecopper-oxygen planes, the main building block of the cuprates (copper-based superconductors). These correlations were first found in the curate $YBa_2Cu_3O_{6+\delta}$ (YBCO) by means of resonant X-ray scattering and X-ray diffraction studies, and then successfully detected in other cuprates, demonstratingtheir universal presence in this group of materials [1,2,3].

Following the initial discovery of the incommensurate CDW order in underdoped YBCO, we have extensively studied the CDW correlations in the model,hole doped cuprate$HgBa_2CuO_{4+d}$ (Hg1201). The observed doping dependence of the CDW wavevector, along with tight-binding calculations, provides strong evidence for Fermisurface reconstruction by bidirectional (*checkerboard*) CDW order [5,6].In contrary, resonant X-ray scattering measurements in YBCO demonstrated that the CDW order is consistent of locally unidirectional *stripes* [7]. Subsequent hard X-ray diffraction experiments, in which atomic displacements associated with the CDW order were studied, are inconsistent with stripe order and suggest *checkerboard*-type order, in accordance with our results [8]. In light of these contradicting results, anovel approach of studying charge correlations is needed.

We employed a uniaxial pressure as a symmetry breaking field thatdeforms not only the structure and a local electronic environment of the material but also has an impact on the charge correlations along copper-oxygen planes. If the CDW order's form factor is compatible with the *stripe* picture, applying the external pressure along one of the axes in copper-oxygen planes is expected to align the CDW domains making the two suggested models (*checkerboard* and *stripes*)distinguishablein the X-ray scattering experiments.

The effect of uniaxial pressure on the electronic order was studied in the model, tetragonal, electron doped cuprate$Nd_{2-x}Ce_xCuO_4$ (NCCO). Using He_2 gas-driven pressure cellstress is applied along one of the [010] crystallographic directions, and theresonant X-ray scattering measurements at the copper L_3-edgewere performed at the UE46-PGM1 beamline of BESSY II in Berlin.

The pressure device is based on a solution where He_2 gas is injected to one of two bellows. The pressurized gas drives the piston and creates pressure on the sample. While one of the bellows induces the compressing force, the secondone generates the tensile force. The cell is connected to the gas supply by means of small capillaries, allowing thusthe in-situ control of the applied pressure from the outside of the XUV chamber. It also allows compensating the changes in the pressure caused by the temperature variation.

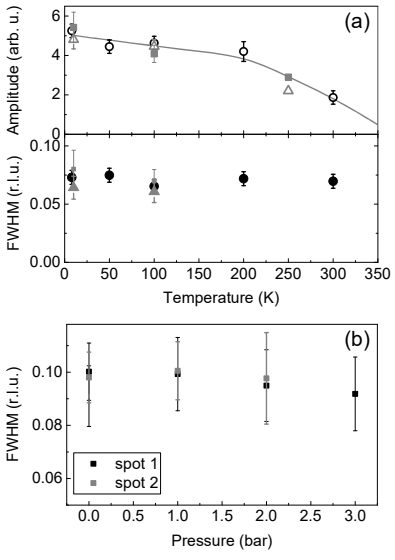

Figure 1. (a) Temperature dependence of the amplitude and width of the CDW peak in NCCO (x=0.11). (b) Pressure dependence of the CDW peak in NCCO. The parameters are extracted from the Gaussian function fit to the experimental data. The error bars corresponds to the fitting uncertainty. The different collors correspond to different spots on the samples the data were collected

The results indicate that the effect of the applied pressure does not significantly modify the CDW order (Figure 1).The very minimal decrease of the correlation length is consistent withthe scenario,where the CDW order is *checkerboard*-type. The external pressureslightly interrupts the correlation length, rather than significantly influencing the CDW peak, as expected for the *stripe*-like order.

Recent X-ray diffraction studies [9] demonstrated that uniaxial pressure applied along the cooper oxygen planes inorthorhombic YBCO may cause change in the amplitude of the CDW effect, and furthermore generate anaddition to the previously discussed charge correlations. These induced charge modulations are also correlated in the direction perpendicular to the planes, and thus called three-dimensional (3D) CDW order. Similar 3D CDW order has been demonstrated at external magnetic fields above approximately 18 T,in the same compound [10]. Thus a natural question arises regarding the origin of 3D CDW effect and its impact on superconductivity.

We have addressed this question by performing systematic X-ray absorption spectroscopy measurements at the Cu K-edge in pulsed magnetic fields up to 28 T in single crystals of YBCO ($\delta = 0.55$), Hg1201 ($p \approx 0.9$), $La_{2-x}Sr_xCuO_4$ ($x = 0.125$) and NCCO ($x = 0.15$). The doping level for each compound was selected such that the CDW order, in the absence of magnetic field, is maximized. Since the field-induced 3D CDW correlations were previously detected only in YBCO, the first aim was to determine if the field-induced transition is a generic behaviour for all cuprates. The second one was to determine which of the structural components (copper-oxygen layer, reservoir layer) contribute to the formation of the novel field-induced electronic order in YBCO.

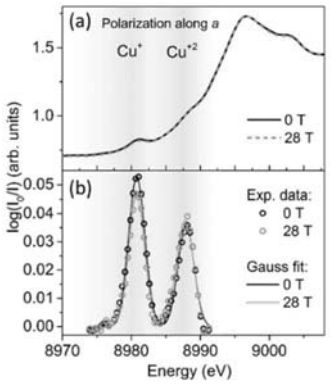

Figure 2. (a) X-ray absorption spectra of YBCOwith the polarization along a axis (also perpendicular the copper-oxygen chains). The absorption edge features two distinct peaks originating from two inequivalent copper valences, Cu^+ and Cu^{2+} at 8983 and 8988 eV, respectively. (b) Spectra from panel (a) after subtracting the step at the absorption edge. The two pre-peaks are prominent

The experiment was performed at energy dispersive-X-ray absorption beamline in ID24, ESRF.The beamline is particularly suited for the time-resolved experiments in pulsedfields due to the simultaneous acquisition of the absorption spectra in the entire energy range. The combinationof the dispersive method and multiframe detection system allows the precise determination of the small valence(or absorbing atoms surroundings) changes, as the full-energy spectra and field-dependences are measured at thesame time rather than constructed point by point.The presented technique is unique on a world-wide scale and has been developed in collaboration with LNCMI Toulouse and the ESRF in Grenoble.As X-ray absorption near edge spectroscopy is site elective probe it can differ between two nonequivalent cooper statesin YBCO structure. The observation of the changes in the lower-energy peak (Figure 2)intensity (associated to Cu^+ ions within the cooper-oxygen chains) indicates that the chains, characteristic for YBCO, contribute to the formation of the high magnetic field induced 3D CDW order. The initial analysis points towards the possibility that the field induced state may be specific to YBCO due to the underlying crystal structure (e.g., the existence of the copper-oxygen chains, orthorhombic distortion). This conclusion is further supported by the lack of the magnetic field induced changes in the absorption spectra in Hg1201, LSCO and NCCO.

In summary, the existence of contradicting results regarding the nature of the CDW correlations in the cuprates required additional verification. Solving this issue required an unconventional approach. In this work, twosuch novel experimental setups in combination with synchrotron X-rays were used. The presented studies, performed in the extreme conditions allow to distinguish between to proposed models of the form factorof the CDW order. It furthermore provides the clue regarding the origin of the field-induced 3D CDW order in the cuprates.

Acknowledgements: This work was supported bythe European Research Council (ERC Consolidator Grant No725521).

[1] J. Chang *et al.*, *Nature Phys.* **8** (2012) 871.
[2] G. Ghiringhelli *et al.*, *Science* **337** (2012) 821.
[3] S. Blanco-Canosa *et al.*, *Phys. Rev. B* **90** (2014) 054513.
[4] D. Pelc *et al.*, *Science Adv.* **5** (2019) 1.
[5] W. Tabis *et al.*, *Nature Comm.* **5** (2014) 5875.
[6] W. Tabis *et al.*, *Phys. Rev. B* **96** (2017) 134510.
[7] R.Comin, A. Damascelli, *Annu. Rev. Condens. Matter Phys.***7** (2016) 369.
[8] E.M.Forgan. *et al.*, *Nat. Comm.* **6** (2015) 10064.
[9] H.-H. Kim *et al.*,*Science* **362** (2018) 1040–1044.
[10] S. Gerber *et al.*, *Science* **350** (2015) 949.

O-23A **Thursday, 13.06., 18^{30}-18^{50}**

3D Multipoint-projection X-ray microscopy

K. M. Sowa[1]*, M. P. Kujda[1] and P. Korecki[1]

[1]*Institute of Physics, Jagiellonian University, Kraków, Poland*

Keywords: X-ray tomography, polycapillary optics, single exposure 3D imaging

*e-mail: k.sowa@doctoral.uj.edu.pl

The inspiration of multipoint-projection X-ray microscopy comes from our recent work, in which we showed that point defects in the structure of a polycapillary optical element directly lead to the formation of high resolution X-ray projections of objects that are placed at the focal plane of the optics [1]. However, the main problem of this defect-assisted method is randomness and lack of control over the distribution of defects. Although tailored optics would be a solution for such an issue, fabrication of tailored optical element is a hard and demanding task. In this presentation we show that this problem can be overcome in multipoint-projection microscopy [2]. An array of multiple mutually incoherent but partially coherent secondary X-ray micro-sources are multiplexed at the object placed in the focal spot of the optics (the experimental setup of multipoint-projection microscopy is presented in Fig. 1a). If several conditions are fulfilled, multiple projections of the object do not overlap at the detector plane, are perfectly demultiplexed (Fig 1b) and give rise to projections of highly-absorbing samples at submicron resolution with only a few photons per detector pixel, as shown in Fig. 1c). The spatial resolution is limited to ~400 nm by a single capillary channel diameter at the exit of the focusing element. In the presentation, we will also present propagation based in-line phase-contrast imaging realized with the Gabor holography geometry [3,4]. Moreover, we will show that multipoint-projection geometry is capable to provide 3D images from a single x-ray exposure [5] in a way similar to a plenoptic or light-field camera [6]. 3D imaging of artificially prepared objects and biological samples will be discussed. Our experiments were performed with a table-top experimental setup that uses a micro-focal X-ray tube. However, the setup can be easily modified for operation at a synchrotron radiation beamline. Since polycapillary optical elements are achromatic, multi-point projections microscopy is compatible with polychromatic radiation from a bending magnet and could be used at SOLARIS synchrotron in Kraków.

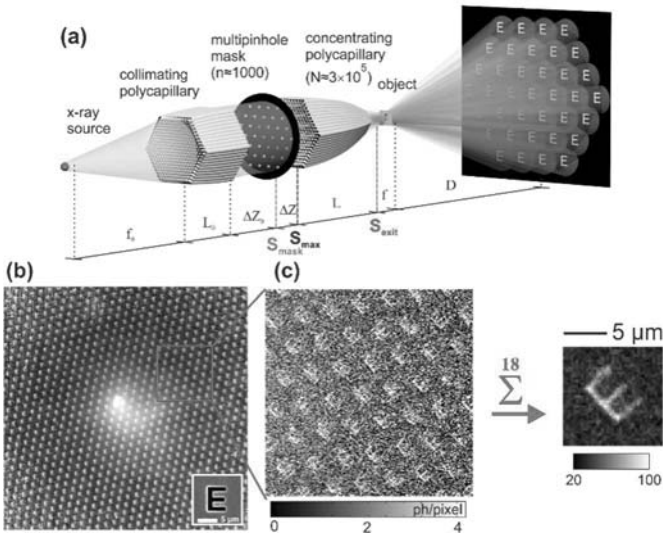

*Figure 1.*Principle of multipoint-projection X-ray microscopy. a) experimental setup: two polycapillary optical elements (collimating and focusing) and a laser-drilled multi-pinhole mask in between. Each capillary generates an X-ray secondary micro-source and therefore, the object placed in the focal spot of the optics is illuminated by an array of mutually incoherent but partially coherent micro-sources, b) over one thousand shadow projections of the object demultiplexed at the detector plane, c) projections of the object acquired with a noise-free hybrid-pixel detector. Projections can be averaged in order to massively improve the signal-to-noise ratio

Acknowledgements: This work was financially supported by the National ScienceCentre, Poland (grant no. 2017/25/B/ST2/00152). KMS acknowledges support from Polish Ministry of Science and HigherEducation (project no. 7150/E-338/M/2017).
Authors thank B.R. Jany for performing SEM imaging and FIB nanostructuring.

[1] P. Korecki, K. M. Sowa, B. R. Jany, F. Krok, *Phys. Rev. Lett.* **116** (2016) 233902.
[2] K. M. Sowa, B.R. Jany, P. Korecki, *Optica* **5** (2018) 577.
[3] D. Gabor, *Nature* **161** (1948) 777–778.
[4] T. E. Gureyev *et al*., *Phys. Rev. Lett.* **86** (2001) 5827.
[5] K. M. Sowa, M. P. Kujda, P. Korecki, *submitted*
[6] E. Y. Lam, *J. Opt. Soc. Am. A* **32** (2015) 2021-2032.

O-24A **Thursday, 13.06., 18^{50}-19^{10}**

XNLD as the means of studying near surface crystallographic structure in pristine and TM doped single crystals bismuth chalcogenides

J. Stępień[1]*, M. Jurczyszyn[1], K. Maćkosz[1], A. Kozłowski[2], Z. Kąkol[2] and M. Sikora[1]

[1]*AGH University of Science and Technology, Academic Centre for Materials and Nanotechnology, Mickiewicza 30, 30-059, Kraków, Poland*
[2]*AGH University of Science & Technology, Faculty of Physics & Applied Computer Science, Mickiewicza 30, 30-059 Krakow, Poland*

Keywords: bismuth chalcogenides, XAS, XNLD

*e-mail: jstepien@agh.edu.pl

The best recognized feature of topological insulators (TI) is the existence of metallic states whenever the TI material breaks its continuity, e.g. on the surface [1], [2]. In such a case, the linear dispersion relation exist in a form of a Dirac cone, on top of otherwise insulating bulk energy gap. Additionally, for surface metallic states the spin is perpendicular to the momentum vector. This results in the remarkable property: surface electrons cannot be back-scattered, i.e. they are robust against perturbations. This fact can be utilized in spintronic applications and in devices carrying quantum information where avoiding decoherence is of outmost importance.

Magnetic topological insulators reveal modification of valence band structure in the bulk TI, i.e., for a few quintuple-layers (QLs) of doped and intercalated topological insulators. The correlation between systematically modified bulk electronic properties of TI and topological properties at the surface is of particular importance for spintronic devices, since the electron (spin) injection occurs not only in the interface but also in the bulk.

The influence of magnetic and nonmagnetic adatoms on the electronic structure on the surface states in TI has intensively been studied, including the evolution of electronic bandstructure and its influence on the distribution and magnetic anisotropy of dopants [3-5]. However, little is known about the influence of dopants on the near-surface crystal structure, which is crucial in determination of the extraordinary electronic transport. There is also deficient information on the influence of ion etching and deposition of metal contacts, i.e. the typical steps in engineering of electronic nanodevices by means light assisted lithography, on the near surface atomic structure of TI.

In this contribution we show thatthe robustness of crystal structure of TI can be probed using X-ray Natural Linear Dichroism (XNLD) in total electron yield collected absorption spectra.We have measured XNLD signal at Te M-edge for Bi_2Te_3 and Bi_2Te_3 doped with Mn. The experiment was performed on surfaces of in-situ cleaved single crystals, surfaces exposed to air, surfaces exposed to erosion by means of Ar^+ ion beam, and surfaces covered with Au film. Experiments were performed at XAS endstation of PEEM/XAS beamline at Solaris simultaneously with LEED/AES surface analysis.

Preliminary results show that XNLD related to strong structural anisotropy at the surface is preserved upon exposure to air and deposition of metal films, however it is deteriorated upon high fluence/energy of ion etching. Detailed analysis of the results, supported by FDMNES modelling will be presented.

Acknowledgements: The experiment was performed thanks to collaboration of SOLARIS Staff. Work supported by National Science Centre, Poland (grant number:2015/17/B/ST3/00128).

[1] M. Z. Hasan, C. L. Kane, *Rev. Mod Phys.***82** (2010) 3045.
[2] H. Zhang, C. X. Liu, X. L. Qi *et al.*, *Nature Phys.* **5** (2009) 438.
[3] I. Vobornik, G. Panaccione, J. Fujii *et al.*, *Nano Lett.* **11** (2011) 4079.
[4] T. Eelbo, M. Sikora, G. Bihlmayer *et al.*, *New J. Phys.* **15** (2013) 113026.
[5] M. Waśniowska, M. Sikora, M. Dobrzański *et al.*, *Phys. Rev. B* **92** (2015) 115412.

O-25B **Thursday, 13.06., 16^{50}-17^{10}**

SAXS investigation of nanostructure-property relationship of composite materials

M. Zienkiewicz-Strzałka[1*], A. Bosacka[1] and S. Pikus[2]

[1]*Department of Physicochemistry of Solid Surface, Maria Curie-Skłodowska University, sq. Maria Curie-Skłodowska 3, 20-031 Lublin, Poland*
[2]*Department of Crystallography, Faculty of Chemistry, Maria Curie-Skłodowska University, sq. Maria Curie Skłodowska 3, 20-031 Lublin, Poland*

Keywords: mesoporous silica, small angle scattering

*e-mail: malgorzata.zienkiewicz@poczta.umcs.lublin.pl

The idea of combining inorganic networks and polymers, biopolymer or metallic nanoparticles has opened a wide field in materials science.Nanocomposites are nanotechnology products with a constantly growing importance, mainly due to the possibility of modifying and adapting properties to specific applications [1-2]. Biocomposites create a new generation of multi-element materials. A lot of effort is given to the development of sustainable and environmentally friendly methods of obtaining and processing nanocomposites.A many types of hybrid organic-inorganic materials havebeen produced by sol-gel guidelines, where in both inorganic and organic parts contribute to the overall properties of the composite by their own specific properties. The size, shape and clustering of nanosized objects in the nanocomposites are of fundamental interest to understand the microstructure of these heterogeneous materials When the clear difference in electron density between the embedded objects and the matrix are significant, small angle X-ray scattering (SAXS) gives valuable information about the structure of the composites.

Small angle X-ray scattering can be applied to analyse the structural changes in composite matrix after any modification. Scattering patterns can be also obtained due to the crystal structures (particles or metal nanoparticles) are present in samples [3-5]. The porous materials where the nanoobjects are represented by porous system can be also analyzed by SAXS. In general, the nanocomposite systems include the crystalline, amorphous and background regions with characteristic differences in electron densities. When the differences in electron densities are significant, the significant changes in the SAXS spectra are observed.

The aim of this work was to investigate the structural and interfacial properties of various composite samples including silica, mesoporous silica, carbon, polymer and biopolymer composites. The investigated samples varied in the intensity of scattering. SAXS data reveals a single correlation between the size of the silver nanophase and X-ray scattering at small angles and may suggest the properties of nanoparticles in/on the nanocomposite body.

.

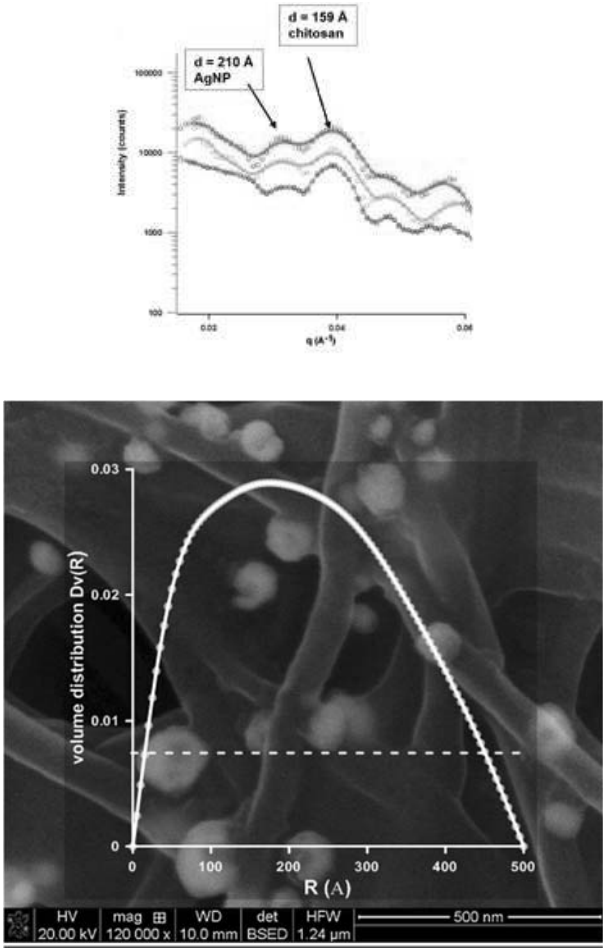

Figure 1. Experimental SAXS profiles for AgNP/chitosan composites and radial distribution function, Dv(R) obtained from the SAXS data compared with SEM images

[1] T. Tanaka, G.C. Montanari, R. Mulhaupt, *IEEE Transactions on Dielectrics and Electrical Insulation*, **11** (2004) 763 - 784.
[2] C. Sanchez, F. Ribot, *New J. Chem*. **18** (1994) 1007.
[3] C. Becker, H. Krug, H. Schmidt, *Mater. Res. Soc. Symp. Proc*,**435** (1996) 237.
[4] C. J. T. Landry, B. K. Coltrain, M. R. Landry, J. J. Fitzgerald,V. K. Long, *Macromolecules* **23** (1993) 3702.
[5] E. P. Giannelis, *Adv. Mater*. **8** (1996) 29

O-26B **Thursday, 13.06., 17^{10}-17^{30}**

Ultrafast crystallization of thin film metallic glasses: an X-ray diffraction study

R. Sobierajski[1]*, P. Zalden[2], K. Sokolowski-Tinten[3], R. Minikayev[1], K. Georgarakis[4], D. Klinger[1], F. Bertram[5], M. Chaika[1],M. Chojnacki[1], P. Dłużewski[1], K. Fronc[1], A. L. Greer[6], I.Jacyna[1], M. Klepka[1], M. Kozłowski[1], M. Kłomski[7],K. Ławniczak-Jabłońska[1], Ch. Lemke[8],O. Magnussen[8], B. Murphy[8],K. Perumal[5], A. Pietnoczka[7],U. Ruett[5], J. Warias[8] and J. Antonowicz[7]

[1]*Institute of Physics Polish Academy of Sciences, al. Lotników 32/46, 02-68 Warszawa, Poland*
[2]*European XFEL, Holzkoppel 4, 22869 Schenefeld, Germany*
[3]*Universitaet Duisburg-Essen, Universitätsstraße 2, 45141 Essen,Germany*
[4]*Cranfield University, College Rd, Cranfield, Bedford MK43 0AL,United Kingdom*
[5]*Deutsches Elektronen-Synchrotron DESY, Notkestrasse 85, Hamburg 22607, Germany*
[6]*University of Cambridge, Trinity Ln, Cambridge CB2 1TN,United Kingdom*
[7]*Warsaw University of Technology, Pl. Politechniki 1, 00-661 Warsaw, Poland*
[8]*Christian-Albrechts-Universitaet, Christian-Albrechts-Platz 4, 24118 Kiel,Germany*

Keywords: x-ray diffraction, metallic glasses, laser heating, crystallization

*e-mail: ryszard.sobierajski@ifpan.edu.pl

Among other glass-forming materials, metals are typically difficult to vitrify since they crystallize on cooling immediately after the melting (or liquidus) point is reached. The stability of the supercooled liquid is usually described in terms of the time-temperature-transformation (TTT) diagram which is a graphical representation of the time required to initiate crystallization in the supercooled liquid at a given temperature. This time is strongly temperature-dependent and its minimum is in the high-temperature regime, near the equilibrium melting point. Due to the timescale limitation, fast crystallization kinetics of the metallic glasses is extremely difficult to assess experimentally by conventional characterization techniques.

In this work we study crystallization kinetics in ~30 nm thin metallic glasses ($Cu_{67}Zr_{33}$ and $Pd_{1-x}Si_x$, with x in the range of 5-20 at. %) sputtered on a sapphire substrate. The proposed approach is based on repeated ultrafast heating (10^{14} K/s) by femtosecond optical pulses followed by extremely rapid cooling ($10^{10\text{-}12}$ K/s) by heat dissipation into the film substrate [1,2]. The frozen-in intermediate stages of transformation are characterized by consecutive microbeam X-ray diffraction (XRD) snapshots taken at PETRA III source.

By quantitative analysis of the XRD patters, we evaluated the crystalline volume fraction as a function of the number of laser pulses (N) and their fluence (F). Since N is proportional to the effective annealing time and F to the maximum sample temperature, the equivalent of the TTT diagram was obtained. By comparing the resulting diagrams obtained for various alloy compositions and laser annealing atmosphere (in-air vs. in-vacuum) we determined the effect of silicon concentration (in Pd-Si systems) and demonstrate the influence of surface oxidation on crystallization kinetics.

The XRD studies were supported by analysis of the scanning and transmission elecrtron microscopy images providing information about the changes of surface morphology and local structure induced by laser irradiations again as a function of N and F.

The applied unique technique allows to overcome timescale limitations related to ultrafast crystallization (nucleation and growth of the crystalline phases) of thin metallic glass films and to quantify its kinetics over a wide range of effective crystallization temperatures.

.

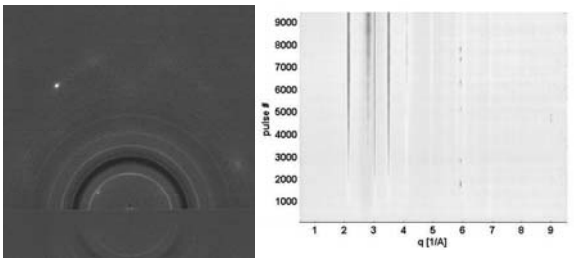

Figure 1. (left) 2D XRD differential pattern resulting from subtraction of the image obtained for laser-irradiated from as-grown $Cu_{67}Zr_{33}$sample. A broad dark ring corresponds to the lacking amorphous phase in the irradiated sample while fine bright rings originate from the crystallization products. (right) The evolution of the azimuthaly integrated XRD pattern as a function of the number of irradiating pulses

Acknowledgements: This work was supported by National Science Centre, Poland, grant agreement Nº 2017/27/B/ST3/02860. XRD results have been obtained in the frame of the Project Nº I-20160581 EC and I-20170745 EC at PETRA III facility.

[1] M. Von Allmen, S. S. Lau, M. Mäenpää, B. Y. Tsaur, *Appl. Phys. Lett.* **37** (1980) 84.
[2] P. Zalden, A. Hoegen, P. Landreman, M. Wuttig, A. Lindenberg, *Chem. Mater.* **27** (2015) 5641.

O-27B **Thursday, 13.06., 17^{30}-17^{50}**

XAFS study on the Co(II), Ni(II) and Cu(II) complexes with chlorophenoxyherbicides

A. Wolska[1]*, A. Drzewiecka-Antonik[1], P. Rejmak[1], M. T. Klepka[1] and W. Ferenc[2]

[1]*Institute of Physics, Polish Academy of Sciences, Al. Lotnikow 32/46, 02-668 Warsaw, Poland*
[2]*Faculty of Chemistry, Maria Curie-Skłodowska University, PlacMarii Curie-Skłodowskiej 2, PL-20031 Lublin, Poland*

Keywords: synchrotron radiation, EXAFS, XANES, herbicides, transition metal complexes

*e-mail: wolska@ifpan.edu.pl

Herbicides are widely used in agriculture for weed control. They are being applied for protection of crops, lawns and orchards creating the risk of pollution of soils and waters. Their remainders can be adsorbed by the organic and mineral components of the soil and sediment. They can also form complexes with metal ions. Comprehensive studies are needed in order to understand how they can affect the environment. The structural and biological studies have to be carried out. However, many of the newly formed compounds are in a non-crystalline form which makes structural investigations difficult.

The methodology based on X-ray absorption fine structure (XAFS) spectroscopy developed in our laboratory can be used to structurally characterize non-crystalline compounds [1-3]. In case of the metal complexes with organic ligands, the coordination of the ligands to the metallic center is of interest, therefore metal's surrounding is investigated. Extended X-ray absorption fine structure (EXAFS) spectroscopy provides information onthe type and number of the nearest neighbors, as well as their distances to the absorbing atom. This data is a base for building a set of preliminary structural models which are subsequently used in the ofX-ray absorption near edge structure(XANES) spectra calculations. The shape of XANES spectra strongly depends not only on the bond lengths but also on the spatial arrangements between the neighboring atoms. Therefore, the XANES spectra can be used in the selecting the most probable model. Finally, the best model isoptimizedbythe density functional theory(DFT) and then again checkedand confirmed in the EXAFS analysis.

During the presentation structural investigations on the non-crystalline compounds will be described on the examples of theCo(II), Ni(II) and Cu(II) complexes with chlorophenoxyherbicides.

The XANES and EXAFS measurementswere performed at the XAFS beamline at ELETTRA synchrotron (Trieste, Italy). The K-edges of Co, Ni and Cu for complexes in the form of powder were recorded in the transmission mode. The EXAFS analysis was performed using the Athena and Artemis programs [4]. Theoretical ab-initio XANES calculations were carried out using FEFF 9.6 code [5]. The geometry of the models was adjusted by a LigandRot program [6]. DFT studies were performed using Turbomole ver. 6.5 computational package [7].

[1] M. T. Klepka, D. Kalinowska, C. A. Barboza, A. Drzewiecka-Antonik, K. Ostrowska, A. Wolska, *Rad. Phys. Chem.* doi: 10.1016/j.radphyschem.2018.11.001.
[2] A. Drzewiecka-Antonik, W. Ferenc, A. Wolska, M. T. Klepka, B. Cristóvao, J. Sarzyński, P. Rejmak, D. Osypiuk, *Chem. Phys. Lett.* **667** (2017) 192.
[3] A. Drzewiecka–Antonik, W. Ferenc, A. Wolska, M. T. Klepka, C. A. Barboza, B. Cristóvao, D. Osypiuk, J. Sarzyński, B. Tarasiuk, E. Grosicka-Maciąg, D. Kurpios-Piec, M. Struga, *Polyhedron* **165** (2019) 86.
[4] B. Ravel, M. Newville, *J. Synchr. Radiat.***12** (2005) 537.
[5] J. J. Rehr, J. J. Kas, F. D. Vila, M. P. Prange, K. Jorissen, *Phys. Chem. Chem. Phys.***12** (2010) 5503.
[6] A. Wolska, M. T. Klepka, W. Ferenc, A. Drzewiecka, *X-raySpectr*. **44** (2015) 323.
[7] R. Ahlrichs, M. Bär, M. Häser, H. Horn, C. Kölmel, *Chem. Phys. Lett* .**162** (1989) 165.

O-28B **Thursday, 13.06., 17^{50}-18^{10}**

Local atomic environment of Cu and Ag ions of new bioactive 1,5-disubstituted tetrazole complexes investigated using multi–technique approach methodology

D. Kalinowska[1]*, M. T. Klepka[1], D. Szulczyk[2;3], M. Struga[2;3] and M. Mielczarek[2]

[1]*Institute of Physics Polish Academy of Sciences, Al. Lotnikow 32/46, 02-668 Warsaw, Poland*
[2]*Medical University of Warsaw, Department of Biochemistry, First Faculty of Medicine, 02-097 Warsaw, Poland*
[3]*Medical University of Warsaw, Laboratory of Centre for Preclinical Research, 02-097 Warsaw, Poland*

Keywords: XAS, EXAFS, XANES, bioactive, metal complexes

*e-mail: diana.kalinowska@ifpan.edu.pl

Although the quality of healthcare has increased with the invention of antibiotics, nowadays the antimicrobial resistance remains a global and critical healthcare issue. WHO reports about the growing threat of bacterial infections, that may become the top cause of mortality in the world within the next three decades.Greater effort is required in research and development of the novel class of compounds effective against pathogens [1, 2]. Tetrazole derivatives are a potential in this field of research. Their wide range of biological activity and polynitrogen planar structure make them perfect template aimed at the development of new bioactive compounds [3–9].

Structural characterization of new, bioactive 1,5-disubstituted tetrazole-derivative complexes with Cu and Ag ions will be presented. The studies have been carried out for compounds in a form of solvates with growth cell culture medium as a solvent. It simulate living environment of the cells and is commonly used for various biological assays. Solvent molecules may modify the surrounding of metal ion and enhence the activity of a compound. Since the potential of pharmacological action depends on the chemical structure, there is an interest in detailed investigation of complex's molecular structure.

Due to fact that diffraction methods are inapplicable in case of compounds in form of solution, methodology deleoped in our laboratory has been used. It assumes using the X–ray absorption spectroscopy (XAS),which provides information about the local atomic order around the specific elementregardless of their form or state. With support oflaboratory based techniques(e.g. FTIR spectroscopy, elemental analysis) and DFT calculationsapplpying methodology made it possible to propose the three-dimensional models of the analyzed compounds.

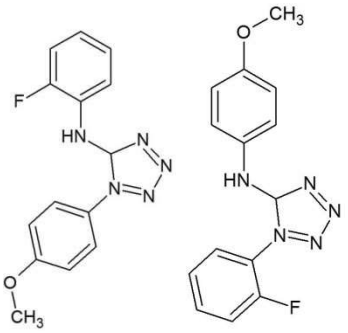

Figure 1. Schematic structure of two tautomeric forms of 1,5–substituted tetrazole-derivative ligand used as ligands in coordination reaction

Acknowledgements: The authors acknowledge Elettra-Sinctrotrone Trieste S.C.p.A. for beamtime at the XAFS beamline.

[1] A. Bielenica *et al.*, *Eur. J. Med. Chem.* **101** (2015) 111.
[2] J. Stefańska *et al.*, *Pol. J. of Microbiol.* **65** (2016) 451.
[3] D. Szulczyk *et al.*, *Eur. J. Med. Chem.* **156** (2018) 631.
[4] M. Staniszewska *et al.*, *Eur. J. Med. Chem.* **145** (2018) 124.
[5] C. X. Wei *et al.*, *Molecules* **20** (2015) 5528.
[6] A. Qian *et al.*, *Bioorg. Med. Chem. Lett.* **28** (2018) 344.
[7] V. A. Ostrovski *et al.*, *Russ. Chem. Bull.* **61** (2012) 768.
[8] L. L. Dai *et al.*, *Med. Chem. Comm.* **6** (2015) 147.
[9] R. Sribalan *et al.*, *J. Mol. Struct.* **1175** (2018) 577.
[10] M. T. Klepka *et al.*, *Chem. Phys. Lett.* **691** (2018) 190.
[11] M. T. Klepka *et al.*, *Radiat. Phys. Chem.* **6** (2018) https://doi.org/10.1016/j.radphyschem.2018.11.001

O-29B **Thursday, 13.06., 18^{10}-18^{30}**

The off-resonant excitations and two-photon absorption cross-sections Z-dependence for the 3d elements

K. Tyrala[1*], J. Czapla-Masztafiak[1], A. Wach[1], K. Wojtaszek[1], W. M. Kwiatek[1] and J. Szlachetko[1]

[1]*Institute of Nuclear Physics Polish Academy of Sciences, 31-342 Krakow, Poland*

Keywords: X-ray spectroscopy, synchrotron radiation, free-electron laser

*e-mail: krzysztof.tyrala@ifj.edu.pl

Two-photon absorption (TPA) is a simple nonlinear process where the electron of the atom is excited by two separate photons. This phenomenon is for many years known and used as a research tool at optical wavelengths [1,2]. Giving the fact, that TPA process follows the quadrupole selection rules ($\Delta l = \pm 2,0$), it may be possible to use it in X-ray spectroscopy for probing forbidden in the linear regime *1s → 3d or 1s → 4d* transitions. However at X-ray energies, the process is possible to beinducedat very high intensities, that may be provided only by X-ray Free Electron Lasers [3,4]. Recent research suggests that the process is dominated by a sequential variant [5], that is mediated by a virtual, intermediate state.

Another process, mediated by the same virtual intermediate state is the off-resonant excitation, or Resonant Raman Scattering (RRS). This one-photon process involves the core-shell electron excitation with photon energy lower than the ionization threshold of a given element, that may be considered as the first step in sequential TPA.As a consequence, the cross-sections relations between the one photon off-resonant excitation and the two-photon absorption can be studied and it is possible to derive the cross-sections value for TPA based on the one-photon interaction data [6].

For many years the off-resonant excitation was observed by the use of monochromatized radiation from X-ray tubes [7–8] or synchrotrons [9–12]. Yet, the cross-sections values were determined so far only for a handful of elements, usually by means of low energy resolution measurements. Herein we report the determination of the cross-section values for elements from 3d group, based on the measurements performed at synchrotron with the use of high energy resolution X-ray spectroscopy. Based on the experimental data, we estimate the cross-sections dependence on the atomic number. Based on the obtained results, we will discuss expected dependences for cross-sections for nonlineartwo-photon absorption mechanisms and examine the influence of the intermediate state lifetime.

Acknowledgements: This work was partially supported by National Science Centre, Poland (NCN) under grant no. 2017/27/B/ST2/01890.

[1] M. Göppert-Mayer, *Ann. Phys.* **401** (1931) 273.
[2] W. Denk, J. H. Strickler, W. W. Webb, *Science* **248** (1990) 73-76.
[3] P. Emma, R. Akre, J. Arthuret *et al.*, *Nat. Photonics* **4** (2010) 641.
[4] J. Amann, W. Berg, V. Blank *et al.*, *Nat. Photonics* **6** (2012) 693.
[5] K. Tamasaku, E. Shigemasa, Y. Inubushi *et al.*, *Nat. Photonics* **8** (2014) 313.
[6] J. Szlachetko, J. Hoszowska, J.-C. Dousse *et al.*, *Sci. Rep.* **6** (2016) 33292.
[7] C. J. Sparks, *Phys. Rev. Lett.* **33** (1974) 65.
[8] K. Hamalainen, S. Manninen, P. Suortti *et al*., *J. Phys. Condens. Matter* **1** (1989) 5955.
[9] H. J. Sánchez, M. C. Valentinuzzi, C. Pérez, *J. Phys. B At. Mol. Opt. Phys.***39** (2006) 4317.
[10] J. P. Briand, D. Girard, V. O. Kostroun *et al*, *Phys. Rev. Lett.* **46** (1981) 1625.
[11] S. Manninen, P. Suortti, M. J. Cooper*et al*., Phys Rev. B **34** (1986) 8351.
[12] J. Szlachetko, J.-C. Dousse, J. Hoszowska *et al.*, *Phys. Rev. Lett*. **97** (2006) 73001.

O-30B **Thursday, 13.06., 18^{30}-18^{50}**

Changes in the structure of XAS spectra and kinetics of phase transformation for thermally oxidized titanium at different temperatures

K. Wojtaszek[1]*, A. Wach[1], K. Tyrała[1], M. Nowakowski[1], M. Zając[2], J. Stępień[3], W. Stańczyk[4], J. Czapla-Masztafiak[1], W. M. Kwiatek[1] and J. Szlachetko[1]

[1]*Institute of Nuclear Physics Polish Academy of Sciences, 31-342 Krakow, Poland*
[2]*National Synchrotron Radiation Centre Solaris, Jagiellonian University, Krakow, Poland*
[3]*Academic Centre for Materials and Nanotechnology AGH, Krakow, Poland*
[4]*AGH University of Science and Technology, Faculty of Electrical Engineering, Automatics, Computer Science and Biomedical Engineering, Krakow, Poland*

Keywords: X-ray Absorption Spectroscopy, Total Electron Yield mode, TiO_2, thermal oxidation, biomaterials

*e-mail: klaudia.wojtaszek@ifj.edu.pl

Thanks to mechanical properties and biocompatibility, titanium and titanium alloys are widely used in implantology.In many works, it has been shown that the titanium dioxide layer on titanium implants can protect implants against corrosion and promote cell adhesion [1,2,3]. Thermal oxidation of titanium is a simple and economical solution, facing the problem of the formation of too thin TiO_2 passive layer on implants to ensure sustained wear resistance [3,4]. Thermal oxidation not only increases the thickness of the oxide layer but also promotes the formation of the rutile phase, which is characterised by excellent adhesion to the titanium substrate, low friction and excellent wear resistance [5].

In the presented work, we have shown changes in the structure of XAS spectra and kinetics of phase transformation for thermally oxidized titanium at different temperatures (25ºC-800ºC)of titanium metal discs. The process was followed by ex-situ measurements using X-ray Absorption Spectroscopy method in total electron yield (TEY) mode, which gave information about surface states of titanium discs. It is important to note that the oxide layer was formed on a surface of high-purity Ti discs exposed to air at room temperature. In order to obtain XAS spectra for pure Ti (without the presence of thin oxide layer), metallic disc was sputtered using a broad Ar ion beam at XAS end station. In order to study kinetics of phasetransformation, the XAS spectra obtained at different oxidation temperatures were fitted with reference spectra using the Athena program.

Acknowledgements: Authors would like to acknowledge National Science Centre, Poland (NCN) for partial support under grant no. 2015/18/E/ST3/00444.

[1] M. C. Advincula *et al*., *Biomaterials* **27** (2006) 2201-2212.
[2] R. Zhang, Y. Wan, X. Ai, Z. Liu, D. Zhang, *Proc Inst Mech Eng H* **231** (2017) 1.
[3] G. Wang *et al*., *Sci Rep*., **6** (2016) 31769.
[4] K. Aniołek, M. Kupka, A. Barylski, Ł. Mieszczak, *Arch. Metall. Mater*. **61** (2016) 2.
[5] D. Siva Rama Krishna, Y. L. Brama, Y. Sun, *Tribology International* **40** (2007) 153.

O-31B **Thursday, 13.06., 18^{50}-19^{10}**

Electronic structure of photocatalystsprobed by means of X-ray spectroscopy techniques

A.Wach[1]*,W. Błachucki[2], K. Wojtaszek[1], K. Tyrała[1], J. Czapla-Masztafiak[1], W. M. Kwiatek[1] and J. Szlachetko[1]

[1]*Institute of Nuclear Physics Polish Academy of Sciences, Krakow, Poland*
[2]*Institute of Physical Chemistry, Polish Academy of Sciences, Warsaw, Poland*

Keywords: X-ray spectroscopy, photocatalysts

*e-mail: anna.wach@ifj.edu.pl

With the rapid development of the society, a number of associated challengesis emerging such as energy shortage and environmental pollution. As a result, an extensive research has been carried out to develop clean and renewable energy technologies [1]. One of the promising approaches relies on photocatalytic materials, by means of which renewable solar energy is directly converted into chemical energy [2]. Semiconductor metal oxides, typically titaniumdioxide (TiO_2), zinc oxide (ZnO), iron oxide (Fe_2O_3) and tungsten oxide (WO_3),have been studied as light-harvesting materials due to their outstanding properties: chemical stability, good photocatalytic properties and low cost

In the present study we demonstrate capability of the X-ray spectroscopy to investigate electronic structure of semiconducting materials TiO_2 and WO_3, at working conditions.The electronic structure of occupied (valence band) and unoccupied (conduction band)states of these materials is directly related with its photocatalytic properties[3]. The energy band gap, separating the valence and conduction bands, determines the range of solar spectrum that can be absorbed.We used a combination of valence-to-core X-ray emission (v2c-XES) and high-resolution X-ray absorption (HR-XAS) techniques to probe the highest occupied and the lowest unoccupied electronic states, respectively. The obtained experimental data were also compared with theoretical calculations of the DOS performed with the FEFF9.6 program.

Moreover, the process of metal to semiconductor transition (the band gap creation) was studied with an *in situ*time-resolved Resonant X-ray Emission Spectroscopy (RXES). The *in situ* RXES was proved to be an ideal tool to follow the electronic structure transformationduring thermal oxidation of metallic W to WO_3 (Figure 1). Application of the high energy resolution spectroscopy allowed us to detect splitting of W 5d states by the ligand field into t_{2g} and e_g orbitals. From the measured data we derived contributions of atomic orbitals to the valence and conduction band and performed quantitative analysis of the ligand field splitting.

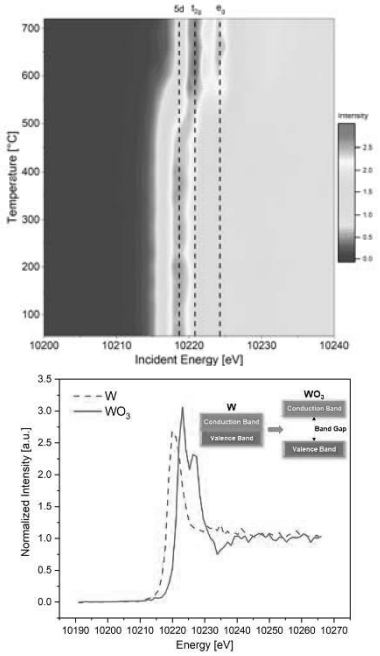

Figure 1. Electronic structure changes in the conduction band of W induced by metal to metal-oxide transition

Acknowledgements: Authors would like to acknowledge National Science Centre, Poland (NCN) for partial support under grant no. 2015/18/E/ST3/00444. W.B. acknowledges the Polish Ministry of Science and Higher Education for support from the budget allocations for science for years 2016-2019 within the IDEAS PLUS II project of number IdPII2015000164.

[1] H. Yamashita, K. Mori, Y. Kuwahara, T. Kamegawa, M. Wen, P. Verma, M. Che, *Chem. Soc. Rev.* **47** (2018) 8072.
[2] K. Maeda, K. Domen, *J. Phys. Chem. Le*tt. **1** (2010) 2655.
[3] J. Szlachetko, J. Sá, *CrystEngComm* **15** (2013) 2583.

O-32 **Friday, 13.06., 10^{20}-10^{40}**

Structural and biophysical studies of the plant m6A methyltransferase complex

M. Taube[1;2]*, I. Zhukov[3], K. Szutkowski[4], A. Jarmołowski[2], Z. Szweykowska-Kulinska[2] and M. Kozak[1]

[1]*Department of Macromolecular Physics, Faculty of Physics, Adam Mickiewicz University, Uniwersytetu Poznanskiego 2, 61-614 Poznan, Poland*
[2]*Department of Gene Expression, Institute of Molecular Biology and Biotechnology, Faculty of Biology, Adam Mickiewicz University, Uniwersytetu Poznanskiego 6, 61-614 Poznan, Poland*
[3]*Institute of Biochemistry and Biophysics Polish Academy of Sciences, Pawinskiego 5A, 02-106 Warszawa, Poland*
[4]*NanoBioMedical Centre, Adam Mickiewicz University in Poznan, Wszechnicy Piastowskiej 3, 61-614 Poznan, Poland*

Keywords: small-angle X-ray scattering, SAXS, NMR, m6A, RNA methylation, plants

*e-mail: mtaube@amu.edu.pl

Recently, widespread N6-methyladenosine (m6A) modification of messenger RNA (mRNA) and non-coding RNA has been discovered in yeast, flies, mammals and plants [1]. It has been shown that this modification could affect mRNA fate within the cell: changing its splicing pattern, promoting transport to the cytoplasm, increasing degradation rate and enhancing translation. Moreover, m6A modification of primary miRNA transcripts promotes miRNA biogenesis in human cell lines. At the functional level, m6A plays an important role in many biological processes, including: stem cell differentiation, circadian clock in mammals, functioning of the nervous system and development in plants [2]. In mammals two methyltransferases: METTL3 and METTL14, together with the adaptor protein WTAP are required for m6A methylation [3], while in plants - MTA and FIP37, identified as homologs of METTL3 and WTAP, respectively [3].

Here we present results of our structural and biophysical characterization of the plant m6A RNA methylation machinery. Using the small angle X-ray scattering (SAXS) we have shown that adaptor proteins WTAP and FIP37 oligomerize and have dynamic structure in solution. Moreover we showed that three coiled-coil domains of FIP37 created homodimers. Using the yeast two-hybrid system we showed that C-terminal part of FIP37 and N-terminal domain of MTA are responsible for the interactions. In addition we proved that N-terminal part of the MTA possessed additional conserved motif. The circular dichroism and SAXS data provided evidence that this fragment is folded and stable in solution. To further characterize this domain we apply nuclear magnetic resonance spectroscopy (NMR) to solve its three dimensional structure. The structure of this domain shows the new fold specific for the plant m6A RNA methyltransferases.

Acknowledgements: This work was supported by the international grant POLTUR2/3/2017 from National Center of Research and Development and research grant UMO 2017/27/B/ST4/00485 from the National Science Centre.

[1] Y. Yue, J. Liu, C. He, *Genes Dev.* **29** (2015) 1343.
[2] J. Y. Roignant, M. Soller, *Trends Genet.* **33** (2017) 380.
[3] D. L. Balacco, M. Soller, *Biochemistry* **58** (2019) 363.

P-01

Epitaxial ultra thin film of Bi_2O_3 on α-Al_2O_3 (0001) surface

D. M. Kamiński[1*], M. Mirolo[2], P. Andreazza[3], T. R. J. Bollmann[4] and M. Jankowski[5]

[1]*Department of Chemistry, Maria Curie-Sklodowska University, Pl. M. Curie-Skłodowskiej 5, Poland*
[2]*Paul Scherrer Institut, Forschungsstrasse 111, 5232 Villigen PSI, Switzerland*
[3]*CNRS - Universitéd'Orléans, 1b rue de la Férollerie, CS 40059 45071, Orléans cedex 2, France*
[4]*University of Twente, Inorganic Materials Science, MESA+ Institute for Nanotechnology, PO Box 217, NL-7500AE Enschede, The Netherlands*
[5]*ESRF-The European Synchrotron,71 Avenue des Martyrs, F-38000 Grenoble, France*

Keywords: synchrotron radiation, SXRD, WinRod

*e-mail: daniel.kaminski@poczta.umcs.lublin.pl

Nanostructured ultrathin Bi films have recently attracted a ot of interest as they reveal exotic magneto-electronic properties making them appealing materials for spintronic applications. Especially the spin-momentum locked surface states of topological insulating Bi films, make them very attractive candidates for spintronic devices. To develop and optimize topological insulators towards applications, thin films of high quality are a necessity. The direct growth onto a suitable substrate should be preferred as it leads to a well defined interface and highest possible film quality. We demonstrate the controlled growth of a-Bi_2O_3 (111) film on an α-Al_2O_3 (0001) substrate by surface x-ray diffraction and x-ray reflectivity using synchrotron radiation, see Figure 1. At temperatures as low as 40 K, unanticipated pseudo-cubic Bi(110) films are grown with thicknesses ranging from a few to tens of nanometers. By mild heating at 400K roughness of the Bi film is reduced and domains with orientation Bi(110) are transformed to Bi(111). A treatment with atomic oxygen at 500K gives a-Bi_2O_3 (111) layer see figure 2.

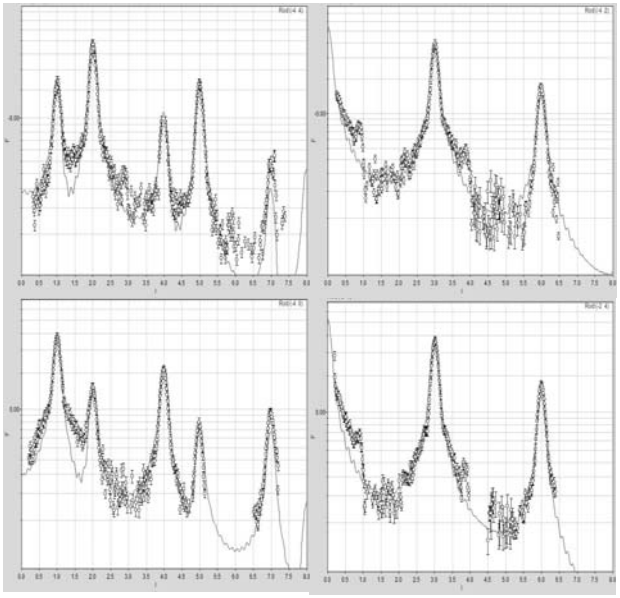

Figure 1. Selected surface x-ray diffraction ROD's and a best fit model of the 3 nm thin a-Bi2O3 (111) film. The model and fitting were done in WinRod program (which bases on the ROD program of Prof. E. Vlieg)

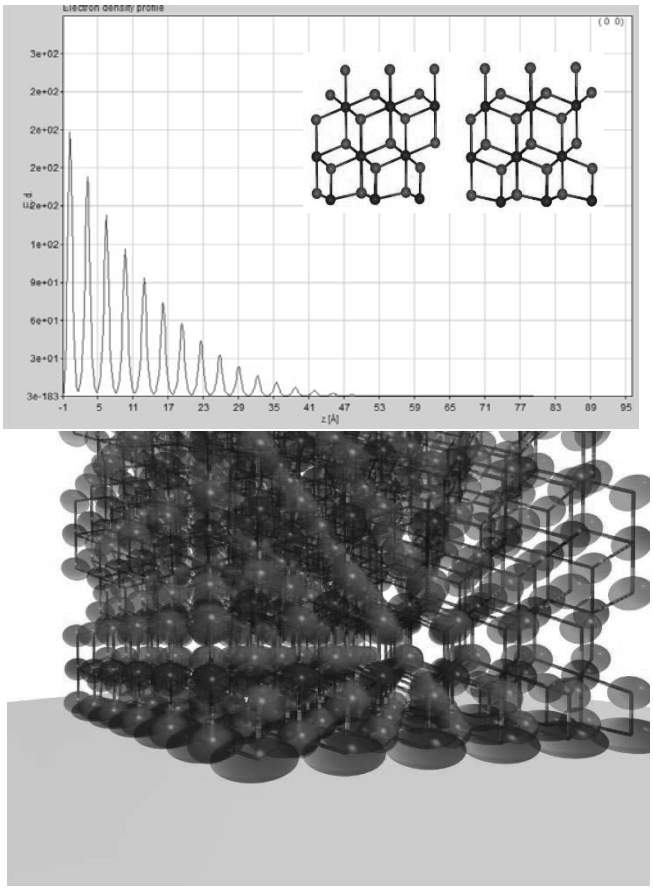

Figure 2. A profil of thin film layer as seen by x-ray (top). The layer consist tow domains (inset). The α-Bi_2O_3 (111) is incommensurate to the substrate. This leads to differences in position between oxygen atoms from sapphire and first Bi layer, which is seen as higher in-plane Debye-Waller parameter of first Bi layer (bottom). The Bi layer is also displaced up

Acknowledgements: This work is part of the research programme of the Foundation for Fundamental Research on Matter (FOM), which is part of the Netherlands Organisation for Scientific Research (NWO). TRJB acknowledges ESRF beamtime granted for this study under proposal no MA-2475.

P-02

The structure of mesoporous materials synthesized using selected natural aluminosilicates

S. Pikus[1]*, M. Zienkiewicz- Strzałka[2] and M. Skibińska[1]

[1]*Department of Crystallography, Faculty of Chemistry, Maria Curie-Skłodowska University, sq. Maria Curie Skłodowska 3, 20-031 Lublin, Poland*
[2]*Department of Physicochemistry of Solid Surface, Maria Curie-Skłodowska University, sq. Maria Curie-Skłodowska 3, 20-031 Lublin, Poland*

Keywords: mesoporous silica, aluminosilicates, nanomaterials, composites.

*e-mail: stanislaw.pikus@poczta.umcs.lublin.pl

SBA-15 is a mesoporous silica material with a hexagonal structure and a pore diameter between 5-15nm. It is characterized by high thermal stability and a large surface area in the range of 400-900 m2/g, that is why it has great application possibilities. The physicochemical properties of this material can be controlled by changing the conditions of the synthesis process, e.g. pH, mixing time, the temperature of the aging process, the addition of solvents, the reagents used. Typically SBA-15 is synthesized by the sol-gel method using tetraethylorthosilicate (TEOS) as a source of silica. However, due to the high processing costs of TEOS, was looking for new reagents which will be an alternative solution and can be used as a substitute.

The aim of this research was to use selected natural aluminosilicates in the synthesis of SBA-15 material as an alternative to TEOS silica source.

A classic synthesis of SBA-15 material was carried out using bentonite, halloysite and diatomite in which the amount of TEOS was decreased and the amount of added aluminosilicate was increased. These materials were characterized using the XRD method, SAXS, nitrogen adsorption/desorption and TEM. Fig. 1 shows small-angle diffraction patterns. Only for the first four samples of BTS1-4 there were observed three peaks (110, 110, 200) characteristic for the ordered hexagonal structure of SBA-15. In other cases, where the amount of bentonite was already significant, the amount of TEOS was small and the amorphous material was obtained. In the wide-angle range, small peaks from montmorillonite can be seen in each of the samples. However, their intensity indicates that most of the bentonite used for the synthesis of SBA-15 has built into the structure.

X-ray diffraction results confirmed by the TEM method. TEM / EDX analysis indicates that as the amount of mineral added increases, the aluminum and iron content in the samples increases too.

Specific surface area of the materials decreases and is lower than in the case of the classical SBA-15, also the micropore surface and the pore volume decrease. However, in the case of the last sample containing only bentonite without TEOS, the surface is also significant and much higher than for pure mineral. The changes are also noticeable in the case of nitrogen adsorption/desorption isotherms, where for the first four samples we obtain a type IV isotherm with a wide hysteresis loop. However, as the quantity of mineral added increases and TEOS decreases, an isotherm is obtained with less developed hysteresis loops. Similar results were obtained when halloysite was used while the use of diatomite gave much worse results.

The use of selected aluminosilicates in the synthesis of mesoporous materials has a very beneficial effect on the ordering of SBA-15 materials. Especially materials synthesized with bentonite and in the absence of TEOS show high adsorbent capacities. Hence, bentonite may be an alternative to TEOS as a source of silica in the synthesis of mesoporous materials.

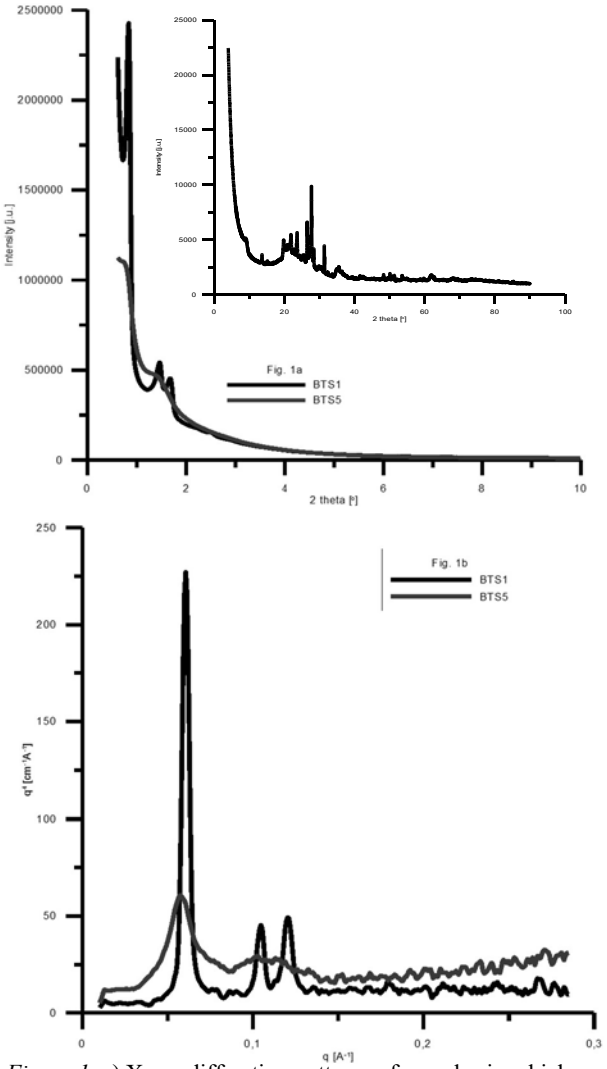

Figure 1. a) X-ray diffraction patterns of samples in which increasing amount of bentonite was used (BTS1 to BTS9) b) Porod plots

P-03

Compression of gold in silicone oil: A false friend in the powder HP/HT experiment?

P. Piszora[1]* and J. Darul[1]

[1]*Department of Materials Chemistry, Faculty of Chemistry, Adam Mickiewicz University, UniwersytetuPoznańskiego 8, 61-614 Poznań*

Keywords: powder X-ray diffraction, gold,hydrostaticity, uniaxial stress

*e-mail: pawel@amu.edu.pl

Operating with pressure opens up the possibility of obtaining novel materials. However, from the point of view of reproducibility of measurements, it is important to distinguish between hydrostatic and non-hydrostatic pressure component.Takemuradefined the ‘‘hydrostatic limit’’ as the pressure whereany sign of deviation from hydrostatic conditions is experimentally detected [1]. In most HP experiments, it is not a simple task to find the pressure where the stress causes nonnegligible effect on one of physical properties.

In the powder diffraction experiments,in order to achieve hydrostatic conditions, the sample must be immersedin a medium that displays hydrostatic behavior. Many pressure transmitting media has been tested to determine the pressure range in which hydrostatic conditions would be ensured [2, 3]. Avoiding non-hydrostatic conditions in an experiment is a common choice, however compression in the non-hydrostatic conditions can be applied to move the phase transition pressure to lower pressure value, to involve the structural phase transition [4] and to modify the relative evolution of cell parameters of crystalline samples with pressure [5].

The equation of state of gold is widely used as an X-ray pressure standard. Gold is chosen as a pressure calibrant because of its moderate compressibility, chemical inertness, and large X-ray scattering power. The determination of volume by powder X-ray diffraction is, however, severely affected by the presence of uniaxial stress in the sample at high pressures. If a crystal lattice deforms under uniaxial stress, the measured d-spacings deviate from the hydrostaticvalues, depending on the geometry of the X-ray diffraction experiment. The lattice strain is accumulated asymmetrically along the gold nanoparticles and an asymmetrical distribution of the appliedpressure took place during compression.As a result of the above, below 12 GPa an orthorhombic distortion in Au nanoparticles was induced [6]. Compression at nonhydrostatic condition could generate plastic deformation also in large particles [7]. Under high pressure, uniaxial stress varies depending on the experiment, in particular on the pressure medium used.This variable could bethe major reason for the discrepancy of the lattice parameter of gold measured at high pressure. The microscopic state of stress can be indicated by analyzing the change in FWHM of X-ray diffraction peaks.

The structural properties of Au at high pressure and at two temperatures, 300 K and 380 K, were studied in situ up to 13 GPa by X-ray powder diffraction at the MSPD-BL04 beamline of the ALBA Synchrotron Light Source using monochromatic radiation, at a wavelength $\lambda = 0.4246$ Å. High pressure (HP) and high pressure high temperature (HP/HT) experiments were carried out by using a membrane-type diamond anvil cell (DAC). A pair of 300 μm culet-size diamond anvils were used. Gaskets made from rhenium, pre-indented to a thickness of ~60 μm and then drilled to a diameter of ~140 μm, served as the sample chamber. A piece of polycrystalline gold with a purity of 999.9 and of about 30 μm in diameter was loaded into the sample chamber. The pressure transmitting medium was a polydimethyl-siloxane oil of the type ‘Rhodorsil 47V1000’ (VCR) which behaves hydrostatically up to 2.5 GPa and quasi-hydrostatically up to 10 GPa with a small maximum of nonhydrostaticity at about 6 GPa [3]. Heating was carried out by using a resistance-heating system, and the temperature was measured by a Pt90Rh10–Pt100 thermocouple, which was attached to the pavilion of the diamond. Analyses of all the patterns were carried out by means of the Rietveld refinement procedure implemented in the EXPGUI/GSAS software package.

For all patterns, the diffraction peak profile was fitted with pseudo-Voigt function. Anisotropic peak broadening mainly caused by lattice strain was observed with broadening of the diffraction peaks. The phenomenological microstrain model of Stephens was used to model the anisotropy in FWHM of the individual peak profiles.

Non-hydrostaticstresses create inhomogeneous strain in the crystal and thusbroadening of the diffraction peaks from the sample.Based on the observed structural and microstructural properties of gold, some general comments will be made about the silicone oil as a pressure medium.

Acknowledgements: These experiments were performed at the MSPD-BL04 beamline at ALBA Synchrotron with the collaboration of ALBA staff.

[1] K. Takemura, *J. Appl. Phys*. **89** (2001) 662.
[2] R. J. Angel, M. Bujak, J. Zhao, G. D. Gatta, S. D. Jacobsen, *J. Appl. Cryst*. **40** (2007) 26.
[3] S. Klotz, J. C. Chervin, P. Munsch, G. Le Marchand, *J. Phys. D: Appl. Phys.* **42** (2009) 075413.
[4] J. Darul, C. Lathe, P. Piszora, *RSC Adv*. **4** (2014) 65205.
[5] K. Takemura, *Phys. Rev. B* **60** (1999) 6171.
[6] R. Mendoza-Cruz, P. Parajuli, H. J. Ojeda-Galván, A. G. Rodriguez, H. Navarro, J. J. Velazquez-Salazar, L. Bazan-Diaz, M. J. Yacaman, *CrystEngComm*. (2019) DOI: 10.1039/C9CE00104B.
[7] Y. Bao, B. Zhao, X. Tang, D. Hou, J. Cai, S. Tang, J. Liu, F. Wang, T. Cui, *Appl. Phys. Lett*. **107** (2015) 201909.

P-04

Comparison of local structure within $Pb_{1-x}Sn_xTe$ solid solution

R. Knura[1;2;3]*, T. Parashchuk[1], A. Yoshiasa[3], and K. T. Wojciechowski[1;2]

[1]*The Lukasiewicz Research Network – The Institute of Advanced Manufacturing Technology, Wroclawska 37, 30-011 Cracow, Poland*
[2]*AGH University of Science and Technology, Mickiewicza 30, 30-059 Cracow, Poland*
[3]*Kumamoto University, 2 Chome-39-1 Kurokami, ChuoWard, 860-8555 Kumamoto, Japan*

Keywords: XAFS, $Pb_{1-x}Sn_xTe$, solid solution

*e-mail: rafal.knura@agh.edu.pl

PbTe is a narrow bandgap semiconductor widely used in thermoelectric research and applications. Pb can be substituted with Sn which allows tuning the bandgap[1]. Furthermore, creation of solid solution could also lead to a decrease of lattice contribution to thermal conductivity, which makes this material very profitable for thermoelectric application[2]. However, till this time, the local structure, bonds, charge distribution and their effect on physical and chemical properties remain unclear.

In order to examine structural properties, the pristine PbTe and $Pb_{1-x}Sn_xTe$ (x=0.1, 0.25, 0.5) were synthesized by melting raw materials in evacuated quartz ampoules at 1273 K and quenching in air. X-ray Powder Diffraction measurements confirmed NaCl type structure and lattice constants corresponding to Sn concentration in a manner described by Vegard's law. X-ray Absorption Fine Structure measurements were performed at beamlines AR-NW10A (Pb L_{III} and Sn K) and BL-9C (Te L_I and L_{III}) in Photon Factory, Tsukuba, Japan. Analysis of the EXAFS results was performed using ATHENA and ARTEMIS packages[3].

Fourier transforms of the k-weighted EXAFS function were performed and the first neighbor shell was fitted. Due to a large number of correlations between edge energies (E_0) and obtained distances to nearest neighbors, after initial fitting, E_0 was averaged and uniformed for all studied samples and the fitting was repeated. Amplitude reduction factor (S_0^2) was fitted for all relevant spectra simultaneously.

Analysis of Pb L_{III} XANES spectra revealed shifting of the edge energy towards higher energies, accompanied by splitting of the position of the maximum of spectra first derivative. These effects could be attributed to increasing in ionic contribution to the bond character with increasing overall Sn concentration, which also depends on the local concentration of Sn atoms around scattering Pb atom. A decrease in the depth of minimum at 16 eV above E_0 was also observed.

No significant change in position of the first maximum at XANES spectra of Sn K edge was observed leading to the conclusion that the oxidation state of Sn was independent of composition in the studied samples. One can, however, observe the splitting of a maximum of XANES spectrum first derivative which might be a result of a solid solution.

The L_I XANES spectra showed a gradual increase of first to second maximum intensities with increasing Sn concentration. Additionally, Te L_{III} spectra are shifted towards higher energies with increasing Sn concentration.

EXAFS analysis of Pb L_{III} (R-factor below 1%) revealed a decrease of Pb-Te bond distance with increasing Sn concentration.

Although PbTe and SnTe exhibit the same crystal structure at room temperature and have unlimited solubility within each other the local structure of the solid solution is determined by the local concentration of elements. This could influence transport properties i.e. by further lowering thermal conductivity through a scattering of phonons caused by changes in local structure stiffness within a solid solution.

Acknowledgements: This work was financed by the "New approach for development of efficient materials for direct conversion of heat into electricity" project which is carried out within the TEAM -TECH programme of the Foundation for Polish Science co-financed by the European Union under the European Regional Development Fund and the beneficiary of this project is The Lukasiewicz Research Network - The Institute of Advanced Manufacturing Technology in Cracow (Poland).

[1] Y. Gelbstein, Z. Dashevsky, M. P. Dariel, *Physica B* **391** (2007) 256.
[2] M. Orihashi, Y. Noda, L. Chen, T. Hirai, *Mater. Trans. JIM* **41(9)** (2000) 1196.
[3] B. Ravel, M. Newville, *J. Synchrotron Radiat.* **12** (2005) 537.

P-05

Structural, electronic and electrical properties of MCo_4Sb_{12} (M= In, Sb, Bi,Te) materials

T. Parashchuk[1], R. Knura[2], A. Yoshiasa[3] and K. Wojciechowski[1;2]

[1]*The Lukasiewicz Research Network- The Institute of Advanced Manufacturing Technology, 37A Wroclawska, 30-011 Krakow, Poland*
[2]*Thermoelectric Research Laboratory, Department of Inorganic Chemistry, AGH University of Science and Technology, 30 Mickiewicza Ave., 30-059 Krakow, Poland*
[3]*Kumamoto University, 2 Chome-39-1 Kurokami, ChuoWard, 860-8555 Kumamoto, Japan*

Keywords: electronic calculation, structural properties, synchrotron radiation

*e-mail: taras.parashchuk@ios.krakow.pl

Thermoelectric materials are used in devices converting heat into electricity or for construction of solid-state heat pumps [1-2]. The main advantages of these devices are high reliability and a significantly long period of continuous operation. Nowadays, one of the promising groups of new thermoelectric materials are compounds with the skutterudite structure. The general formula of skutterudites can be written as $A_xM_4X_{12}$ (A can be a lanthanide, actinide or some *s* and *p* block element; M= Co, Rh, Ir, Ni, Fe; X is a pnictogen atom such as P, As, Sb). The subgroup of compounds which do not contain the A element has a structural void in the 2a Wyckoff position and is called unfilled skutterudites. Consequently, compounds containing the A atoms are called filled skutterudites (A atoms are named fillers).

However, the concept of the occupation of the void position by many possible fillers is under the intensive discussion of scientists. In this work, an excess amount of In, Sb, Bi, and Te are introduced as fillers in the skutterudite structure (MCo_4Sb_{12}, M= Sb, In and Bi) and study its influence on structural, electronic, and electrical properties of the materials. All the samples are preparedbyhigh-pressure high temperature (HPHT) method (p= 7.8 GPa, T=700°C). The powder XRD results of the HPHT treated samples confirm that the foreign atoms (Sb, In, Bi and Te) can enter into the void site (2*a* position) of $CoSb_3$structure, which is evidenced by the extinguishing of the lower angle Bragg reflections. Also, a significant increase of lattice parameter for all the samples could indicate the void occupancy by filler atoms. Further, it is also supported by the electrical property measurements. Temperature dependence behavior of Seebeck coefficient data demonstrates that the excess amount of filler atoms (Sb, Bi and In) can occupy the void site (2*a* position) of $CoSb_3$ structure. Powder XRD of the samples after thermopower measurement revealed that a partial dis-insertion of filler atoms, which is confirmed by the intensification of extinguished low angle Bragg reflections. Our experimental findings are well supported by theoretical calculations for the MCo_4Sb_{12}, M= Sb, In and Bi samples.

For exact determination of the location of the foreign atoms, the XAFS analyzes were done. X-ray Absorption Fine Structure measurements were performed at beamlines AR-NW10A (Bi L_{III}) and BL-9C (In K, Sb L_I and L_{III}, Te L_I and L_{III}) in Photon Factory, Tsukuba, Japan. Analysis of the EXAFS results was performed using ATHENA and ARTEMIS packages [3].

The results indicate that the behavior of considered atoms in $CoSb_3$ structure is complicated due to their possible occupations of main atoms positions, as well as void positions. And also, different type of atoms do not show similar tendency.

Acknowledgements: Authors thank the Foundation for Polish Science (TEAM-TECH/2016-2/14 Grant "New approach for the development of efficient materials for direct conversion of heat into electricity"), co-financed by the European Union under the European Regional Development Fund for financial support to The Lukasiewicz Research Network - The Institute of Advanced Manufacturing Technology.

[1] G. J. Snyder, E. S. Toberer, *Nat. Mater* **7** (2008) 105-114.
[2] J. P. Heremans, V. Jovovich. E. S. Toberer, A. Saramat, K. Kurosaki, A. Charoenphakdee, S. Yamanaka, G. J. Snyder, *Science* **321** (2008) 554.
[3] B. Ravel, M.Newville, *J. Synchrotron Radiat.* **12** (2005) 537.

P-06

Analysis of tea samples by Fourier Transform Infra-Red microspectroscopyfor authentication, provenance and contamination

K. Banas[1]*, A.Banas[1], J. Loke[2] and M. H. B. Breese[1]

[1]*Singapore Synchrotron Light Source, National University of Singapore, 5 Research Link, Singapore 117603*
[2]*Forensic Management Branch, Criminal Investigation Department, Police Cantonment Complex 391 New Bridge Road #20-04 CID Tower Block C, Singapore 088762*

Keywords: FTIR, spectral processing,food provenance, contamination

*e-mail: slskb@nus.edu.sg

This research is a part of Coordinated Research Project Enhancing Nuclear Analytical Techniques to Meet the Needs of Forensic Science guided by International Atomic Energy Agency. The main objective of our project is to establish a reliable and robust model for fast identification and detection of counterfeited food products by using FTIR spectroscopy in conjunction with R Platform for statistical computing.

At the first stage of the project our focus was on coffee and tea samples of various origin. We developed and tested detailed protocols for sample preparation, experimental routines and data evaluation procedures in order to deliver representative and repeatable results.

Spectra pre-processing, data analysis (dimension reduction, clustering and identification) and visualization was conducted by using of R Platform, open-source environment for statistical computing [1-3]. As a part of our project development of the Shiny [4] Viewer started.

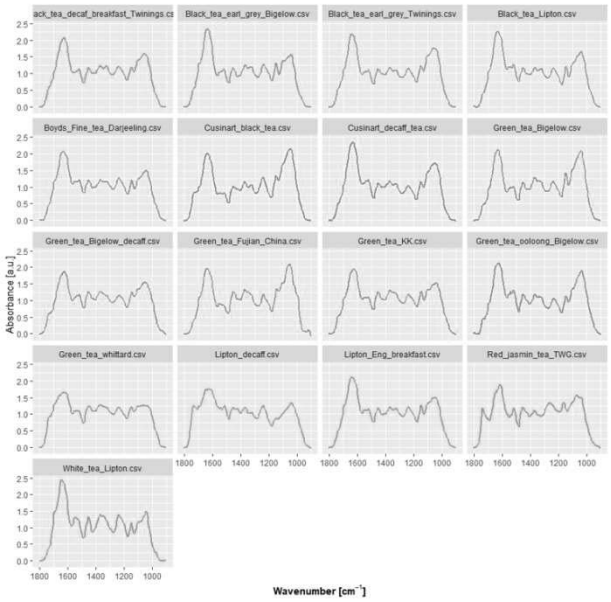

Figure 1. Representative infrared spectra of various tea brands presented for fingerprint region

Acknowledgements: Singapore Synchrotron Light Source (SSLS) is a National Research Infrastructure under the National Research Foundation Singapore.

[1] R Core Team. R: A Language and Environment for Statistical Computing, 2019. http://www.r-project.org/.
[2] R Studio: Integrated development environment for R, 2019. http://www.rstudio.com/.
[3] H Wickham,. *ggplot2: elegant graphics for data analysis*. (Springer New York, 2009)
[4] W. Chang, J. Cheng, J.J Allaire,Y. Xie,J. McPherson, (2018). shiny: Web Application Framework for R. R package version 1.1.0. https://CRAN.R-project.org/package=shiny

P-07

X-ray pinhole camera for emittance measurement in Solaris storage ring

A. Kisiel[1], T. Zbylut[1], A.Marendziak[1], S. Cabala[1], M. Ptaszkiewicz[1], P. Klimczyk[1] and A. Wawrzyniak[1]*

[1]*National Solaris National Synchrotron Radiation Centre, Krakow, Poland*

Keywords: synchrotron radiation, emittance

*e-mail: adriana.wawrzyniak@uj.edu.pl

The transverse beam emittance is a crucial parameter determining the brightness of an electron storage ring based synchrotron radiation source. The measurement of the emittance can be done indirectly by measuring the transverse beam size using the synchrotron radiation produced by an electron beam. Several techniques to measure the beam size were developed for variety of storage rings. The X-ray pinhole camera is widely used system for the transverse beam profile measurement and emittance feedback. The pinhole beamline depicts the electron beam by analyzing the emitted X-rays. However this method is predominantly applied to the middle and high energy storage rings. At Solaris storage ring with the nominal energy of 1.5 GeV and critical photon beam energy of c.a. 2 keV, the design of the beamline was modified to provide sufficient X-ray photon flux for proper imaging.

The Solaris is a third generation light source consisting of 0.6 GeV S-band linear accelerator with thermionic RF gun, a vertical dog-leg transfer line and 1.5 GeV storage ring with 96 m circumference. More details about the machine layout and design can be found in [1-4] whereas the main storage ring design parameters are presented in Table 1.

Table 1. The SOLARIS storage ring main parameters

Parameter	Value
Energy	1.5 GeV
Max. Current	500 mA
Circumference	96 m
Main RF frequency	99.93 MHz
Harmonic number	32
Horizontal emittance (without insertion devices)	6 nm rad
Coupling	1%
TuneQ_x, Q_y	11.22; 3.15
Electron beam size (straight section centre) σ_x, σ_y	184 μm, 13 μm
Electron beam size (dipole centre) σx, σy	44 μm, 30 μm
Max. number of insertion devices	10
Momentumcompaction	3.055×10^{-3}
Total lifetime of electrons	13 h

The Solaris has been operating with the beam in storage ring since May 2015 and currently services two beamlines (PEEM/XAS with two end-stations, and UARPES with one end-station), three more PHELIX, XMCD and second diagnostic beamline LUMOS have received funding and will be installed and commissioned in next few years.

The first X-ray diagnostic beamline was installed and commissioned in the Solaris storage ring in the mid of 2018. This X-ray diagnostic beamline has been designed to measure the transverse beam profile and to monitor the emittance and their stability during the beam decay.The bending magnets in the storage ring produce photons in the broad energy range from infrared to hard X-ray. In case of PINHOLE beamline, the synchrotron radiation passes from vacuum to air through a 0.4 mm thick CVD (*chemical vapour deposited*) diamond window, which acts also as filter. The bandwidth of the source filtered by the window goes from approximately 3 keV to above 35 keV with peak photon flux at 7 keV. The pinhole is placed behind the CVD window, 2.75m from the X-ray source point.

A rectangular pinhole was made from horizontal and vertical tungsten slits. Whole tungsten block of rectangular pinhole is mounted on four-axis optical table. After passing through the pinhole, X-ray beam is converted to the visible light at the image plane by a thin (0.2 mm) LuAG(Ce) (Lutetium Aluminium Garnet - Lu3Al5O12:Ce) scintillator crystal with a peak emission of 535 nm. LuAG(Ce) phosphor screen is located an additional 3,98 m downstream of the pinhole, so that the image is magnified by a factor of 1.45. An image is obtained with a CCD camera. The emittance is calculated from the size of the image. The relationship between the measured beam size and the electron beam emittance depends on the lattice optical functions, the screen resolution, pinhole size and photon beam divergence.

Figure 1. The image of the electron beam at 250 mA, horizontal/vertical emittances are 7.893/0.0626 nm respectively

The successful installation and commissioning of the X-ray pinhole beamline allows now to measure the emittance and helps in proper 3rd harmonic cavities tuning against the coupled bunch instabilities and avoiding transverse emittance blow-up on uncoupled higher order modes of RF cavities.

[1] MAXIV Detailed Design Report, https://www.maxlab.lu.se/node/113
[2] S.C. Leemann,*Proc. Of IPAC2012*, New Orleans, US, TUPPP024 (2012) 1662.
[3] A.I. Wawrzyniak*et al*.,*Proc. of IPAC2011*, San Sebastian, Spain, THPC123 (2011) 3173.
[4] A. I. Wawrzyniak, R. Nietubyc*et al*., *Proc. of IPAC2013*, Shanghai, China, MOPEA047 (2013) 184.

P-08

Comprehensive strategy for efficient generation of well-diffracted crystals

M. Senda[1]* and T. Senda[1]

[1]*Structural Biology Research Center, Photon Factory, Institute of Materials Structure Science, High Energy Accelerator Research Organization, 1-1 Oho, Tsukuba, Ibaraki, 305-0801 Japan*

Keywords: crystallization, post-crystallization treatment

*e-mail: miki.senda@kek.jp

Protein crystallography is a powerful tool for obtaining 3D structural information of proteins at atomic resolution. Its special advantage is high-throughput structure determination of a great number of protein-compound complexes for pharmaceutical and biochemical sciences. In order to achieve the high-throughput crystal structure determination, however, a robust procedure is needed for an efficient generation of well-diffracted crystals.

At the initial crystallization screening, we can use a fully automated robot consisting of three parts: crystallization system, incubators at 293K and 277K, and observation system [1]. The observation system, PXS-PReMo, automatically takes photos of all droplets following the setup schedule. It is possible to check results of screening from our own computers *via* VPN connection from outside of our laboratory.

One of the frequently occurring problems in crystallization is poor quality of crystals obtained at the initial crystallization screening even if we used the fully automated robot. When crystals were obtained under a several conditions, choice of the best crystallization condition is quite important. Interestingly, quality of bad-looking crystals is sometimes much better than that of good-looking crystals. It is impossible to select well-diffracted crystals only from the appearance of crystals without diffraction images.

When no crystals have sufficient quality at the initial screening, we need to optimize the crystallization conditions in a try-and-error manner. We have accumulated a lot of experiences of crystal quality improvement. These experiences are helpful for efficient improvement of crystal quality.

When collecting diffraction data, protein crystals are frozen at ~100K. Cryoprotectant is usually used for avoiding the ice formation inside the crystals. Several studies have shown that cryoprotectants sometimes interact with protein and stabilized them. In our experience, crystal structure analysis of histone-chaperone TAF-Iβ showed that the trehalose used as a cryoprotectant bound to TAF-Iβ in the crystal [2]. In this case, when the trehalose-soaked crystals were flash-cooled, crystal quality was improved from 5.5 Å to 2.3 Å resolution by changing the space group from *C*2 to *P*2(1). Since protein stabilization would contribute to the crystal quality improvement, we have attempted to use cryoprotectant not only as a cryoprotectant but also as a protein-stabilizing reagent.

The most difficult example in our experience was CagA, which is derived from *H. pyroli.* Initially obtained CagA crystals only diffracted to 7.5 Å resolution at room temperature, suggesting that the crystals were intrinsically of poor quality. In order to improve crystal quality of the CagA crystal, we developed a multi-step soaking method, in which a crystal is sequentially soaked in 2-3 different cryoprotectant solutions. Using the multi-step soaking method, we successfully improved the crystal quality of CagA from 7.5 Å to 3.1 Å resolution, thereby solving the crystal structure of CagA [3].

High resolution crystal structures are required for pharmaceutical and biochemical sciences. Therefore, we usually perform cryoprotectant screening for every crystal except that crystals diffracted very well using glycerol which is the most popular cryoprotectant. We have a standard protocol and recommended cryoprotectants based on our experiences [4]. Quality of several crystals have been improved using our strategy even if original crystals were of poor quality as shown in Table 1 [2, 3, 5, 6, 7]. We believe that our strategy would be applicable to many other protein samples.

Table 1. Typical successful examples of crystal quality improvement using our strategy

Protein	Before [Å]	After [Å]	Cryoprotectant
TAF-Iβ	5.5	2.3	trehalose
CagA	7.5	3.1	trehalose+PEG1K
PI5P4Kβ (human)	3.5	2.1	PVP + EG
BphA4	1.6	1.1	sucrose + PEG200
tandemSH2–peptide	2.3	2.1	diethyleneglycol
CbnR DBD–DNA	2.9	2.5	glycerol
Protein X–DNA	7.5	3.6	erythritol

Acknowledgements: This work was supported by Basis for Supporting Innovative Drug Discovery and Life Science Research (BINDS) from Japan Agency for Medical Research and Development (AMED).

[1] Hiraki *et al.*, *Acta Cryst. D* **62** (2006) 1058.
[2] Muto *et al.*, *PNAS* **104** (2007) 4285.
[3] Hayashi *et al.*, *Cell Host Microbe* **12** (2012) 20.
[4] Senda *et al.*, *Crystal Growth & Design* **16** (2016) 1565.
[5] Sumita *et al.*, *Molecular Cell* **61** (2016) 1.
[6] Hayashi *et al.*, *Cell Reports* **20** (2017) 2876.
[7] Koentjoro *et al.*, *FEBS Journal* **285** (2018) 97.

P-09

Effect of photofunctionalization process on the deposition of hydroxyapatite layer on titanium dioxide substrate

J. Kubacki[1]*, M. Roy[2], K. Dudek[3], A. Szczurek[4] and J. Krzak[4]

[1]*A. Chelkowski Institute of Physics, University of Silesia, 75 PulkuPiechoty 1a, 41-500 Chorzow, Poland*
[2]*Prosthodontic Department, Poznan University of Medical Science, Bukowska 70 – 60-812 Poznan, Poland*
[3]*Institute of Ceramics and Building Materials, Refractory Materials Division Gliwice, Toszecka 99, 44-100 Gliwice, Poland*
[4]*Department of Mechanics, Materials Science and Engineering, Wroclaw University of Technology, Smoluchowskiego 25, 50-370 Wroclaw, Poland*

Keywords: synchrotron radiation, free-electron laser

*e-mail: jerzy.kubacki@us.edu.pl

Implant dentistry is striving to improve success by introducing new materials and methods to modify their surfaces. At present most implants and prosthodontic abutments were composed of titanium dioxide, which is very popular material in dental implantology. The reason for the great interest is the very good biocompatibility of these materials with human bone tissue. The osteointegration process plays a special role in the analysis of the usefulness of these materials in dental implantology [1]. The performed studies have shown that the speed of osteointegration can be increased by surface functionalization in two ways: by depositing of a hydroxyapatite layer on the implant surface or UVC ultraviolet surface irradiation. The first method leads to an increase in the number of active centres to increase the amount of chemical bonds of implant-bone tissue. The second method known as photofunctionalization process removes significantly the amount of hydrocarbons from the implant surface, which also leads to an improvement in the amount and improvement of the quality of chemical bonds. In case of the oxide surface like TiO_2 after production is very reactive with the atmospheric agents and gets contaminated with layer hydrocarbons in 4 weeks since its production. The phenomena of contamination it has been called biological ageing and it is inevitable. It results in a reduction of interaction between the material and the cells resulting in an incomplete integration. Thanks to photofunctionalization it is possible to reverse the process of hydrocarbon contamination and restore the almost carbon free surface typical of the oxide immediately after production [2]. Decreasing of intensity of C1s line and atomic concentration of carbon was about fourfold as was presented in figure 1. An important issue is also the adhesion of hydroxyapatite layers to the implant surface.

The aim of this work was to examine the quality of hydroxyapatite layer deposited on the TiO_2 discs with diameter of 10 mm and different degrees of surface granulation. The hydroxyapatite layers were deposited on substrate before and after applied of the photofunctionalization process. All layers were produced by electrophoresis method at the same current-voltage parameters. The process of surface photofunctionalization of the discs was carried out using the standard commercial procedure with Ushio Therabeam® SuperOsseo device. The X-ray Diffraction method was used to check the quality of the layer.

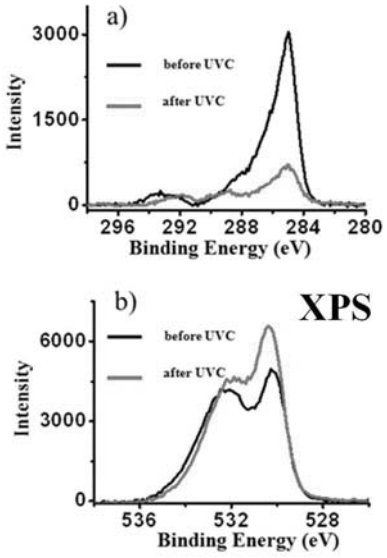

Figure 1. Influence of UVC irradiation on the hydrocarbons contamination of Ti surface [2]

A very good method for the chemical analysis of the deposited layers is the X-Ray Photoelectron Spectroscopy XPS. In addition to the chemical composition, we also get information about the electronic structure which allows to determine the type of bonds of the analyzed layer. The surface morphology was determined by means of an electron microscope combined with the analysis of the Auger electrons. This made it possible to make maps of the chemical distribution of the particular elements of the deposited layers. Adhesions measurement was carried out using Anton Paar Micro-combi-tester devices.

The morphology analysis showed a homogeneous layer of hydroxyapatite independent of the photofunctionalization process. On the other hand, minor differences could be noticed in the electronic structure of the O1s, C1s, P2p, Ca2p lines and the chemical composition of deposited layers, depending mainly on the degree of surface granulation. Significant differences occurred in the measurements of adhesion. Photofunctionalization ofthesubstrate leads to changes in the structure of deposited hydroxyapatite layer especially in the electronic structure and adhesion.

[1] F. Iwasa, N. Hori, T. Ueno, H. Minamikawa, M. Yamada, T. Ogawa, *Biomaterials* **31** (2010) 27172-27.
[2] M. Roy, A. Pompella, J. Kubacki , J. Szade, R. Roy, W. Hedzelek, *PLoS One* **11** (2016) e0157481.

P-10

Impact of doping on electronic structure calculated for $(Fe_{1-x}Mn_x)_2P_{1-y}Si_y$ series

J. Czerniewski[1]* and J. Goraus[1]

[1]*University of Silesia, Faculty of Mathematics, Physics and Chemistry, Institute of Physics,75 PułkuPiechoty 1A, 41-500 Chorzów, Poland*

Keywords: magnetic intermetallics; magnetic properties; ab-initio calculations; electronic structure, calculations

*e-mail: jacekczerniewski@poczta.fm

We present the evolution of the band structure in Fe_2P type series where iron was substituted by manganese and phosphorus was substituted by silicon which was studied in [1-9].

Density Functional Theory (DFT) based calculations show that shifts in the calculated densities of states are much more pronounced for the p-element substitution than for the d-element substitution. Calculations were performed using SPR-KKR-CPA code [10] with 36 energy points and broadening parameter ϵ=0.01 Ry. Manganese can occupy two inequivalent Wyckoff sites in Fe_2P type structure, the differences in simulated spectra for these two structural models are, however, subtle.

We also present the simulation of the X-ray Absorption Spectroscopy (XAS) results which show some observable difference for two structural models considered. These differences should be visible in experimental XAS spectrum, and could resolve which structural model is present in a real sample.

Total densities of states calculated for two structural models.

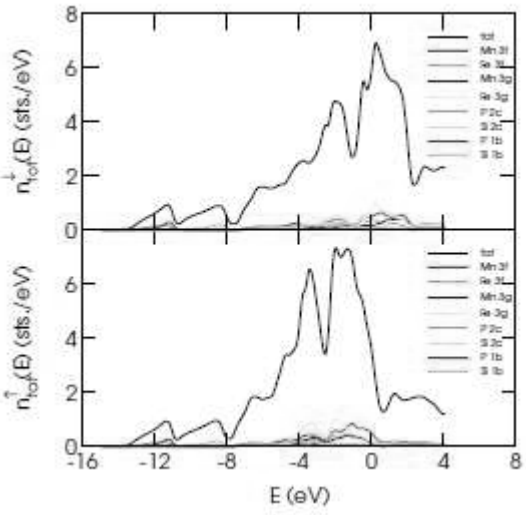

Figure 1. Band structure calculated for the situation when arbitrarily chosen value of $\frac{2}{3}$ of Mn occupies 3f site

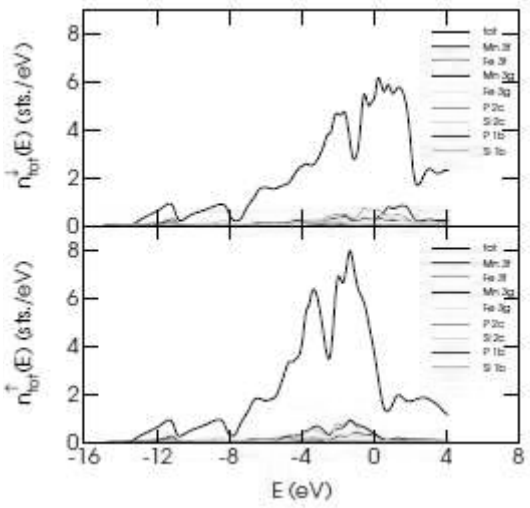

Figure 2. Band structure calculated for the situation when arbitrarily chosen value of $\frac{2}{3}$ of Mn occupies 3g site

[1] E. Brück, *J. Phys. D: Appl. Phys.* **38** (2005) 381.
[2] L. Häggström, J. Sjöström, T. Ericsson, *J. Magn. Mag. Mat.* **60** (1986) 171.
[3] M. Hudl, L. Häggström, E. K. Delczeg-Czirjak, V. Höglin, M. Sahlberg, L. Vitos , O. Eriksson, P. Nordblad, Y. Andersson, *App. Phys. Lett*. **99** (2011) 152502.
[4] V. Höglin, J. Cedervall, M. S. Andersson, T. Sarkar, M. Hudl, P. Nordblad, Y. Andersson, M. Sahlberg, *RSC Advances* **5** (2015) 8278.
[5] V. Höglin, M. Hudl, M. Sahlberg, P. Nordblad, P. Beran, Y. Andersson, *J. Solid State Chem*. **184** (2011) 2434.
[6] Viktor Höglin, M. Hudl, L. Caron, P. Beran, M. H. Sorby, P. Nordblad, Y. Andersson, M. Sahlberg, *J. Solid State Chem* .**221** (2015) 240.
[7] M. J. Neish, M. P. Oxley, J. Guo, B. C. Sales, L. J. Allen, M. F. Chisholm, *Phys. Rev. Lett.* **114** (2015) 106101.
[8] N. H. Dung, L. Zhang, Z. Q. Ou, L. Zhao, L. van Eijck, A. M. Mulders, M. Avdeev, E. Suard, N.H. van Dijk, E. Brück, *Phys. Rev. B* **86** (2012) 045134.
[9] J. Goraus, Ł. Hawełek, P. Włodarczyk, *Solid State Commun*. **224** (2015) 41.
[10] H. Ebert, D. Kodderitzsch, J. Minar: *Rep. Prog. Phys*. 74 (2011) 096501., The Munich SPR-KKR package, version 6.3, H. Ebert *et al*.,http://ebert.cup.uni-muenchen.de/SPRKKR

P-11

Chemically induced nanocrystalline peak shift and asymmetry

Z. Kaszkur[1]*, M. Zieliński[1] and I. Smirnov[1]

[1]*Institute of Physical Chemistry PAS,Kasprzaka 44/52, Warszawa 01-224, Poland*

Keywords: synchrotron radiation, in situ diffraction

*e-mail: zkaszkur@ichf.edu.pl

Wide angle powder diffraction patterns of nanocrystalline metals (Pt, Pd, Au) supported on amorphous silica have been measured in Debye-Scherrer geometry, in capillary connected to various atmosphere (O_2, He, H_2). The measurements were done at ID22 beamline of ESRF using flat panel Perkin Elmer XRD 1611CP3 detector.

The work aimed at developing methodology of powder diffraction analysis for nanocrystalline metals.

Usually not realized an inherent feature of their diffraction pattern is the peak asymmetry, that can be either left or right hand side depending on the state of the crystal surface. Dependence of effective lattice parameter (LP) on the crystal size comes from the surface unsaturated bonds and results in the strongest effect for the surface layers. The real effect is different than estimated from small model fragments of the perfect lattice. The asymmetry depends on the state of the crystal surface and its changes on adsorption, the more the smaller the crystal.

The objective of the work is to verify the proposed by us method [1] of analysis of the asymmetry on high quality diffraction data spanning up to high scattering vector values K (~30 A^{-1}) or more). A proof of the method assumes comparison between the peak shape for bare crystal surface and the surface with saturated by adsorbate bonds and requires measurement in oxidative (air or oxygen) and innert after reduction (diluted hydrogen) atmospheres.

The proposed method [1] basing on diffraction profile decomposition into Voigt functions that are especially suitable for analysis as having analytic Fourier Transform. It results in both: LP dependence from crystal size and a column length distribution (CLD) (in cases when microstrain is negligible). The method is based on the Balzar work [2] on a peak shape analysis with added arguments originating from our atomistic simulations for metal nanocrystals proving the deviations from Bragg's Law [3] and their dependence on interaction with the adsorbate on different crystal faces [4 with supplementary info].

The added value of the method is determination of the real peak background level, based on the physical requirement of Column Length Distribution (CLD) positivity.

We have tested several approaches to extract intensity scattered by the nanometal phase from capillary and silica support contributions in Debye-Scherrer geometry. To analyze details of the structure response to varying atmosphere due to very small crystal sizes (Au) we use combined approach of fitting the overlapping peaks with analytical functions and of modelling the atomic Pair Distribution Function (PDF) calculated from the wide angle intensity distribution using developed by us method [5].

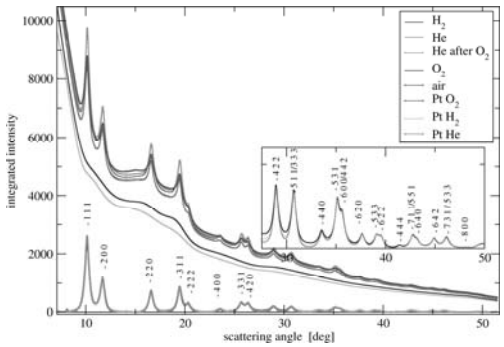

Figure 1. Diffraction patterns of Pt/silica sample exposed to a number of atmospheres together with the empty capillary and silica patterns. Below are the metal (Pt) phase patterns with Miller indices marked

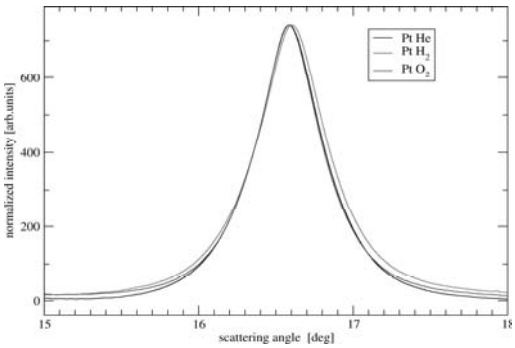

Figure 2. Pt 220 peak of Pt/silica sample exposed to a number of atmospheres

Acknowledgements: This work was supported by ESRF grant MA-3959

[1] Z. Kaszkur, M. Zielinski, W. Juszczyk, *J. Appl. Crystall.* **50** (2017) 585.
[2] D. Balzar, *J. Res .Natl. Inst. Stand. Technol.* **98** (1993) 321.
[3] Z. Kaszkur, *Z. Kristallogr.* **2** (2006) 147.
[4] Z. Kaszkur, P. Rzeszotarski, W. Juszczyk, *J. Appl. Crystall.* **47** (2014) 2069.
[5] Z. Kaszkur, *J. Appl.Crystall.* **23** (1990) 180.

P-12

Time and angle resolved photoemission study of hot electron behavior in doped Bi_2Te_3

T. Sobol[1;2; 3]* and J. Szade[2;3]

[1]*Central European Research Infrastructure Consortium, CERIC-ERIC, Dyna Chiro project, S.S. 14 - km 163,5 in AREA Science Park, 34149 - Basovizza, Trieste - ITALY*
[2]*National Synchrotron Radiation Centre SOLARIS, Jagiellonian University, Czerwone Maki 98,30-392 Kraków, Poland*
[3]*Institute of Physics, University of Silesia, 75 PułkuPiechoty 1A, 41-500 Chorzów, Poland*

Keywords: topological insulators, Bi_2Te_3, higher harmonic generator,synchrotron radiation.

*e-mail: tomasz.sobol@ceric-eric.eu

Interactions of photoexcited electrons in topological insulators is one of the most important topics in the physics of these materials. Spin to charge conversion, electron phonon interaction and other phenomena are related with the processes involving surface and bulk states in the time scale of femto- and pico seconds.

Moreover, it is of crucial importance to recognize the effects taking place at the interface of topological insulator and other metals, including the magnetic ones. Any device which is going to use the effect of spin to charge conversion will face that problem.

Generally, transition metals are expected to destroy the linear band dispersion and helical spin structure of surface states. It was found that covering of topological insulators, including Bi_2Te_3 (BT) by thin film of Fe film leads to the formation of the energy gap although other papers did not confirm that [see eg. 1,2].

The time and angle resolved photoelectron spectroscopy was shown to be a perfect tool to study the electron dynamics for robust topological insulators. Sobota et al. and other groups have shown how the electron relaxation time depends on the location of the electrons excited by the infrared femtosecond impulse and populating various regions of the bulk and surface Brillouine zone [see e.g. 3,4].

The aim of our project was to study electronic structure and electron dynamics in BT capped with a very thin Fe layer. Oxidation effect was studied in a controllable way. Additionally, the effect of Fe doping to BT grown as a thin film was checked. Doping was realized in a co-deposition mode during the MBE growth.

Acknowledgements: This work is created as part of the Dyna Chiro project that is a CERIC internal research project.

[1] M. R. Scholz, J. Sanchez-Barriga, D. Marchenko, A. Varykhalov, A. Volykhov, L. V. Yashina, O. Rader, *Phys. Rev. Lett.* **108** (2012) 256810.
[2] L. A. Wray *et al.,* Nature Phys. **7** (2011) 32.
[3] J. A. Sobota *et al*., *Phys. Rev. Lett.* **113** (2014) 157401.
[4] J. Sánchez-Barriga *et al.*, *Phys. Rev. B* **95** (2017) 125405.

P-13

Hydrothermal synthesis and characterization of molybdenum disulfide and strontium molybdate nanocomposite

S. Ramanavičius[1]* and A. Jagminas[1]

[1]*State research institute Center for Physical Sciences and Technology, Savanoriųave. 231, LT-02300 Vilnius, Lithuania*

Keywords: synchrotron radiation, free-electron laser

*e-mail: simonas.ramanavicius@ftmc.lt

To design new compounds with specific, tailor-made qualities, 2D layered structures recently are investigated with much interest [1].

In this study, highly crystalline nanostructured composite comprised of strontium molybdate and molybdenum disulphide is fabricated at the conductive substrate by a simple one-pot hydrothermal synthesis approach. For this, an aqueous solution of ammonium heptamolybdate, strontium nitrate, and thiourea has been successfully used for the first time. The formation of highly crystalline composite film composed of nanoplatelet species, densely packed and well attached to conductive Ti/TiO_2 substrate, is obtained and verified by scanning and transmission electron microscopy, X-ray diffraction, and electrocatalytic water splitting tests. Note that the hybridization of MoS_2 with $SrMoO_4$ resulted in the formation of electrocatalyst possessing a lower hydrogen evolution overvoltage by ≅ 50 mV compare to that at a pure 2H-MoS_2 nanoplatelet electrode [2].

To increase the HER activity and durability, further compositional improvements of this catalyst are envisaged.

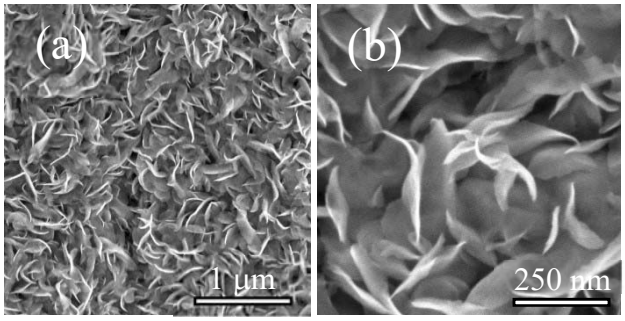

Figure 1. Top-side SEM image (a) and XRD pattern (b) of the film formed at the anodized titanium substrate by one-pot hydrothermal synthesis way at 220 °C for 10 h

[1] M. Graf, M. Lihter, M. Thakur, V. Georgiou, J. Topolancik, B. R. Ilic, K. Liu, J. Feng, Y. Astier, A. Radenovic, *Nat.Protoc.* **14** (2019) 1130–1168.
[2] Z. Wu, B. Fang, Z. Wang, C. Wang, Z. Liu, F. Liu, W. Wang, A.Alfantazi, D. Wang, D. P. Wilkinson, *ACS Catalysis* **3** (2013) 2101–2107.

P-14

Structural and conformational changes of amyloid beta peptides assemblies induce by the presence of surfactants

M. Wilkowska[1]*, B. Peplińska[2] and M. Kozak[1;3]

[1]*Department of Macromolecular Physics, Faculty of Physics, Adam Mickiewicz University, Uniwersytetu Poznańskiego 2, 61-614 Poznań, Poland*
[2]*NanoBioMedical Centre, Adam Mickiewicz University, Wszechnicy Piastowskiej 3, 61-614 Poznań, Poland*
[3]*Joint SAXS Laboratory, Adam Mickiewicz University, Uniwersytetu Poznańskiego 2, 61-614 Poznań, Poland*

Keywords: Alzheimer disease, amyloid beta peptide, SAXS, FTIR, CD, AFM, TEM

*e-mail: mskupin@amu.edu.pl

In recent years, it is believed that the primary role in the formation of the Alzheimer's Disease (AD) plays soluble oligomeric assemblies of amyloid beta peptides (Aβ). The oligomerization process of Aβ peptide is relatively fast and it can be affected by many variables [1,2]. The control of Aβ aggregation is very hard to achieve, but the use of selected specific surfactants and investigation of their interaction with peptides may contribute to a better understanding of this process.

The aim of this study was characterization of the structural and conformational changes in beta amyloid peptides induced by the presence of a different types of surfactants in various concentrations. The effect of surfactant concentration in solution was tested on amyloid beta 1-40 fibrils and their short variants..

The size distribution of Aβ peptide aggregates in the solutions of selected surfactants was evaluated using atomic force microscopy (AFM) and transmission electron microscopy (TEM). AFM and TEM allowed the visualization the morphology of fibrils and aggregates of Aβ peptides. AFM measurements allowed estimation of the heights, but TEM studies allowed a more accurate estimation of the width of obtained aggregate structures. The changes in secondary structure of Aβ peptides in the presence of different concentrations of surfactants were tested using FTIR spectroscopy and circular dichroism (CD) methods. Small angle scattering of X-ray (SAXS) studies by the use of synchrotron radiation were performed for selected solutions of tested surfactants and Aβ aggregates. The kinetics of aggregation behavior of Aβ peptides in the surfactant environments was studied using fluorescence spectroscopy with Thioflavin T assay.

In order to verify the suitability of chosen surfactants for therapeutic purposes, preliminary examination of their cytotoxicity on HeLa and fibroblast cells was conducted.

Acknowledgements: The study was supported by research grant, Grant Diamentowy"from Ministry of Science and Higher Education (Poland) - DEC:0011/DIA2015/44.

[1] J. Hardy, D. J. Selkoe, *Science*, **297** (2002) 353.
[2] J. A. Loureiro, S. Rocha, M. do C. Pereira, *J. Pept. Sci. Off. Publ. Eur. Pept. Soc.* **19** (2013) 581.

P-15

Tricationic and tetracationic surfactants as transgene carriers – comparison of their physicochemical properties

W. J. Andrzejewska[1]*, B. Peplińska[2], M. Kempka[1], D. Clemens[4], U. Keiderling[5], E. Härk[4], Z. Kochovski[4] and M. Kozak[1;3]

[1]*Department of Macromolecular Physics, Faculty of Physics, Adam Mickiewicz University, Uniwersytetu Poznańskiego 2, 61-614 Poznan, Poland*
[2]*NanoBioMedicalCentre, Wszechnicy Piastowskiej 3, 61-614 Poznań Poland*
[3]*Joint SAXS Laboratory, Adam Mickiewicz University, Uniwersytetu Poznańskiego 2, 61-614 Poznan, Poland*
[4]*Institute for Soft Matter and Functional Materials, Helmholtz-Zentrum Berlin, Hahn-Meitner-Platz 1, Berlin 14109, Germany*
[5]*Department Experiment control and data acquisition, Helmholtz-Zentrum Berlin fürMaterialien and Energie, 14109 Berlin, Germany*

Keywords: small angle X-ray scattering, small angle neutron scattering, siRNA, polycationic surfactants, gene carriers

*e-mail: weronika.andrzejewska@amu.edu.pl

Compounds (dicationic and oligocationic surfactants, charged polymers) that are used for binding and transport of nucleic acids should be characterized by high biocompatibility and ability to form stable lipoplexes with nucleic acids [1]. In practice, they should support efficient transfer of therapeutic material (transgene) to the pathological cells. Introduced transgene by interaction with the corresponding cellular genome induces a permanent curative effect [2,3].

It is supposed that polycationic surfactants which are structurally similar to natural lipids may have good transfection properties. The physicochemical properties of these compounds promote their ability to create stable and nontoxic complexes with dsDNA and siRNA [4].

In this work we present results of structural studies of polycationic surfactants and their complexes with short nucleic acid oligomers (dsDNA and siRNA, 21 bp). These systems were examined by selected biophysical methods like small angle X-ray scattering (SAXS), small angle neutron scattering (SANS), electron microscopy, spectroscopy etc.

The studies have shown different structural properties of studied surfactants, depending on the size of their molecules (number of positively charged subunits) and ability to form stable lipoplexes.

Acknowledgements: This work was supported by research grant(UMO-2016/23/N/ST4/01637) from National Science Centre (Poland).Special thanks to collaborators from Helmholtz Zentrum Berlin and NanoBioMedicalCentre.

[1] C. Amoruso *et al.*, *SIAM J. on App. Math*. **71** (2011) 2334-2358.
[2] J. Pernak *et al., Chem. Eur. J.* **13** (2007) 3106-3112.
[3] F. Mutelet *et al., J. Chem. Eng. Data* **57** (2012) 918-927.
[4] W. Andrzejewska *et al.*, *Biophys. J*. **114**(3) Supplement 1, (2018) 438a.

P-16

Changes in secondary structure of human prion protein peptide 30-90 induced by the presence of cationic gemini surfactant

J. Ludwiczak[1]* and M. Kozak[1]

[1]*Adam Mickiewicz University,Uniwersytetu Poznańskiego 2, 61-614 Poznań, Poland, Poznań,Poland*

Keywords: Prion protein, surfactants, secondary structure

*e-mail: jj13800@amu.edu.pl

Human prion protein (PrP) is a small, glycosylated macromolecule located in the extracellular surface of neurons and involved in the signal transduction. Misfolding of PrP proteins followed by its aggregation in different organisms (human, sheep, cow etc.) is associated with development of several neurodegenerative diseases [1]. Therefore, understanding the mechanism of the PrP misfolding process is of enormous interest in the scientific community. Conformational changes observed for human prion protein peptide 30-90 are closely related to the ability of full-length protein to undergo aggregation and fibrilization.

By interaction of human prion protein peptide 30-90 with gemini surfactant we can monitor changes in secondary structure (e.g. β-sheets) content, which is connected with formation of amyloid deposits. The present study was aimed at determination of the influence of selected cationic gemini imidazolium surfactant with different spacer on secondary structure of human prion protein peptide 30-90 in native form and at different pH conditions by the use of spectroscopic techniques (FTIR, circular dichroism).

Acknowledgements: This work was supported by research grant (UMO-2016/23/N/ST5/02013) from National Science Centrę (Poland). Surfactants were generous gift from dr Andrzej Skrzypczak (Poznań University of Technology, Poland).

[1] N .J. Cobb , W. K. Surewicz, *Biochemistry* **48** (2009) 2574 – 2585.

P-17

Radiation damage of proteins caused by synchrotron radiation – a case study based on bioSAXS experiments

A. Moliński[1;2]*, M. Taube[1], Z. Pietralik[1], M. Gielnik[1] and M. Kozak[1;3]

[1]*Department of Macromolecular Physics, Faculty of Physics, Adam Mickiewicz University in Poznań, Uniwersytetu Poznańskiego 2, 61-614 Poznań, Poland*
[2]*Nano-Bio-Medical Centre, Adam Mickiewicz University in Poznań, Wszechnicy Piastowskiej 3, 61-614 Poznań, Poland*
[3]*Joint Laboratory for SAXS Studies, Faculty of Physics, Adam Mickiewicz University in Poznań, Uniwersytetu Poznańskiego 2, 61-614 Poznań, Poland*

Keywords: radiation damage, bioSAXS

*e-mail: augmol@amu.edu.pl

To investigate the structure and dynamics of biomolecules there is a wide spectrum of different techniques based on diffraction or scattering of synchrotron radiation or neutrons. Amongst others, the most popular ones are macromolecular crystallography and small angle X-ray scattering (SAXS), that take advantage of the accessibility of modern synchrotron light sources. High intensity of X-ray radiation allows us to reduce the time needed for experiment and obtainhigh-quality data. However, it could also cause severe damage to samples both crystalline and in solution. Particularly, protein solutions studied by SAXS are prone to aggregation and degradation after irradiation [1,2]. Nevertheless, scientists developed numerous methods of preventing investigated samples from those damages like the addition of the stabilizing agent to the solution [3]. Nonetheless, despite those efforts, some proteins are still prone to damage from the high intensity of X-ray beams. In this study, we will present our own experience with protein degradation (human cystatin C, human prion protein) during synchrotron SAXS experiments.

Acknowledgements: This research was supported by a research grant (2014/15/B/ST4/04839) from National Science Centre (Poland) and the grant POLTUR2/3/2017 from National Centre for Research and Development (Poland)

[1] J. B. Hopkin, R. E. Thorne, *J. Appl. Crystallogr.* **49** (2016) 880–890.
[2] C. M. Jeffries, M. A. Graewert, D. I. Svergun, C. E. Blanchet, *J Synchrotron Radiat.* **22** (2) (2015) 273-279.
[3] S. P. Meisburger, M. Warkentin, H. Chen, J. B. Hopkins, R. E. Gillilan, L. Pollack, R. E. Thorne, *Biophys J.* **104**(1) (2013) 227–236.

P-18

Influence of zinc ions on secondary structure of PrP (58-93) peptide variants containing octarepeat region

J. Wolak[1]*, A. Szymańska[2] and M. Kozak[1]

[1]*Faculty of Physics Adam Mickiewicz University in Poznan, ul. Uniwersytetu Poznańskiego 2, 61-614 Poznań, Poland*
[2]*Faculty of Chemistry, University of Gdańsk, ul. WitaStwosza 63, 80-308 Gdańsk, Poland*

Keywords: prione peptide, molecular dynamic

*e-mail: joanna.wolak@amu.edu.pl

Neurodegenerative diseases are one of the greatest challenges of modern medicine and it is hard to find a good strategy of their treatment. Development of new treatment routes and design of new drugs require recognition of all components (peptides and proteins) involved in the disease process.

Creutzfeldt–Jakob disease (CJD) is a fatal neurodegenerative disease of central nervous system classified as transmissible spongiform encephalopathy. CDJ is caused by the process of aggregation of misfolded isoforms prion peptides (PrPSc), which shorten fragments of prion protein (PrPC). The human prion protein is the membrane protein that consists of two domains: structured C-terminal domain and N-terminal flexible domain which include four octarepeated fragments. In this region histidine residue which is able to coordinate divalent cations can be identified. Divalent ions like copper or zinc can force changes in the secondary structure of prion protein leading to aggregation processes [1].

The aim of this study was to examine the conformational changes in mutants of PrP (58-93) peptide induced by the presence of zinc ions. The study was performed on the synthesized peptides with histidine residues replaced by alanine at different positions. To examine the influence of zinc on the structure of prion peptides, molecular dynamics simulations were carried out using the programs GROMACS and YASARA. Moreover, changes in the secondary structure studied peptides were analysed by Circular Dichroism Spectroscopy (CD) and Fourier Transform Infrared Spectroscopy (FTIR).

AcknowledgementsThis research was supported by a research grant (2014/15/B/ST4/04839) from National Science Centre (Poland).

[1] K. Pan, C. W. Yi, J. Chen, Y. Liang, *Biochim.Biophys. Acta*, **8** (2015) 1854

P-19

High energy XAS beamline at SOLARIS possible data quality

M. T. Klepka[1]*, D. Kalinowska[1], W. Klysubun[2] and A. Wolska[2]

[1]*Institute of Physics Polish Academy of Sciences, Al. Lotnikow 32/46, 02-668 Warsaw, Poland*
[2]*Synchrotron Light Research Institute, Nakhon Ratchasima 30000, Thailand*

Keywords: XAS, beamline, SOLARIS synchrotron

*e-mail: mklepka@ifpan.edu.pl

XAS beamline at SOLARIS synchrotron is under construction. Three way letter of cooperation between Hochschule Niederrhein – University of Applied Sciences in Germany, Synchrotron Light Research Institute in Thailand (SLRI) and Jagiellonian University has been signed in December last year. The beamline is planned to be ready within two years.

XAS group from the Institute of Physics PAS is involved from scientific point of view in this project. BL8 beamline at the SLRI is a twin beamline to the one which will be constructed at SOLARIS. Its energy is up to 13 keV what gives possibility to cover EXAFS region for all 3d tramsitionmetals. Test measurements at Cu K-edge have been performed and compared to the results obtained for the same samples at the XAFS beamline at Elettra synchrotron (Trieste Italy).

Results of the comparison will be presented and discussed.

[1] W. Klysubun, P. Sombunchoo, N. Wongprachanukul, P. Tarawarakarn, S. Klinkhieo, J. Chaiprapa, P. Songsiriritthigul, *Nucl. Instr. Meth. Phys. Res. A* **852** (2007) 87-89.

[2] W. Klysubun, P. Tarawarakarn, N. Thamsanong, P. Amonpattaratkit, C. Cholsuk, S. Lapboonrueng, S. Chaichuay, W. Wongtepa, *Radiat. Phys. Chem.* 2019 in press

P-20

Amyloids β aggregation in the presence of human serum albumin and human cystatin C – structural investigation

A. Żyła[1;2]*, M. Taube[3], M. Kozak[1;2;3] and W. Bal[4]

[1]*Department of Macromolecular Physics, Faculty of Physics, Adam Mickiewicz University in Poznań, UniwersytetuPoznańskiego 2, Poznań, Poland*
[2]*NanoBioMedical Centre, Wszechnicy Piastowskiej 3, Poznań, Poland*
[3]*Joint Laboratory for SAXS Studies, Faculty of Physics, Adam Mickiewicz University in Pozna, Uniwersytetu Poznańskiego 2, Poznań, Poland*
[4]*Department of Biophysics, Institute of Biochemistry and Biophysics, Polish Academy of Sciences,Pawinskiego 5a, Warszawa, Poland*

Keywords: HSA, HCC, amyloid β, SAXS, SANS, Molecular Docking, Molecular Dynamics. Structural investigation

*e-mail adrzyl@amu.edu.pl

Development of neurodegenerative disorders (Alzheimer's, Parkinson's diseases) correlates with the extended lifetime in our population and these diseases are a serious challenge for science. Still we have no effective drugs that would be able to combat these diseases. The discovery of molecules (proteins and peptides) [1] responsible for development of these diseases was a milestone in understanding them at molecular level, and determination of three-dimensional structures of these macromolecules permitted understanding some of the mechanisms of protein aggregation and the formation of their neurotoxic oligomers or amyloid deposits. There are also promising studies showing that proteins like human serum albumin (HSA) [2] or human cystatin C (HCC) [3] could be involved in the inhibition of Aβ peptides aggregation into toxic amyloids. For further studies it will be crucial to characterize the structural properties of these complexes but also to resolve the mechanism of binding in the atomic scale.

Figure 1. Human serum albumin with docked Aβ 1-42 and equilibrated by Molecular Dynamics

We have optimized a protocol of production and purification of HSA and HCC proteins and synthesis of some variants Aβ peptides. Purified proteins will be used in the investigation of Aβ peptides aggregation by biophysical methods like nuclear magnetic resonance (NMR), circular dichroism (CD). Recently, we have initiated the studies of HSA complexes with Aβ using small angle X-ray/neutron scattering (SAXS /SANS). We also proposed a theoretical model of binding the Aβ peptides to the HSA molecule.

Acknowledgements: The studies were supported by research grant 2017/27/B/ST4/00485 from National Science Centre, POWR.03.02.00-00-I032/16 from European funds and international grant POLTUR2/3/2017 from National Center of Research and Development.

[1] M. A. Castell, S. Soriano, *Ageing R.s Rev.* **13** (2014) 10-2.
[2] T. S. Choi et al., *J. Am. Chem. Soc*. **139** (2017) 15437-15445.
[3] M. Spodziejaet al., *J. Mol. Recognit*. **30** (2017) 2.

A-01

SOLARIS Synchrotron accelerators

A. Wawrzyniak[1,*]

[1]National Solaris National Synchrotron Radiation Centre, Krakow, Poland

SOLARIS is a third generation light source constructed at the Jagiellonian University (JU) in Kraków, Poland. The project was started in 2010 as a greenfield project with unique cooperation between JU and the MAXLab in Lund, Sweden. Within this framework, two twin 1.5 GeV storage rings were designed and built. The installation of the SOLARIS machine started on May 2014 and one year later was completed. In November 2014, the subsystem tests and conditioning of the SOLARIS linear accelerator (linac) was started and in the end of February 2015, the 300 MeV electron beam at the end of the linac was observed for the first time. After this achievement, the machine was shut down for 2.5 months to complete transfer line and storage ring installation. In May 2015, the commissioning of the linac together with the transfer line and storage ring began. In June, the first turns and then the accumulated beam were observed. On 19 June, a 0.07 mA current was stored at an energy of 380 MeV and the first synchrotron light from the dipole was detected on the fluorescent screen at the PEEM beamline's front end.

Linear accelerator: The SOLARIS injector consists of a 0.6 GeV S-band linac with a thermionic RF gun and a vertical dog-leg beam transfer line. The electron source is a thermionic RF gun with a BaO cathode that has been chosen for simplicity of operation. This gun was designed and manufactured at MAX IV Laboratory. The energy of the electron beam exiting the gun is 2.8 MeV and the average current of the bunch train right after the gun is 200 mA. To focus the bunches, two solenoid magnets are installed after the gun. The beam is transported through the chopper section and an energy filter in order to compress and clean the beam. The linear accelerator consists of six five-meter long S-band travelling wave accelerating structures combined in three accelerating units. Each accelerating unit contains one SLED (SLAC Energy Doubler) cavity and two linac structures and is powered by an RF amplifier. Between the linac structures, quadrupoles, steering magnets and diagnostics instruments are placed to focus and guide the beam. The transfer line efficiently transports the beam from the linac to the storage ring. The main components of the transfer line are the dipoles, with a total bend angle of 27 degrees, which bend the beam in the vertical plane, as well as six focusing quadrupoles. The last element is a septum magnet, which connects the injector with the storage ring. The total length of the injector is ca. 54 meters.

***Storage ring*:** The SOLARIS 1.5 GeV storage ring is composed of twelve double bend achromat (DBA) cells. Most of the magnets in the DBA are multifunction:

- bending magnets with defocusing gradient and pole face strips,
- focusing quadrupoles with focusing sextupole content
- defocusing sextupoles with trim coils for skew quads
- correction sextupole magnets with additional coils of steering magnets.

All the magnets within one DBA cell are shaped in one Armco block. This innovative approach allows the mutual alignment of magnets within the DBA cell to be within a 25 μm tolerance range and makes the cell short, merely 4.2 m. This implementation, however, comes at the cost of the challenging manufacturing requirements of the magnets and vacuum chambers as well as their assembly. There are twelve 3.5 m-long straight sections in the storage ring. Two of them are completely occupied with diagnostic instruments, a vertical pinger, the injection septum magnet (1st straight), two 100 MHzRF cavities, and two Landau cavities (12th straight). Additionally, in the 3rd straight section a dipole injection kicker magnet is installed. All the other straight sections are fully dedicated for insertion devices (IDs). The optical functions for the achromat are shown in figure 1.

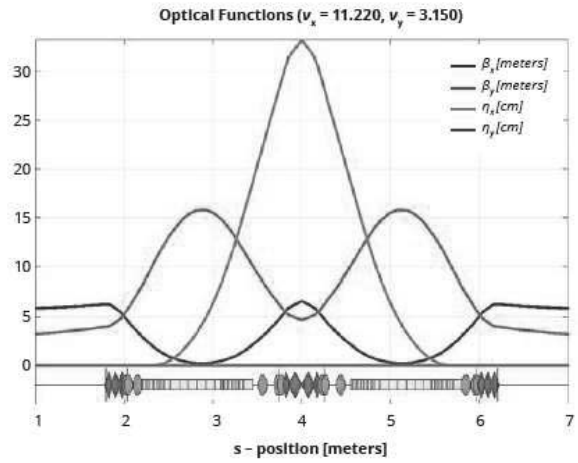

Figure 1. The optical functions for the single DBA cell

As one can see, the beta functions and dispersion have low values, reducing the need for large vacuum chamber apertures. The cross section of the vacuum chambers has inner dimensions of 40/20 mm (horizontal/vertical), however at the center of the double-bend achromat the aperture is increased to 56/28 mm.

Beam injection into the storage ring is done by a single pulsed dipole magnet installed in the 3rd straight section.

Machine operation: The commissioning of the storage ring started in May 2015 and was divided into three phases. Phase I took place between May and July 2015. During this period, the first electrons were injected into

the storage ring at an energy of ca. 400 MeV, the first turns were observed, and later accumulation and a stored beam of a few mA was obtained. During this phase, the main effort was put into matching the linac, transfer line and storage ring energy. However, the working point of the SR differed from the design one. During summer shutdown, the aluminum vacuum chamber and undulator in the 5th straight section was installed. After summer shutdown, phase II of the commissioning started. The main achievements were to bring the tune values to the design ones, correct the chromaticity to +1, improve the orbit correction, increase the stored current and ramp the beam up to the final energy of 1.5 GeV. At the end of this phase, the maximum current possible to store was 200 mA. The beam current*lifetime product (I. τ) at that time was about 0.5 Ah (see figure 2). During the long winter shutdown, the 3rd harmonic cavities were installed and in spring 2016 the 3rd phase of storage ring commissioning started. The goals of this phase were to improve the injection rate and ramping speed, make beam-based alignment, increase the lifetime by vacuum conditioning and tuning the Landau cavities. Between April and December 2016, the time for the storage ring commissioning was shared with the commissioning of the UARPES beamline. The magnet shunting was done at the early commissioning phase based on the magnetic measurements, but now after Linear Optics from Closed Orbit (LOCO) optimization some additional changes in the shunting are needed. Nowadays, the linac delivers an electron beam with an energy of 535 MeV. The beam is injected to the storage ring with the repetition rate of 1 Hz. In the beginning, a chopper was not used and the 3 GHz bunches were injected as a long bunch train of 184 ns. Therefore, during the injection process a high radiation level was registered at the experimental hall. The estimated injection efficiency at that time was 30%. In 2017, the chopper system was commissioned and put into operation. This improved the injection efficiency up to 60% and drastically reduced the loss rate during the injection process. The ramping is executed in less than 4 min., therefore the whole injection process together with Landau cavities tuning and beam stabilization takes less than 30 min. During commissioning phases, a good performance level of the SOLARIS storage ring was reached. The beam optics was brought close to the design values. The measured storage ring parameters with respect to the theoretical values are presented in table 2. However, studies of betatron function revealed beta beating in the range of several percent. This, in addition to closed orbit, phase advance and dispersion studies indicate that the shunting of individual magnets has to be revised. After ca. 400 Ah of beam cleaning, the vacuum condition allowed 400 mA of the beam current to be stored at the final Energy with a total lifetime of 8 h. Moreover, after reaching the 575 Ah of the integrated current (winter 2018), the nominal current of 500 mA at full (1.5 GeV) Energy was stored. However, vacuum conditioning of the RF cavities is still required for high currents. The evolution of the I. τ product with respect to the integrated current from the start-up of the storage ring up to now is shown in figure 2.

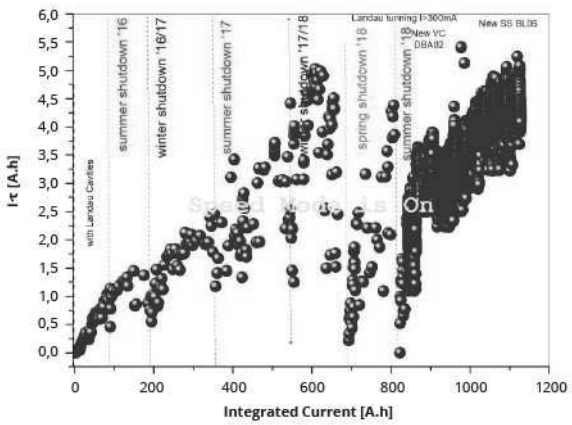

Figure 2. The I.τ product versus integrated current in the storage ring

The degradation of the lifetime after a few shutdown periods is mostly connected with the installation of the new vacuum chambers (IDstraight sections; frontends; bending magnet section; diagnostic beamline) and/or some leaks and their repairs in the RF section. Some longitudinal instabilities that are present have been cured by tuning the Landau cavities to the 3rd harmonic resonance. Moreover, once the Landau cavities are tuned, the Touschek lifetime increases by a factor of 3. Since the commissioning of the experimental beamlines as well as user operation is on-going, beam stability and reproducibility is of great interest. These studies have shown that the electron orbit can be restored from injection to injection within a tens of microns range when orbit correction is applied. The main concern is the thermal stability of the storage ring, which for the moment oscillates within a range of 1.5ºC, having an impact on the beam oscillations. Some changes in the cooling water system are planned in the near future to improve thermal stability at SOLARIS. Recently, the closed orbit was improved and now the rms values of the closed orbit in both planes are below 1 um. Moreover, during the summer shutdown in 2018 the X-ray pinhole diagnostic beamline was installed and put into operation. The successful installation and commissioning of the X-ray pinhole beamline allows the emittance to now be measured and helps in proper tuning of 3rd harmonic cavities against coupled bunch mode instabilities. In 2016, 21 weeks of operation were dedicated for machine studies and commissioning, and 17 weeks were devoted to beamline commissioning. The machine was shut down in total for 14 weeks. In 2017, 14 weeks were also scheduled for the shutdown period. Due to ongoing installation and improvements on the existing beamlines, only 15 weeks were dedicated to the beamlines and the rest of time (23 weeks) was used for machine optimization. Since 1 October 2018, the SOLARIS storage ring has been in the user operation mode. In 2018, the SOLARIS storage ring ran more than 1 328 h for beamline commissioning and users. A total beam availability of 90.4% was reached. About 376 h were dedicated to the optimization of the accelerators for the users. The time distribution between machine and beamlines is presented in figure 6. In table 3, the current delivered to the users over first 3 months of user operation is presented.

The average operating current was 270 mA. The mean time before failure (MTBF) in 2018 was 16.3 h, whereas the mean time to recover (MTTR) was 1.5 h.

Future plans: A very good level of performance of the SOLARIS synchrotron has been reached over the last 2 years of operation. However, some fine-tuning of the linac and storage ring optics is still required. For the near future, measurements of emittance, energy spread, Twiss parameters, LOCO, lifetime, etc. are planned. Since there is continuous work on injection efficiency improvement, a chopper system upgrade will be implemented to increase the injection efficiency from 60% up to 100%. The SOLARIS storage ring is under permanent development. New insertion devices for new Beamlines are planned to be installed and made operational. Therefore, an effort to optimize linear and nonlinear optics with new devices is being made. To keep the beam stable for long time, beam instabilities are being studied and cured with bunch by bunch feedback systems which are planned to be developed and installed. Moreover, to keep the beam stable during IDs operations, fast orbit feedback is planned to be installed and made functional. A new diagnostic beamline based on visible light is going to be installed in 2019. This will make it possible to measure the transversal as well as the longitudinal electron beam parameters. There are also ongoing studies on a full energy linac and top-up injection. From the operational point of view, the preparation work is being done to have the facility delivering a beam to users for more than 5 000 h per year, which means 24 h/7 days operation.

A-02

SOLARIS Synchrotron beamlines

collaborative work edited by J. Szade[1,2*]

[1]*National Solaris National Synchrotron Radiation Centre, Krakow, Poland*
[2]*University of Silesia in Katowice, Poland*

Active Beamlines

UARPES: the beamline delivers vacuum ultraviolet photons for research using angle-resolved photoemission-spectroscopy (ARPES). This technology occupies an exceptionally important place among techniques for structural studies as it makes it possible measurement of the fundamental electron parameters: energy and momentum. Thanks to this technology, it is possible to quickly and precisely study band structure in 3Dwith allowance for electronic correlation effects. TheARPES research technology is of prime importance for the development of science and technology as it allows for experimental demarcation of the electronic band structure of matter. The electronic structure in turn determines all of the physical and chemical properties of the material. Some of the possible applications for research using the UARPES beamline include research on superconductors, new electronic materials, and low dimensional materials.

PEEM/XAS: the PEEM/XAS is a bending magnet based beamline dedicated to microscopy and spectroscopy in the soft X-ray energy range. The beamline is designed to study chemical and electronic, structural and magnetic properties by means of XAS, XNLD(X-ray natural linear dichroism), XMCD (X-ray magnetic circular dichroism), and XMLD (X-ray magnetic linear dichroism). The beamline is equipped with two end stations: a photoemission electron microscope (PEEM), and a universal station for X-ray absorption spectroscopy (XAS). The PEEM/XAS beamline can be used in material sciences, physics, chemistry, geosciences
and biosciences.

Beamlines under construction

XMCD: the beamline will use variable polarization radiation, the source of which will be the EPU (elliptically polarizing) undulator. The concept of the beamline assumes the coexistence of two measurement branches, in which the research end stations will be the PEEM microscope (photoemission electron microscope) and STXM (scanning transmission X-ray microscope). The PEEM branch will also contain an octupole station. The octupole end station will be dedicated to measurements of magnetic circular dichroism in the absorption of X-rays. The PEEM end station with standard equipment will allow for the creation and modification of research systems and imaging of their surfaces in a wide range of temperatures and with high resolution. The main advantage of the method is the ability to select the energy of excitations and the possibility to tune to the characteristic edge of the absorption. The STXM end-station will provide chemical analysis at the nanoscale through the combination of X-ray absorption spectrometry and microscopy. Potential applications of the XMCD beamline include magnetic order research, domain structure research, imaging of chemical composition, biomolecular spectroscopy, and fluorescence detection. The beamline will be accessible for scientists in 2020.

PHELIX: PHELIX is a beamline using soft X-rays, the source of which is an APPLE II undulator with permanent magnets. This type of insertion device gives the opportunity to obtain a variable polarization of light: linear polarization at any angle as well as circular and elliptical polarization. The PHELIX end station will enable a wide range of spectroscopic and absorption studies characterized by different surface sensitivity. Besides collecting standard high-resolution spectra, it will allow, among other things, the band structure to be mapped and the spin

to be detected in three dimensions. The beamline will be used in research of new materials for spintronics and magneto-electronics, topological insulators, thin films and multilayer systems including samples obtained in-situ, surface of bulk compounds, surface magnetism, spin polarized surface states, chemical reactions taking place on the surface, and biomaterials. The beamline will be put into operation in 2020.

SOLABS: an X-ray absorption spectroscopy beamline, whose synchrotron light source will be a bending magnet. The line will deliver photons within a broad energy range, allowing measurements to be conducted at the absorption edges of many elements. The end station will therefore be intended for materials research of both a basic and applied nature. The project leader, thanks to whom the research infrastructure will be created, is Hochschule Niederrhein, University of Applied Sciences of Germany, while the project partner is the Synchrotron Light Research Institute of Thailand.

SOLCRYS: a wiggler-based, high energy X-ray beamline for structural studies. End stations will enable measurements in various modes:
-single crystal diffraction (in particular protein crystallography)
-small-angle X-ray scattering
- powder diffractometry.
Its end stations will enable basic and applied studies, such as:
-comprehensive studies on crystalline structures of various materials, including biological samples (proteins, protein complexes, nucleic acids, etc.), biological macromolecules in solutions, nanoparticle suspensions, new nanomaterials (polymer systems, molecular sieves, nanocomposites, liquid crystals, etc.);
- studies on crystalline structure of functional materials under high pressure;
- studies on structural phase transitions under high pressure;
- studies on structure of unstructured objects (proteins, membrane and spherical proteins, macromolecular complexes, viruses and virus-like particles, biological membranes, nucleic acids and their complexes with proteins and / or drug delivery systems).
The construction of the beamline will involve the extension of the SOLARIS Centre's experimental hall. The investment's completion is planned for 2022. The SOLCRYS beamline will be built thanks to the cooperation of the Jagiellonian University with the Joint Institute for Nuclear Research in Dubna (Russia).

Planned Beamlines

At present, the Ministry of Science and Higher Education is considering three applications from SOLARIS for funding of investment in large research infrastructure.
The applications regard the construction of two beamlines, the FTIR and POLYX, as well as the construction of an STXM end station.

FTIR: an absorption infrared microscopy beamline (FTIR) with imaging. The construction of this beamline will allow for micro-scale chemical analysis and research on intermolecular forces in a broad range, from far infrared through mid-wavelength to near infrared. Such a broad spectra range on a single device is uncommon and will make possible a new level of research to be undertaken, including developmental and application studies in biomedicine, nanotechnology, environmental studies and many other scientific disciplines. The planned studies will facilitate, among others, targeting of the synthesis of potential medicines and their design. If the project receives co-financing from the budget of the Ministry of Science and Higher Education, construction of the beamline will begin in 2019 and be completed in 2022.

POLYX: a beamline which will enable high-resolution multi-modal imaging in the hard X-ray range. The use of innovative solutions in X-ray optics, pixel detectors, and experimental techniques will allow parameters to be achieved which are typical for synchrotrons which are much larger than SOLARIS. Depending on the experimental configuration and technique used, the POLYX beamline will enable imaging of samples of various sizes with spatial resolutions of from 50 μm to as much as 100 nm. The end stations on the POLYX beamline will be capable of being easily modified, allowing for the application of different synchrotron measurement methods. Additionally, the POLYX beamline may be used for testing new solutions in X-ray optics and detectors. If the project receives co-financing from the budget of the Ministry of Science and Higher Education, the construction of the beamline will begin in 2019 and be completed in 2022.

STXM: an end station for scanning transmission microscopy which will comprise an element of the XMCD beamline. The X-ray scanning microscope is one of the most universal types of X-ray microscopes, one which allows researchers from many scientific disciplines to conduct imaging research at the nanoscale. The device will enable, among others, nanoscale chemical analysis via a combination of X-ray absorption spectrometry and microscopy. In recent years, microscopes of this type have been installed at many synchrotrons around the world. Thus, nearly all modern synchrotron research facilities either already possess, are in the process of constructing, or plan to construct at least one STXM microscope. If the project receives co-financing from the budget of the Ministry of Science and Higher Education, the construction of the end station will begin in 2019 and be completed in 2021.

SOLARIS Experiment Reports

Experiment title:
Determination of spin state transition in $Ba(La,Gd)Co_2O_6$ layered perovskites

Beamline: **PEEM/XAS**

Beamtime from 8:00 19.10.2018
Beamtime to 8:00 20.10.2018

Beamline scientist: Marcin Zając

Experiment team: 1. Aleksandra Mielewczyk-Gryń, 2. Agnieszka Witkowska, 3. Sebastian Wachowski

Abstract (description of the experiment):
Summarise the purpose of your experiment at SOLARIS for the non-specialist. Please limit your entry to 200 words.

Proton Ceramic Cells (PCCs), comprising Fuel Cells and, are highly efficient electrochemical energy converters utilizing – or producing – both hydrogen and hydrogen-based fuels. PCCs are particularly suitable for application in large scale renewable energy systems and may thus be important constituents in the transformation into a more efficient, sustainable and low-carbon energy future. The performance of PCCs is currently limited by the electrode functionality, which relies on the functional properties of mixed protonic and electronic conducting ceramics (MPECs) used as positrode materials. Layered perovskites with general formula $BaLn_xLn'_{1-x}Co_2O_{6-\delta}$ (Ln, Ln' - different lanthanides) have the most promising electrochemical performance as a positive electrode for PCCs. Transport properties in oxides in general depend on the defect structure, which in turn can be influenced by order-disorder transitions on both cation and anion sublattices. Therefore, identifying the structural properties underpin the understanding of mixed protonic-electronic conductivity. The project was dedicated to $BaGd_xLa_{1-x}Co_2O_{6-\delta}$ compounds exhibiting varied hydration susceptibility and electrical performance on x function, correlated with changes in crystal symmetry and oxygen vacancies occupancy. Using X-ray absorption spectroscopy realized mainly on O K-edge and Co L_{23}-edges we would determine the Co oxidation state and the spin state of cobalt 3d electrons (low, intermediate or high spin configuration), which will allow us to understand the role of lanthanide on the hydration processes and open a possibility to improve and tailor MPEC properties for PCC application.

Experiment details:
Please include any relevant details e.g. sample stage, detectors, white or monochromatic beam.
Please limit your entry to 100 words.

NEXAFS spectra of samples with a general formula $BaGd_xLa_{1-x}Co_2O_{6-y}$ where x = 0.2, 0.3, 0.5 and of reference samples such as $BaLaCo_2O_6$ (Co^{+3} high spin state, HS), $BaGdCo_2O_6$ (Co^{+3} intermediate spin state, IS), $LaCoO_3$ (Co^{+3} low spin state, LS) and CoO (Co^{+2} low spin state, LS) were collected on O K-edge, Co L_{23}-edges and on M_{45}-edges of Ba and La. Measurements were performed at RT in TEY detection mode using monochromatic beam with a spot size of 3mm x 3mm. Using also the night shift, a set of all spectra of 9 samples and twice I_o intensity in a whole measured energy range were collected.

Achievements/difficulties:
Please include actual data from the experiment where possible. Please limit your entry to 200 words.

During the measurements we were able to collect data on cobalt L_{23} edge, lanthanum and barium M_{45} edges and oxygen K edge (which was our main interest). Co L_{23} NEXAFS spectra indicate that in all MPEC samples cobalt exhibits mainly the +3-oxidation state. However, detailed analysis of cobalt L_3 edge hits the information about possible Co^{2+} content present in the samples. Moreover, the obtained data on oxygen K edge allowed us to determine the relation between the cobalt spin state and the sample's composition (x value or Gd/La ratio) (Figure 1). This relation is especially important in the context of understanding the properties of this system. The comparative analysis of data presented in Figure 1 shows that the Gd atoms introduced to the $BaLaCo_2O_6$ network induce the transition from a HS state of the Co 3d electrons to IS configuration only for sample with x = 0.3. This behavior closely correlates with the unique susceptibility of this sample to hydration. Additionally, the analysis of lanthanum edges shows the differences in the white line intensities as an effect of both the Gd/La ratio and hydration.

.
We believe that the achieved data will allow us to understand better the structural differences between samples detected by the other methods like e.g. neutron diffraction and synchrotron X-ray diffraction or X-ray absorption.

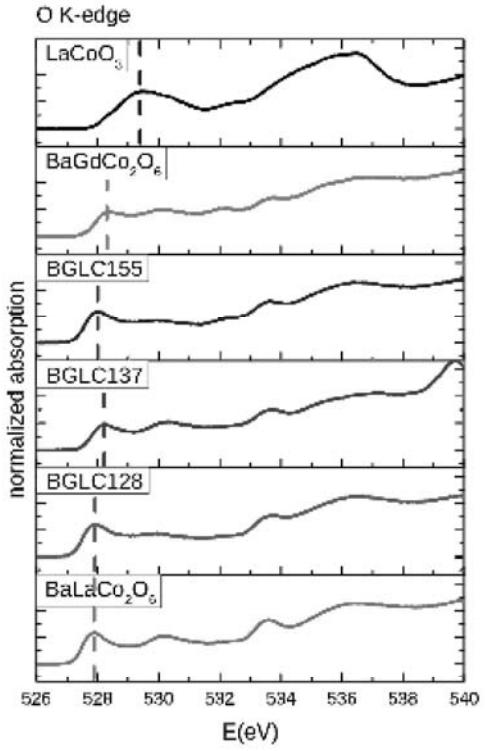

Figure 1. Oxygen K-edge data collected at RT for investigated samples (notation BGLC128 means $BaGd_{0.2}La_{0.8}Co_2O_{6-y}$)

Conclusion for the future:
What will this enable you to do? Do you plan to apply for further beamtime at SOLARIS? Please limit your entry to 200 words.

The quality of obtained NEXAFS spectra is so good that we are able to note changes in oxygen (especially in the pre-edge region) and cobalt spectra structure as a function of lanthanide contents (Gd/La ratio) and hydration level (one test measurement was made for the sample with $x = 0.2$). Thus, we are really interested in high-temperature measurements (application of the compounds in PCC requires 500-800°C as a temperature of operation) which allow us to control temperature-induced phase transition and changes in the electronic and defect structures. The results indicate the strong influence of composition and hydration on the cobalt spin state which is very important information coming from these studies and for sure will be extremely useful for understanding governing principles of hydration of investigated compounds.

Comment:
Please limit your entry to 100 words.

The support of the PEEM/XAFS beamline scientists (dr M. Zając and dr J. Stępień), technical and IT staff was impeccable, problems were solved almost immediately. The system of samples loading is problematic and very uncomfortable (it was a source of problems).
The manner of recording of all data from the experiment in one file is also quite inconvenient, both for checking the results already during the experiment and for subsequent data processing.

Publication resulting from this work:
Please add relevant publications from this study and expected outcomes, contributions to conferences.

SOLARIS Experiment Reports

Experiment title:
Determination of conduction band of photocatalytically-active N/Cu-doped TiO_2 double layer films

Beamline: **PEEM / XAS**

Beamline from – to:
19.02.2019 - 22.02.2019

Beamline scientist:
dr Marcin Zając

Experiment team: 1. dr Anna Wach 2. dr hab.Jakub Szlachetko 3. mgr Klaudia Wojtaszek 4. mgr Krzysztof Tyrała 5. mgr Michał Nowakowski 6. prof. dr hab. Wojciech M. Kwiatek 7. Daniel Sobota 8. Karol Szary 9. Wiktoria Stańczyk

Abstract (description of the experiment):
Summarise the purpose of your experiment at SOLARIS for the non-specialist. Please limit your entry to 200 words.

Photocatalysis is the most promising green route for the conversion of solar radiation into chemical bonds. The most commonly used photocatalyst is titanium dioxide (TiO_2) due to its relatively low cost, high photocatalytic activity, and chemical stability. Unfortunately, TiO_2 has a relatively large band gap (ca. 3.2 eV) and requires excitation with ultraviolet (UV) light, which accounts for only 5% of the solar spectrum. Among several strategies
proposed to increase TiO2 uptake of visible radiation, doping with non-metal anions (such as N, C, S) has been recognized as the most promising one. The improvement of photocatalytic properties relates to the direct modification of TiO_2 electronic structure by the introduction of additional electronic states above the valence band or below the conduction band of the pure metal oxide. The main goal of the experiment was to determine the structure of conduction band of N-N-TiO_2/Cu-TiO_2 double layer films in different stacking configurations. We measured series of X-ray absorption spectra at N, O, K-edges and Cu, Ti L-edges. The measurements provided information about the composition of conduction band of N/Cu-TiO2 doped thin layer films. Additionally, we measured changes in the electronic structure during ex-situ oxidation of Ti-metal discs at different temperatures.

Experiment details:
Please include any relevant details e.g. sample stage, detectors, white or monochromatic beam.
Please limit your entry to 100 words.

The experiment was conducted at XAS end station in the soft x-ray region, covering the photon energy range 200-1200 eV. XAS spectra at N, O K-edges and Cu, Ti L-edges were detected in the Total electron yield (TEY). The measurements were performed on the following samples: TiO_2 doped with copper and/or nitrogen in a bilayer structure with different stacking configurations as well as Ti metal discs oxidized at different temperatures. In addition, the preparation chamber was used to sputter the surface of Ti metal disc.

Achievements/difficulties:
Please include actual data from the experiment where possible. Please limit your entry to 200 words.

In the first part of the experiment, we measured N, O K-edges and Cu, Ti L-edges XAS spectra for N-TiO_2/Cu-TiO_2 double layer films in different stacking configurations. The combination of Ti L2,3-edge XAS spectra with the calculated density of states (FEFF9.0 code) will provide us detailed information about unoccupied electronic states, which are related to the conduction band of semiconductors. In order to study influence of dopants on the electronic structure, we additionally measured reference TiO2 sample with anatase
structure. In the second part of the experiment, Ti L2,3-edge XAS spectra were collected for Ti metal discs oxidised at different temperatures ranging from 200 to 800°C. In the measured spectra we saw four dominant features, which could be attributed to the excitations of Ti 2p3/2 (L3-edge) and Ti 2p1/2 (L2-edge) core levels into empty Ti 3d states. Based on the experimental data, we will follow how the metal electronic structure is transferred into oxide during thermal Ti oxidation.

Conclusion for the future:
What will this enable you to do? Do you plan to apply for further beamtime at SOLARIS? Please limit your entry to 200 words.

Based on experimental data we will determine conduction band electronic states for $NTiO_2$/ Cu-TiO_2 double layer films in different stacking configurations. As shown before (J. Catal. 2017, 353, 116), the stacking order has a great impact on the photocatalytic properties of bilayers structures. The study will allow us to find correlation of material's photocatalytic activity with changes measured in the conduction band of materials. Titanium dioxide TiO_2 has been widely used for various applications ranging from photocatalysis, sensors to dye-sensitized solar cell. Till date, several methods such as thermal evaporation, chemical vapour deposition, sol-gel, hydrothermal and template directed synthesis have been used to prepare the oxide in the most varied morphologies, dimensional arrangement and crystal structures. Possibly the simplest methodology to
form TiO_2 is the thermal oxidation of the metallic substrate. Although substantial experimental work has been devoted to understand oxidation mechanism of titanium, theories and the current understanding are still limited. Based on the experimental data, we will follow how the metal electronic structure is transferred into oxide during thermal Ti oxidation. Moreover, we will identify the intermediates products and mechanisms of metal-oxidation.

Comment:
Please limit your entry to 100 words.

Beamline Scientists provided high quality support over the entire beamtime. They also gave very professional training on the beam-line operation, sample exchange and data acquisition procedures. The beamline was well prepared and operated very smooth. Moreover, the acquisition procedures were clear and easy to be acquainted. We were also extremely impressed by high quality services and competent support from the User Office team.

Publications:
Manuscript from the beamtime is under preparation.

SOLARIS Experiment Reports

Experiment title:
Electronic and magnetic properties of single 2D FeSe(Te) layers ontop of MBE-grown $Bi_2Se(Te)_3$ thin films

Beamline: **UARPES**

Beamtime from 13.11.2018 to 17.11.2018

Beamline scientist: Dr. Natalia Olszowska, Prof. Jacek Kołodziej

Experiment team: Dr. Jan Fikacek, Ing. Martin Vondracek, Dr. Jan Honolka
(ASCR, Institute of Physics)

Abstract (description of the experiment):
Summarise the purpose of your experiment at SOLARIS for the non-specialist. Please limit your entry to 200 words.

We investigate correlations between the electronic band structure of FeSe monolayers and antiferromagnetic phase transitions using angle-resolved photoemission spectroscopy (ARPES) and x-ray magnetic circular dichroism (XMCD) techniques.
This correlation is believed to be the key for an understanding of yet unknown unconventional superconductivity (SC). In particular when FeSe enters the low-dimensional regime, electronic interface effects open the door for efficient modulation of superconducting properties. E.g. oxide-type interfaces have recently been shown capable to stabilize the superconducting phase by a tremendous degree to temperatures as high as 100K.
During experiments at the *XAS* and *UARPES* beamlines, we intended to study monolayer thin FeSe films grown *in situ* ontop of MBE-fabricated Bi_2Se_3topological insulator substrates and contribute to the understanding of the 2016 reported absence of superconducting properties in bulk Bi_2Te_3 crystal based FeSe/Bi_2Se_3 interfaces with respect to the 2017 discovered superconducting twin compound FeTe/Bi_2Te_3.
During the *UARPES* beamtime we were able to take high quality ARPES data of MBE-grown Bi_2Se_3. Despite the promising results, the users were finally not able to grow/measure FeSe with significant coverages within the available time: In contrast to *XAS* beamline experiments (see *XAS*report) the users were not able to optimize Fe evaporation parameters. In addition, the measurement time was shorter than planned, since after an error caused by the users during sample manipulation the *UARPES* preparation chamber had to be opened.

Experiment details:
Please include any relevant details e.g. sample stage, detectors, white or monochromatic beam. Please limit your entry to 100 words.

Sample preparation in the UHV preparation chamber of the *UARPES beamline*:
1) In situ preparation of clean Bi_2Se_3 surfaces via Se decapping at ~ 200°C
2) Verification of clean Bi_2Se_3 surfaces via LEED
3) Fe deposition from an e-beam evaporator. Fluxes were calibrated using a quartz balance
4) Tests to form FeSe by a post annealing step at ~ 300°C

ARPES measurements:
1) ARPES measurements were done at various photon energies (45 eV, 65 eV,95eV, and 100 eV). For overnight scans liquid nitrogen cooling with T ~80K was switched on.
2) Samples studied were (i) decappedMBE-grown Bi_2Se_3, and (ii) MBE-Bi_2Se_3 after Fe deposition and postannealing at 300°C.
3) Core levels of Bi and Se were measured at hv = 100eV

Achievements/difficulties:
Please include actual data from the experiment where possible. Please limit your entry to 200 words.

Achievements:
Our Se decapping procedure to prepare clean *in-situ* prepared Bi_2Se_3surfaces worked well at the *UARPES* preparation chamber [see hexagonal LEED pattern Fig. 1(c)]. High-quality ARPES data of the topological surface state of $Bi_2Se_3$was taken including also time dependent appearance of 2DEG states [see Fig. 1(a) and (b)].Binding energy dependent (kx, ky)-cuts in the region between Γ_0 and Γ_1 points were measured with good statistics and high resolution overnight (liquid N_2 cooling, Slit3 = 0.01, Ep = 10eV).In this particular k-space region one would expect the important high-symmetry M_1 and X_1 points in the presence of FeSe monolayers. A strict 6-fold symmetry in the band structure was visible, which reflects to the formation of 60° domains typical forBi_2Se_3MBE-growth.

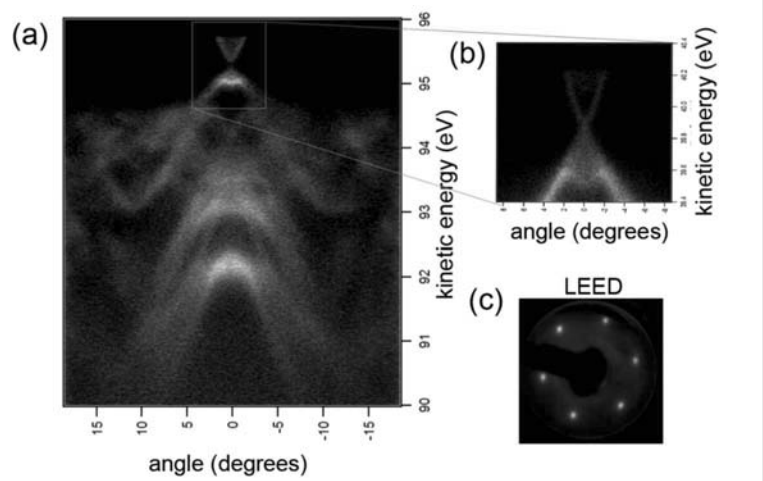

Fig.1: (a) ARPES cut in the DA30L mode (range ~ +/- 0.95 A-1 at hv = 65eV). (b) zoom-in into the topological surface state Dirac cone arounfdΓ_0. (c) LEED image of a decapped MBE-Bi_2Se_3 surface at *UARPES*.

Difficulties:
The project required to deposit smallest amounts of iron atoms with high coverage precision in the submonolayer range. To that purpose the users sent a UHV-compatible-beam evaporator to the *UARPES* beamline. The beamline scientists kindly agreed to install the evaporator before the arrival of the users to gain time and keep the preparation time short. After user arrival and subsequent baking of the evaporator a rough calibration of the iron flux from the evaporator was done using a quartz balance. Since Auger information was not available at the time of the experiment, a direct proof of the formation of FeSe was only possible by searching for a characteristic 12-fold LEED pattern of FeSe/Bi_2Se_3 (see Fig.1 in the *XAS* report). Within three days (until the manipulator incidence caused by the user mistake during sample manipulation) we were unfortunately not able to find optimal iron deposition conditions. A sample which the users hoped to contain FeSe did not show a typical 12-fold symmetric in the ARPES k-space structure (we believe the FeSe coverage was too low).

Conclusion for the future:
What will this enable you to do? Do you plan to apply for further beamtime at SOLARIS? Please limit your entry to 200 words.

Despite the reduced measuring time, our results proved the high potential of the *UARPES* beamline for experiments like those proposed in this project. The good quality of the ARPES data received on clean Bi_2Se_3 surfaces confirms the high spectral resolution in energy and k-space even for MBE-grown samples, which often show a lower degree of crystallinity compared to respective cleaved single crystals. The quality of overnight scans of the band structure for sure meets the criteria to resolve energy bands around the M_1 and X_1 points, which are predicted to determine the superconducting properties of Fe-based SC compounds.
In future proposal calls we would be glad to get the possibility again to measure similar systems at the *UARPES* beamline. For projects with intense *in situ* preparation tasks like the present one on FeSe we would however plan with a longer preparation time of about 4 days before the actual beamtime.

Comment:
Please limit your entry to 100 words.

Publication resulting from this work:
Please add relevant publications from this study and expected outcomes, contributions to conferences.
We might use the ARPES data of the MBE-grown Bi_2Se_3 to discuss the influence of 60deg rotational domains on the band structure of MBE grown samples in comparison to *in situ* cleaved bulk Bi_2Se_3. This result itself however is known (we observed it previously at the ASTRID-2 in Aarhus) and therefore cannot be a major point in a possible publication

Presenting Author's Index